

TAM  
.cb  
CER87/88-9

COPY 2

# ESSAYS ON RIVER MECHANICS

LIBRARIES  
MAY 14 1988  
COLORADO STATE UNIVERSITY

Colorado  
State  
University

Presented by the Graduate Students  
in CE 717 River Mechanics (Spring 1988)

Instructor: P.Y. Julien

May 1988

CER 87 - 88 PYJ-~~111~~<sup>9</sup>

## FOREWORD


I am very pleased to honor the work of my graduate students in the class CE717 - River Mechanics with this report of their technical papers. Each student worked on a particular aspect of river engineering in order to meet the following objectives:

- 1) familiarize with the recent literature and new methodologies not available in textbooks,
- 2) compare various methods (new versus old) and discuss the advancement of engineering technology on a given topic,
- 3) develop skills to point out the key elements of recent technological developments,
- 4) share interesting results with the other students through an oral presentation and a written paper.

The requirements for this project were:

- 1) select a topic relevant to river mechanics and sediment transport,
- 2) conduct a mini literature review including papers published in the past five years,
- 3) compare new methodologies with those detailed in textbooks on either a theoretical basis or through comparison with an appropriate data set,
- 4) write a 40 page report and discuss the major findings in a 30-45 minute oral presentation,
- 5) summarize the analysis and the results in a 15 page paper following the ASCE editorial standards (these papers are enclosed herein)

Not only did the students show great enthusiasm in this class but the reader will certainly agree with me that the objectives were met with great success. I am personally very impressed with the overall quality of the reports presented and can only encourage them to pursue advanced studies in this field.

  
P.Y. Julien

## Table of Content

	<u>Page</u>
Resistance to Laminar Sheet Flow . . . . . By Bahram Saghafian	1
Grain Size Parameters of Debris Flows and Hyperconcentrated Flows . . . . . By Elliott W. Lips	15
The Effect of Channel Width on Bedload Transport . . . . . By Deborah Anthony	27
Design of Stable Alluvial Channels . . . . . By Jayamurni Wargadalam	39
Sediment Extractors . . . . . By Tabassum Zahoor	55
Channel Stabilization . . . . . By Rob Wassum	70
The Techniques of Scaling for Hydraulic Physical Modeling . . . . . By Yi-Ching Chen	86
A Look at Physical Hydraulic Modeling . . . . . By Brian M. Bennett	98
Hinge Pool Effects on Sediment Transport . . . . . By Basil K. Arthur	110
Bed Degradation Below Dams . . . . . By Terry Waddle	123
Local Scour at Abutment . . . . . By Gye Woon Choi	138
Local Scour at Bridge Piers . . . . . By Vincenza Cinzia Santoro	149

(0973R)

# RESISTANCE TO LAMINAR SHEET FLOW

By Bahram Saghafian

**Abstract.** The results of discussion of literature review on resistance to laminar sheet flow are presented. The effects of surface roughness, rainfall, and vegetation are considered. It is believed that the total flow resistance is the sum of the contributions by each effect. Friction factor for the surface roughness effect is directly proportional to relative roughness and inversely to Reynolds number. A power function of rainfall intensity can represent the effect of rainfall on the product of friction factor and Reynolds number. The flow through vegetation requires more studies; however, the different friction factor equations by Chen and Hartley may be used for Bermuda grass and ideal vegetation respectively.

## INTRODUCTION

The flow over natural watersheds and urban drainages due to rainfall is considered to be a thin sheet flow. When the rainfall intensity exceeds the infiltration rate of the surface, if any, a spatially varied sheet flow begins; the flow would be steady unless the rainfall intensity varies with time. The discharge increases in downstream direction during the rainfall and surface runoff rushes down the slope of watersheds or paved roads, side walks, or parking lots in urban areas. After cessation of rainfall, a shallow steady uniform flow continues to create runoff during the time in which base flow source exists; thereafter recession phase starts. Sheet flows can be dealt with as an open channel flow in a broad surface except that if the flow is generated by rainfall, excess resistance will be induced by rainfall effect. Shallow flow is more sensitive to rain impact because of having very low depth.

The primary parameter in mechanics of sheet flow resistance to flow which determines other hydraulic variables such as velocity and shear stress. The focus of this paper will be confined to evaluation of Darcy-Weisbach friction factor for laminar sheet flow in different surface roughness conditions, and with or without rainfall effect. The surface roughness conditions include smooth and rough boundaries in addition to roughness system due to vegetation.

## DIMENSIONAL ANALYSIS

The following analysis shows the most general case of sheet flow over a rough boundary through vegetation with rainfall effect. The variables fall into six categories: 1) channel variables:  $S_0$  = bed slope; 2) roughness:  $k$  = boundary roughness height,  $C$  = roughness concentration defined as the ratio of the plan area of roughness elements to the total plane area of the base; 3) rainfall:  $d$  = rainfall size,  $\lambda$  = rainfall pattern,  $\lambda$  = raindrop shape coefficient,  $i$  = rainfall intensity,  $U$  = velocity of raindrop entering main flow; 4) vegetation:  $S_y$  = average vegetation spacing at depth  $y$ ,  $D_y$  = average diameter or width of the vegetation elements at  $y$ ,  $G_y$  = average gap size at  $y$ ,  $K$  = submerged length along vegetation,  $\psi$  = pattern dimensionless quantity,  $\theta$  = cross-sectional shape dimensionless quantity,  $EI$  = stiffness of vegetation; 5) flow:  $V$  = average flow velocity,  $Y$  = average flow depth,  $S_f$  = boundary loss gradient or head loss gradient; 6) fluid:  $\rho$  = fluid density,  $\gamma$  = specific weight of fluid,  $\mu$  = dynamic viscosity.

The general form of functional relationship may be shown as follows:

$$\text{Func} (V, Y, S_r, S_o, k, C, d, \tau, \lambda, i, U, S_v, D_v, G_v, K, \psi, \theta, EI, \rho, \gamma, \mu) = 0 \dots \dots (1)$$

Eq. 1 for the flow over a rough surface without any effect of rainfall and vegetation takes the form:

$$f = \frac{8gYS_r}{V^2} = \text{func} (V, Y, S_o, k, C, \rho, g, \mu) \dots \dots \dots (2)$$

where f, instead of S<sub>r</sub>, is the dependent variable. Performing Pi theory for constant C and dropping Froude number effect for laminar flow yields:

$$f = \text{func} (S_o, k/Y, R_w) \dots \dots \dots (3)$$

in which R<sub>w</sub> = Reynolds number.

Solving Eq.1 for boundary shear stress due to flow over a smooth surface with rainfall effect yields:

$$\tau = \text{func} (V, Y, S_o, d, \tau, \lambda, U, i, \rho, g, \gamma) \dots \dots \dots (4)$$

where τ is the boundary shear stress equal to γYS<sub>r</sub>. Yoon (1970) performed a dimensional analysis to present:

$$\frac{f}{8} = \frac{\tau}{\rho V^2} = \text{func} \left( \frac{VY}{\gamma}, \frac{V}{\sqrt{gY}}, S_o, \frac{iU}{\gamma}, \tau, \lambda, \frac{iY}{\gamma}, \frac{U}{\sqrt{gY}} \right) \dots \dots \dots (5)$$

where V.Y/γ and V/√gY are the conventional Reynolds number and Froude number respectively. Yoon experimentally found that: 1) iY/γ and U/√gY showed a poor correlation with f. 2) The effect of τ or rainfall spacing was negligible. 3) λ was kept constant and therefore dropped from the analysis. 4) Froude number appeared to be of secondary importance. 5) i/γ is proportional to i for constant γ. Therefore, Eq. 5 becomes:

$$f = \text{func} (R_w, S_o, i) \dots \dots \dots (6)$$

By applying Pi theory on Eq. 1 for the sheet flow through vegetation with rainfall effect and dropping unimportant terms of rainfall parameters based on the previous discussion, the following form is obtained:

$$\text{Func} \left( S_r, S_o, \frac{k}{Y}, \frac{iY}{\gamma}, \frac{S_v}{Y}, \frac{D_v}{Y}, \frac{G_v}{Y}, \psi, \frac{K}{Y}, \theta, \frac{EI}{\rho v^2 y^4}, \frac{\gamma Y}{\rho v^2}, \frac{\mu}{\rho v y} \right) = 0 \dots \dots (7)$$

Chen (1976) uses the experimental result by Yoon (1970) and argues that the effect of rainfall would be maximum for flow on the horizontal smooth surface but would decrease with increasing in both k and S<sub>o</sub>. He continues that since the roughness of turf surface are very high, the effect of rainfall intensity is believed to be insignificant. Also, the data by Chen (1976), Phelps (1970), and Hartley (1980) shows that the

flow resistance for flow through vegetation is much higher than that of flow with rainfall.

After some modifications in Eq.7 and using the relation  $V_{max}.G = V.S$ , Hartley (1980) comes up with the following equation:

$$f = \text{func} \left( S_o, \frac{S_v}{Y}, \frac{D_v}{Y}, \frac{G_v}{Y}, \gamma, \theta, \frac{K}{[EI/\rho V_*^2]^{1/4}}, \frac{V_{max}.D}{\gamma}, \frac{V}{\sqrt{gY}} \right) \dots \dots \dots (8)$$

in which  $V_* = \sqrt{gYS_o}$ . In Eq. 7, term  $k/y$  was dropped by assuming flow through vegetation having smooth boundary. However, the effect of roughness can be added to the vegetation resistance to yield total resistance.

The restrictions and simplifications made by Hartley include: 1) The density of the stream doesn't change with depth. So subscripts of first three terms after  $S_o$  may be dropped. 2) The effect of pattern and slope will be represented by a constant in the final equations. 3) Flexibility effect can be dropped for the experiments with rigid system. Also for rigid system  $K = Y$ . Therefore:

$$f = \text{func} \left( S_o, \frac{S}{Y}, \frac{D}{Y}, \frac{G}{Y}, \frac{V_{max}.G}{\gamma}, \frac{V}{\sqrt{gY}} \right) \dots \dots \dots (9)$$

The Froude number contribution in the laminar flow resistance equation has not been investigated so far. The experiments such as Chen's have been conducted with the attempt to eliminate surface instabilities. However, Hartley reported only small free surface effect even in turbulent flow. Hence, Eq. 9 takes the form of:

$$f = \text{func} \left( S_o, S/Y, D/Y, G/Y, V_{max}.G/\gamma \right) \dots \dots \dots (10)$$

in which  $R_m = V_{max}.G/\gamma = V.S/\gamma$  is the Reynolds number.

GOVERNING EQUATIONS

One of the most common resistance factor is the Darcy-Weisbach friction factor, which will be shown by  $f$  through the paper. The Darcy-Weisbach friction factor for wide open channel flow has been defined by the following equation:

$$f = \frac{8gYS_o}{V^2} \dots \dots \dots (11)$$

where  $S_o$  = energy gradient,  $V$  = velocity, and  $Y$  = flow depth. Eq. 11 may be applied to steady uniform flow in wide channels by substituting  $S_o$  for  $S_o$ .

The sheet flow with rainfall as the lateral inflow is considered to be a shallow spatially varied flow which with constant rainfall intensity and constant base flow would be steady. The derivation of governing equations for steady spatially varied flow with rainfall has been studied by many investigators; among them, Chow (1959), Woo and Brater (1962); and Yen and Wenzel (1970). Probably Yen and Wenzel (1970) derived the most comprehensive dynamic equation for this case by both momentum and energy approaches. Under the following basic

assumptions: 1) one dimensional steady flow; 2) hydrostatic pressure distribution; 3) constant channel slope; 4) constant momentum correction factor along the channel; 5) negligible air entrainment effect; and 6) impervious boundary, Yen and Wenzel (1970) using momentum approach came up with the equation of water surface profile for steady spatially varied flow in a wide channel:

$$\frac{dY}{dx} \left( \cos \theta - \frac{\beta V^2}{gY} \right) = S_o - S_f + \frac{i}{gY} (U \cos \phi - 2\beta V) \dots \dots \dots (12)$$

where x=distance in the flow direction, Y=flow depth at x and normal to channel bed,  $\theta$  = angle between x direction and horizontal direction,  $\beta$  = the momentum correction factor,  $S_f$  = friction slope defined as  $\tau / \gamma Y$ ,  $\phi$  = angle between velocity U and x direction, and other variables have been already defined.

### SURFACE ROUGHNESS EFFECT

The study of laminar sheet flow over bare surface as the most simplified situation is of interest in order to identify the variation of flow resistance coefficient due to surface roughness and Reynolds number. The following general formulation has been adopted by early investigators, such as Izzard (1944) and Woo and Brater (1961):

$$f = \frac{K}{R_w} \dots \dots \dots (13)$$

in which  $R_w$  = Reynolds number. K value varies with the flow regime, surface roughness, rainfall effect, vegetation and probably slope. Theoretically speaking, K is equal to 24 for laminar flow over a smooth wide channel. Horton, Leach, and Van Vliet (1934) experimentally confirmed the K value being 24 for laminar flow in a rectangular channel with a smooth surface, covered by white pine. Allen (1934) found the upper limit of  $R_w$  for true laminar flow regime being about 300 for smooth surfaces. The University of Illinois' data given by Landsford and Robertson (1958) and Chow (1959) determined the same K value as 24 for laminar flow when  $R_w < 500$ .

Woo and Brater (1961) tried to determine friction factor for different boundary surfaces. They partitioned the surfaces into smooth, rough, and very rough. Woo and Brater evaluated the width effect for the flow in rectangular channels, estimating an error of less than 5 percent in K when width depth ratio was 25. Woo and Brater's data for flow over masonite surface representing a typical rough surface showed a value of 30.8 for K. The U.S. Waterways Experiment Station (1935) had already reported K being 31.6 for laminar flow over cement surface. The upper limit of  $R_w$  for laminar flow varied from 400 for a slope of 0.060 to 900 for a slope of 0.001.

Glued-sand with an average diameter of 1 mm on the masonite surface used by Woo and Brater (1961) as a very rough surface on which flow experiments were conducted. It was found that K increased with the slope (except for slopes less than 0.003), having a value of 39.2 for  $S_o = 0.001$  up to 100 for  $S_o = 0.060$ . The laminar flow range was confined between the upper limits of 400 to 800, varying inversely with the

slope. Generally, the data in the laminar range seems inadequate to warrant the results.

If the  $f$  variation with slope is computed based on Woo and Brater's (1961) data, it will be found that for sand surface ( $k=1$  mm) when  $S_0 > 0.003$ :

$$f = \frac{50.85 + 16.667 \log_{10} S_0}{R_*} \dots \dots \dots (14)$$

The application of above equation reduces the slopes less than 0.020 after which the number of data for each slope is lacking.

The idea of correlation of  $f$  with the relative roughness was investigated by Phelps (1975). Phelps tested the flow over spherical roughness elements with diameter of 1.17 mm (.046 in) and grain concentration of 0.1 in the slope range being 0.00048-0.0451. The data confirmed the variation of  $f$  with relative roughness not slope.

Having Phelps' data in Fig.1, the following power equation may be developed to confirm Eq.12 for constant  $k/Y$ :  $f = aR_*^b$ . Table 1 can be filled by using Fig.1 as the reference.

TABLE 1 - Values of a and b Based on Phelps' Data

Relative Roughness (1)	Number of Data (2)	a (3)	b (4)	K (5)
.23	4	35.889	-1.00195	35.498
.27-.28	5	43.584	-1.02503	38.161
.35	7	42.392	-1.00191	42.040
.52-.55	7	31.179	-0.88777	50.61

As it is seen, the exponent  $b$  is very close to -1.0 except for the last series when  $k/Y = .52 - .55$ . As a result, the resistance equation may be written in this form:  $f = K/R_*$ , where  $K = \text{func}(k/y)$ . If a regression is to be performed, the result for  $K$  will yield:

$$K = 65.16 \left(\frac{k}{Y}\right)^{-4.0}, \quad \frac{k}{Y} < .5 \dots \dots \dots (15)$$

The application of resistance equation in the form of  $f = K/R_*$  would be probably limited to  $k/Y$  values less than even .50, according to Phelps' data. The result of power model for  $k/y = .52 - .55$  is not satisfactory to verify the equation for that specific  $k/Y$ . It is possible that free surface instability effect for high  $k/Y$  causes the discrepancies such that the correlation of  $f$  with  $R_*$  decreases indicating the change in flow regime from laminar to transition and turbulent.

Phelps (1975) reported that Woo and Brater's (1961) data also validated Eq.13 as they were grouped based on relative roughness. Assuming so,  $K$  values deduced from Woo and Brater's data are higher than those of Phelps' as much as two times for a constant  $k/Y$ . One may reason that the roughness concentration used by Woo and Brater was the maximum possible similar to Nikurase's work, where the Phelps' selected concentration in his experiments was less and equal to 0.1.



Now, as it is clear, two different independent variables have been worked with in evaluation of flow resistance, i.e. slope and relative roughness. Although Kruse et al. (1965) presented an equation in which slope was the independent variables besides the roughness size, they speculated that the apparent correlation of resistance to slope could be due to relative roughness and local turbulence at the tips of the roughness elements. When slope increased while discharge and hence Reynolds number were kept constant, depth would then decrease and more resistance would be induced due to larger portion of the flow being into contact with the roughness at a higher velocity. Therefore, the basic cause of resistance variation can be relative roughness rather than slope, which in turn is responsible in change in relative roughness. In addition, working with slope as the primary variable requires a series of experiments for each roughness size whereas the  $k/Y$  ratio reflects both roughness size and depth which varies with bed slope in the case of constant discharge. Phelps' work successfully demonstrates the effectiveness of  $k/Y$  being independent variable and the validity of equation  $f = K/R_{*}^2$ .

Yet, some considerations must be taken into account when working with relative roughness. First of all, the roughness concentration has to be held constant for each diagram of  $f$  vs  $R_{*}$  and  $k/Y$ . Second, the  $k$  value, the height of the roughness, needs an accurate measurement. Third, for high  $k/Y$ , free surface instability may bring about additional energy dissipation whose effect on  $f$  in laminar flow region has not been quantitatively determined.

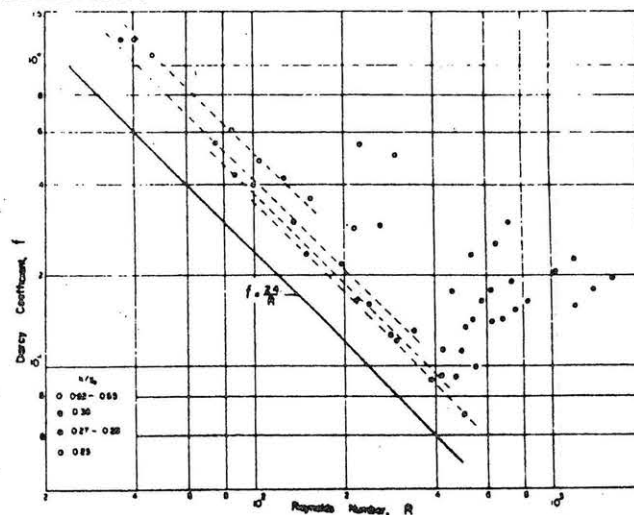


Fig.1. Friction Factor diagram for rough surface, after Phelps (1975)

#### RAINFALL EFFECT

The difficulty in solving the steady spatially varied flow arises when no complete information pertaining the law of the resistance in the presence of rainfall for evaluation of  $S_f$  is available. The efforts by Robertson et al. (1966) and Yu and McNown (1964) during their experiments led to the identification of significant magnitude of  $S_{*}$  and  $S_f$  compared to the other terms of Eq.12.

One of the latest and most complete experimental study on Eq.12 was accomplished by Yoon (1970). Instead of trying for analytical solution of Eq.12, Yoon wrote the following finite difference form of

Eq.12 by substituting  $V = q/Y$ :

$$\frac{\tau}{\gamma Y} = S_0 - \frac{\Delta Y}{\Delta x} \left( \cos \theta - \beta \frac{q^2}{gY^3} \right) - 2 \frac{\beta i q}{gY^2} + \frac{iU}{gY} \cos \theta \dots \dots \dots (16)$$

The simplified notation for Eq.16 is:  $S_f = S_0 - S_1 - S_2 + S_3$ . During a series of tests on sheet flow with rainfall over a smooth boundary, Yoon directly measured water surface profile,  $\Delta Y/\Delta x$ , and boundary shear stress,  $\tau$ , assuming  $\beta = 1$ . He found that the measured boundary shear stress, even with the difficulties in measuring flow depths with rainfall effect, was seemingly in excellent agreement with computed boundary shear stress using Eq.16. Therefore, the application of one dimensional dynamic equation of spatially varied flow appeared to be accurate enough for determination of water surface profile, provided a reasonable resistance law; i.e. and equation for  $f$ . It was also found that  $S_0$  overcame the other terms in magnitude while evaluating  $S_f$ . Each of  $S_1$  and  $S_2$  contributed nearly one tenth of  $S_0$  whereas  $S_3$  was negligible in magnitude.

Izzard (1944) first studied the resistance to sheet flow with rainfall effect. He considered  $K$  value in general Eq.13, could be the sum of a constant and a function of rainfall intensity. Therefore the following function was developed and then used by many other investigators:

$$f = \frac{K}{R_w} = \frac{K_0 + \phi(i)}{R_w} \dots \dots \dots (17)$$

where  $K_0$  is a function of surface roughness. Izzard used a paved rough surface in his experiments. As a result, he determined  $K_0$  being 27 for rough surface. The power function of rainfall intensity turned out to be  $5.67 i^{1.25}$ , where  $i$ (in/h). In addition, Izzard observed increase in  $f$  with increasing bottom slope. However, no slope parameter was included in friction factor equation.

Li (1972) conducted his tests to determine the independent variables of friction factor for laminar flow over smooth surface with rainfall through a dimensional analysis, he assumes the following power equation:  $f = \beta_0 R_w^{\beta_1} i^{\beta_2} S_0^{\beta_3} \epsilon$ , where  $\beta_0, \beta_1, \beta_2, \beta_3$  are constants and  $\epsilon$  is the error in the regression equation. The data covered a range of  $R_w$  from 126 to 900 for laminar regime, 0 to 17.5 in/h for rainfall intensity, and slopes being .0108 and .0064. The result of multiple regression showed that  $f$  equals

$$13.517 R_w^{-0.758} i^{1.413} S_0^{-0.008} \dots \dots \dots$$

According to statistical tests made by Li (1972), bottom slope had an insignificant effect on the product of  $f \cdot R_w$ . Furthermore, the exponent of  $R_w$  approximated to -1.

Before Li (1972), Yoon (1970) had carried out several tests to identify the independent variables affecting friction factor. Yoon (1970) found that the effect of raindrop spacing and raindrop impact velocity were almost negligible on friction factor under his test conditions. However, friction factor increased with increasing rainfall intensity and relatively bottom slope.

Li (1972) performed a regression analysis using his data and Yoon's data to derive the following power function for  $\phi(i)$ :

$$\phi(i) = 27.162 i^{-4.07}, \quad i(\text{in/h}), \quad R_{\infty} < 900 \dots\dots\dots(18)$$

Fawkes (1972) approximated the flow with rainfall as a steady flow with a very flat water surface profile. As a result,  $S_f$  would be almost equal to  $S_o$ . Fawkes then presented  $\phi(i) = 9.982i$ .

Other data based on experiments on sheet flow over smooth and rough surfaces with rainfall given by Kisiel et al.(1973) indicated no significant change in  $f$  due to slope. The data seemed to obey the same general formulation for  $f$ , though no attempt was made to deduce a certain equation for  $f$ .

In order to define friction factor experimentally for sheet flow with rainfall, most of the investigators used the kinematic wave approximation as suggested by Woolhiser (1969). The approximation assumes that all the terms in momentum equation are negligible except  $S_o$  and  $S_f$ , resulting then  $S_f = S_o$ . Then depth and velocity in Eq.11 are measured for a cross section and the variation of  $f$  due to rainfall versus  $R_{\infty}$  will be defined. Izzard (1944), Kisiel et al.(1973), and Fawkes (1972) used the kinematic wave approximation to determine the  $f$  variation.

According to Yoon's study on Eq.16, the kinematic wave approximation may involve up to 20 percent error in  $S_f$  determination. Yoon (1970), and then Li (1972), directly measured the boundary shear stress by hot film sensors, in order to avoid any approximation in their analysis. Having shear stress and flow velocity, they computed friction factor,  $f = 8\tau/\rho V^2$ , for specific rainfall intensity and Reynolds number. Consequently, Eq.17 substituted by  $\phi(i)$  from Eq.18 is the most accurate equation for solving dynamic equation of spatially varied flow.

As already discussed,  $K$  in Eq.13 may be a function of slope,  $S_o$ , or relative roughness,  $k/Y$ . Using a function of  $S_o$  would bring about an approximation by assuming steady uniform flow, which is obviously not true when rainfall exists. On the other hand,  $K$  being a function of  $k/Y$ , as used by Phelps (1975) specifically for steady uniform flow over rough boundary, reflects the effect of non-uniformity of the flow with rainfall effect. As spatially varied flow moves on, the depth changes and the boundary resistance has to change accordingly to yield the relative roughness effect. Therefore, both friction factors yield due to boundary roughness and rainfall will be functions of distance, simply because depth and Reynolds number are not constant for sheet flow with rainfall.

#### VEGETATION EFFECT

It is believed that the total friction factor can be represented by the linear superposition of vegetation drag, bottom effects, and rainfall effect. The last one is minor compared to vegetation drag and the natural bottom roughness of vegetated areas. The bottom effects due to roughness has been already discussed.

The past dimensional analysis indicates that the ideal vegetation resistance is more likely dependent on bottom slope, spacing, roughness diameter, gap size, and flow Reynolds number. The effects of these parameters are as following:

1. Slope: The early investigations of the flow resistance in a laminar flow through vegetation goes back to attempts to determine  $K$  value in Eq.13. As the first investigator, Izzard (1944) conducted a series of experiments on the laminar flow with the rainfall over a turf

surface covered with Kentucky Blue grass. He found K to be as high as 10,000 for bed slope being .01 and with any rainfall intensity.

An extensive study on effect of specific natural vegetation on resistance to sheet flow was carried out by Chen (1976). Bermuda grass and Kentucky Blue grass were used as the typical vegetation in overland areas. Through a dimensional analysis with considering test results, Chen assumed Reynolds number, slope, relative roughness  $k/Y$ , and rainfall intensity as the independent variables in dimensional analysis. Chen concluded that the effect of the rainfall would decrease with increase in roughness size,  $k$ , and bottom slope and therefore it may be neglected for high roughness boundary of grassed area. Later, he dropped  $k$  from the analysis for sake of simplicity and difficulties involved in  $k$  measurement. Finally, the remaining variables became  $R_{*}$  and slope, i.e.  $f = \text{func}(R_{*}, S_{*})$ . The regression analysis showed that K value for laminar flow through Bermuda grass began from 5000 up to 500,000 for slopes being .001 to .555 respectively. It was also found that the upper limit of  $R_{*}$  for laminar flow decreased from  $10^4$  for  $S_{*} = .001$  to  $10^3$  for  $S_{*} = .555$ . The equation suggested by Chen to be applied for Bermuda grass and Kentucky Blue grass surfaces in laminar range is:

$$f = \frac{510,000 S_{*}^{-0.662}}{R_{*}} \dots \dots \dots (19)$$

The increase in slope, if considered as an independent variable, would increase the friction factor of flow on a rough surface when discharge and other parameters held constant. The case of natural vegetation with higher density near the bed yields the same effect for bed slope. To reason such an effect, Kruse et al (1965) explained the phenomena by considering the correspondence of increase in slope and decrease in depth for constant discharge and therefore higher average density opposing the flow. This trend is resulted from Chen's tests on Bermuda grass.

Hartley (1980) superimposed the constant depth lines on Chen's data, as shown in Fig.2. Hartley confirmed the reason stated by Kruse et al (1965) that for constant slope, resistance decreases as depth increases indicating lower average density of vegetation with increasing in depth. Another trend in Fig.2 may be observed along constant depth lines. Generally, the friction factor grows along the path such that the tangent slope to the path starts from zero and increases toward infinity. This implies that constant depth at higher slope ranging from .001 to .164 and higher  $R_{*}$  up to some extent, corresponds to a higher friction factor. Obviously, the preceding conclusion is in contradiction with the case of flow over a rough boundary in which friction factor decreases with slope and  $R_{*}$  with depth held constant. Hartley explains that the increase in resistance along constant depth lines in Chen's data could be due to either instability in free surface as velocity increases or flexibility effects. The former effect requires additional energy dissipation and the latter causes an increase in biomass brought down into the flow due to bending. Kouwen and Unny (1973) state that this effect of flexibility increases resistance as long as the vegetation is not totally overtopped or channelized by the flow.

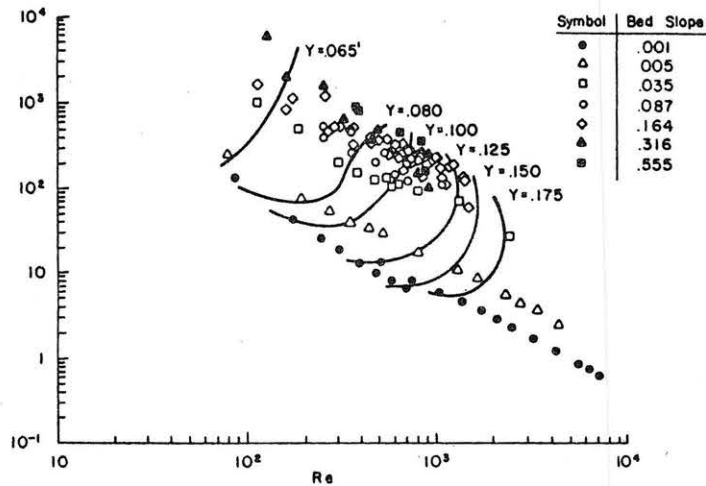


Fig.2. Friction factor diagram for Bermuda grass, after Chen (1976)

In the second part of constant depth line in Chen's data,  $f$  tends to grow very rapidly with constant  $R_{*c}$  and consequently discharge. The trend is true for depths being larger than 0.1 feet and when  $S_{*c} > 0.164$ . This indicates that for steep slope with constant depth, the flow resistance becomes independent of  $R_{*c}$  when  $R_{*c} > 700$  and apparently flow enters the transition regime. Therefore, the upper limit for  $R_{*c}$  for laminar regime in Chen's data would be probably close to 700 for slopes steeper than 0.164, whereas Chen extends it to 1100. One may reason the phenomenon for steep slope in terms of high free surface instability causing turbulence and making the flow exit from laminar regime. For practical purposes, however, steeper slope ( $S_{*c} > 0.164$ ) rarely occurs and the Chen's data on resistance of flow through Bermuda grass can be used for mild slope when  $R_{*c}$  is as large as  $10^4$ .

Even though there exist a debate concerning whether the bed slope can be an independent variable, Chen's data confirms a good agreement in laminar region with the equation  $f = K/R_{*c}$ . Since Chen's equation directly computes the total resistance, there is no need to separate the boundary resistance and deal with it. Also, the equation comes from the experiments in which more similarity with natural situation occurs, particularly density variation with depth.

2. Depth: Instead of bed slope, Phelps (1970) chose depth flow passage ratio as the independent variables. He carried out his experiments with artificial turf of raffia sewn to a jute fabric base. He found that the product of  $f \cdot R_{*c}$  was not a constant for laminar flow but rather decreasing with increase in  $R_{*c}$  for every constant depth. This means a steeper slope than -1 on log-log paper which is the theoretical slope. Phelps (1970) explained this departure in terms of the flexibility of the synthetic turf in response to the flow condition. As the Reynolds number and velocity increased, the expansion of average pore size caused steeper decrease in resistance. Another result of Phelps' experiments was the increasing resistance as depth increased with constant Reynolds number.

The data are depicted in Fig.3 illustrating  $f$  vs  $R_{*c}$  for constant values of  $h/d$ , where  $h$  is flow depth and  $d$  is flow passage dimension which was set to 0.01 feet due to the similarity of flow through turf with groundwater flow through porous media, with convection  $d$  being .01. Therefore, constant lines of  $h/d$  represent constant depths. If one

traces constant depth line in the direction of increasing  $R_m$  or discharge, he will find that the slope is increasing in that direction. As a result, the values of constant slope lines should decrease from the bottom to the top in direction of increasing  $f$ . Now, if for constant  $R_m$  or discharge the bed slope is reduced, the flow depth will increase and so will resistance. However, as indicated before, the same change in slope in Chen's data causes less resistance. One may explain the difference in terms of constant density of artificial turf in Phelps' experiments, but the ability of contraction of pores due to lower velocity. In natural turf used by Chen, average density decreases with depth and induces less resistance at higher depth. As a consequence, Phelps' data doesn't resemble the real condition of most vegetations with varying density. Nevertheless, the effect of flexibility has been of primary cause for change in  $f$  with depth in Phelps' data. The adequacy of Phelps' data is in doubt particularly for higher depths, and may need more experiments to be confirmed.

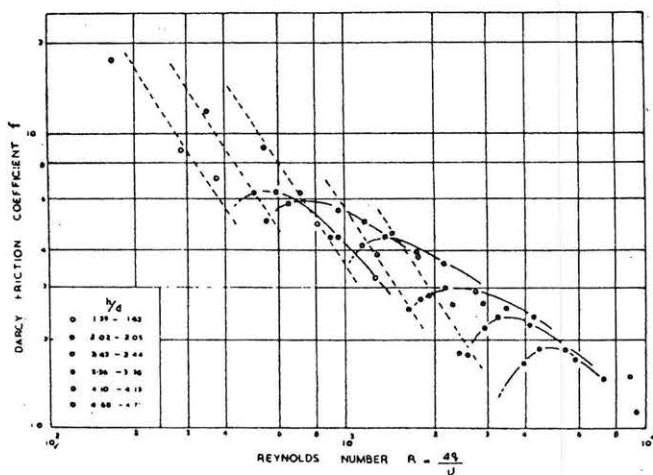


Fig. 3. Friction Factor diagram for simulated turf surface, after Phelps (1970)

Hartley (1980) tested the flow on a smooth surface through 1/4 inch diameter cylinders as the ideal vegetation. He then measured the flow depths and velocities and used the following equation for  $S_f$  being  $(Y_1 - Y_2)/\Delta x + (V_1^2 - V_2^2)/2g\Delta x + S_0$ , where subscripts 1 and 2 stand for upstream and downstream locations with the distance  $\Delta x$  apart. He reported that since the flow was close to a uniform flow, in most cases  $S_f$  showed values quite near  $S_0$ . Then, Hartley separated the bottom resistance friction factor being  $24/R_m$  and computed the friction factor only due to ideal vegetation.

Hartley assumed the following simple power model for laminar flow:  $f = A (Y/D)^B R_d^C$ , where  $A$  depends on density and pattern,  $Y/D$  is the depth diameter ratio, and  $R_d$  is diameter Reynolds number equal to  $V_{max} \cdot D/\nu$ . By performing regression, Hartley confirmed the general form  $f = K/R_d$  as:  $f = A (Y/D) R_d^{-1.0}$ .

Generally, having depth, instead of bed slope, as independent variable is advantageous because in case of non-uniform flow with rainfall the effect of change in depth would be included in flow resistance due to vegetation.

3. Density and Pattern Effects: Incidentally, the increase in vegetation density raises the flow resistance. The quantitative

evaluation of density effect for artificial vegetation has been done by Hartley (1980). He introduced a correction factor for density being  $(D/S)^2$ . Therefore his resistance equation for laminar flow becomes:

$$f = C \frac{DY}{S^2} R_d^{-1} \dots\dots\dots(20)$$

Constant C is dependent on the pattern roughness being 2995, 1366, and 1576 for staggered, parallel, and random patterns respectively.

The restrictions on using Hartley's equations are as follows: 1) Flow is laminar, i.e.  $R_d < 150$ .  $R_d$  may be replaced by  $(V_{max} \cdot D) / \nu = (S/S-D) \cdot (V \cdot D) / \nu$  in which (S-D) equals the gap size. 2) The vegetation surface is smooth and no flexibility effect occurs. 3) The vegetation can be identified as one of staggered, parallel, or random. 4) The vegetation density is approximately constant along the height of stems. 5) The equations only give the vegetation resistance.

4. Flexibility: The flexibility effect of vegetation has not been determined quantitatively for laminar flow through vegetation. Generally speaking, the flexibility effects include streamlining, channelization, vibration and compression. Both streamlinings resulted from bending and channelization, particularly in steep slopes reduce the flow resistance. The vibration effect may be neglected in sheet flow because of small turbulence scale especially for laminar flow in which any disturbance will be diminished. The submergence of excess height of vegetation is called compression which induces more energy dissipation and smaller flow passage size and in turn increases resistance.

#### CONCLUSIONS

The following conclusions were made based on discussion of literature: 1) Total resistance in laminar sheet flow can be represented by the sum of the resistances due to rainfall, roughness, and vegetation. 2) The relative roughness may represent a more general variable compared to bed slope, in flow resistance equation for laminar flow over a rough boundary. 3) According to Phelps' paper, the friction factor equation in the form  $f = K/R_d$  has been verified. K is constant for a given relative roughness. 4) Friction factor depends on Reynolds number and rainfall intensity for flow with rainfall over a smooth boundary; when f is defined as  $8\tau / \rho V^2$ . 5) The resistance equation given by Li (1972) is recommended for the computation of flow resistance with rainfall. Nevertheless, Chen's equation is suggested for total friction factor due to laminar flow through Bermuda and Kentucky Blue grasses. For rigid vegetation with constant density along depth of flow, Hartley's equations may be applied to compute friction factor for different vegetation patterns.

#### APPENDIX I - REFERENCES

1. Allen, J., "Streamline and turbulent flow in open channels", Phil. Mag., 7th series, 17, pp. 1081-1112, June 1934.
2. Chen, C., "Flow resistance in broad shallow grassed channels", Journal of the Hydraulic Division, ASCE, Vol. 102, HY3, pp.307-322, March 1976.
3. Chow, V.T., Open-Channel Hydraulics, McGraw Hill Book Co., New

- York, 1959.
4. Fawkes, P.E., "Roughness in a model of overland flow", Thesis presented to Colorado State Univ., Fort Collins, Colo., in 1972, in partial fulfillment of the requirements for the degree of Masters of Science.
  5. Hartley, D.M., "Resistance to shallow flow through vegetation", Thesis presented to Colorado State Univ., Fort Collins, CO., in 1980, in partial fulfillment of the requirements for the degree of Master of Science.
  6. Horton, R.E., Leach, H.R., and Vliet R.V., "Laminar sheet flow", Trans., American Geophys. Union, Part II, pp.393-404, 1934.
  7. Izzard, C.F., "The surface profile of overland flow", Trans., American Geophys. Union, Vol.25, pp.950-968, 1944.
  8. Kisisel, I.T., Rao, R.A., and Delleur, J.W., "Turbulence in shallow water flow under rainfall", Journal of the Engineering Mechanics Division, ASCE, EM1, pp.31-53, Feb. 1973.
  9. Kouwon, N., and Unny, T.E., "Flexible roughness in open channels," Journal of the Hydraulic Division, ASCE, Vol.99, No. HY5, pp.713-728, May 1973.
  10. Kruse, E.G., et al., "Flow resistance in simulated irrigation borders and furrows", Conservation Research Report No.3, Agricultural Research Services, U.S. Dept. of Agriculture, 56 p., 1965.
  11. Landsford, W.M., and Robertson, J.M., "Discussion of open-channel flow at small Reynolds numbers", by L.G. Stranb et al., Trans., ASCE, vol. 123, pp.707-712, 1958.
  12. Li, R.M., "Sheet flow under simulated rainfall", Thesis presented to Colorado state Univ., Fort Collins, Colo. in 1972, in partial fulfillment of the requirements for the degree of Masters of Science.
  13. Phelps, H.O., "The friction coefficient for shallow flows over a simulated turf surface", Water Resources, Vol.6, No.4, pp.1220-1226, 1970.
  14. Phelps, H.O., "Shallow laminar flow over rough granular surfaces", Journal of the Hydraulic Division, ASCE, Vol. 101, HY3, pp.367-384, 1975.
  15. Robertson, A.F., et al., "Runoff from impervious surfaces under conditions of simulated rainfall," Trans., ASCE, Vol.9, pp.343-346, 1966.
  16. U.S. Waterways Experiment Station paper 17, "Studies of river bed materials and their movement, with special reference to the lower Mississippi River," Vicksburg, Mississippi, Jan.1935.
  17. Woo, D.C., and Brater, E.F., "Laminar flow in rough rectangular channels", Journal of the Geophysical Research, Vol.66, No.12, pp.4207-4217, 1961.
  18. Woo, D.C., and Brater, E.F., "Spatially varied flow from controlled rainfall," Journal of the Hydraulic Division, ASCE, Vol. 88, No.HY6, pp.31-56, 1962.
  19. Woolhiser, D.A., "Overland flow on a converging surface," Trans. ASCE, Vol.12, No.4, pp.460-462, 1969.
  20. Yen, B.C., and Wenzel, H.G., "Dynamic Equations for steady spatially varied flow," Journal of Hydraulic Division, ASCE, Vol.96, HY3, pp.801-814, 1970.
  21. Yoon, N.Y., "The effect of rainfall on the mechanics of steady spatially varied sheet flow, on a hydraulically smooth



boundary," Thesis presented to Univ. of Illinois, Urbana, Ill., 1970, in partial fulfillment of the requirements for the degree of Doctor of Philosophy.  
22.Yu, Y.S., and Mcnown, J.S., "Runoff from impervious surfaces," Journal of Hydraulic Research, IAHR, Vol.2, No.1, pp.2-24, 1964.

## APPENDIX II. - NOTATION

The following symbols are used in this paper:

C = concentration of roughness elements;  
D = average diameter;  
d = rainfall size;  
EI = stiffness of vegetation;  
F = Froude number =  $V/\sqrt{gy}$ ;  
f = Darcy-Weisbach friction factor;  
g = gravitational acceleration;  
G = average gap size;  
i = rainfall intensity;  
K = submerged length along vegetation; also constant for description of f- $R_w$  relationship;  
k = mean boundary roughness height;  
q = unit discharge;  
 $R_w$  = Reynolds number =  $q/\nu$ ;  
 $R_d$  = diameter Reynolds number =  $V.D./\nu$ ;  
S = average vegetation spacing;  
 $S_w$  = bed slope;  
 $S_f$  = friction or energy gradient;  
U = velocity of raindrop entering main flow;  
V = mean flow velocity;  
Y = average flow depth;  
x = distance in the main flow direction;  
 $\beta$  = velocity distribution factor in momentum equation;  
 $\beta_1$  = regression coefficient in regression equation;  
 $\gamma$  = Specific gravity of water;  
 $\epsilon$  = error in regression equation;  
 $\lambda$  = parameter describing raindrop shape;  
 $\rho$  = density of water;  
 $\tau$  = boundary shear stress;  
 $\theta$  = angle between main flow direction and horizontal;  
 $\mu$  = dynamic viscosity of water;  
 $\nu$  = kinematic viscosity of water;  
 $\psi$  = dimensionless vegetation pattern parameter;  
 $\phi$  = angle between the velocity U and x-direction;

## Grain Size Parameters of Debris Flows and Hyperconcentrated Flows

Elliott W. Lips      Department of Earth Resources, Colorado State  
University, Fort Collins, Colorado, 80523

### Abstract

Debris flows and hyperconcentrated flows are members of the sediment-water continuum with distinctly different rheologies. Sedimentological and geomorphic features of the deposits are useful criteria for distinguishing between the flows, however these observations are generally qualitative. This study provides a quantitative analysis of the difference between these two flows.

Sixty-five samples were collected at eight sites of recent debris and hyperconcentrated flows. The deposits were classified in the field based on sedimentological and geomorphic features. Grain size parameters were analyzed and compared to determine which were significantly different for the two types of flows. The best parameters for distinguishing between the flows are sorting, kurtosis and percent clay. Debris flows are very poorly sorted, mesokurtic and have an average of 14.8 percent clay. Hyperconcentrated flows are moderately sorted, very leptokurtic and have an average clay content of 5.8 percent. There is not a statistically significant difference in mean grain size, skewness, or percent silt and clay between the two types of flows.

### Introduction

Debris flows, hyperconcentrated flows and stream flows comprise a continuum of sediment-water processes. The rheologic properties of these flows can be either Newtonian or non-Newtonian, depending in part on sediment concentration, sediment type, and particle distribution (Pierson and Scott, 1985). In order to identify potential runout zones and recurrence intervals for hazard mitigation it is important to distinguish between the types of sediment-water flows. The identification of, and distinction between types of flows is difficult because different terminology and criteria are used by different researchers.

Much of the terminology used in classifying flows comes from Sharp (1938) who used relative velocity and relative sediment concentration to differentiate processes. Varnes (1958, revised in 1978) proposed a slope movement classification based principally on type of material and type of movement. Velocity and moisture content are secondary characteristics. However, this classification does not address the fluid end of the sediment-water continuum and therefore is not useful in distinguishing between debris flows and hyperconcentrated flows.

The distinction between flows at the fluid end of the continuum was first addressed by Beverage and Culbertson (1964) on the basis of sediment concentration. Following this criteria Fan and Dou (1980), Takahashi (1981), Costa (1984) and O'Brien and Julien (1984) have proposed classifications for sediment-water flows. Pierson and Costa (1987) have included velocity as well as sediment concentration into a classification system. Table 1 lists the sediment concentrations and classification of flows reported by these researchers. Three problems exist in this type of classification system. First, there is no consistency in terminology of the flows which makes comparison difficult. Second, there is discrepancy in the reported values of sediment concentration that define the boundaries between types of flows. Third, when examining deposits of sediment-water flows in the field, one cannot establish what the sediment concentration or velocity of the flow was at the time of deposition. Because of these limitations, sediment concentration and velocity are not in themselves adequate discriminators of the type of sediment-water flows.

Table 1. Classification of Sediment-Water Flows (Modified from Bradley and McCutcheon, 1985)

Reference	Concentration Percent by Volume									
	10	20	30	40	50	60	70	80	90	100
Beverage and Culbertson (1964)	High	Extreme	Hyperconcentrated				Mud flow			
Costa (1984)	Water flood		Hyperconcentrated			Debris flow				
O'Brien and Julien (1984)	Water flood		Mud flood		Mud flow	Landslide				
Takahashi (1981)						Debris or Grain Flow			Fall, Landslide, Creep, Sturzstrom, Pyroclastic Flow	
Fan and Dou (1980)										
Pierson and Costa (1987)	Fast		Normal			Slurry Flow (Debris Torrent)		Granular Flow		
	Slow		Hyperconcentrated		Debris and Mud Flow		Sturzstrom, Debris			
					Solifluction		Avalanche, Earthflow			
							Soil Creep			

The second primary criteria used to distinguish sediment-water flows are flow properties, determined from the morphology and sedimentology of the deposits. Examples of the distinction between types of flows are found in the Committee on Methodologies for Predicting Mudflow Areas (1982), Bradley and McCutcheon (1985), Pierson and Scott (1985), O'Brien and Julien (1985), Smith (1986), Pierson and Costa (1987) and Wells and Harvey (1987). Although there is some discrepancy in terminology, most researchers recognize debris flows, transitional (hyperconcentrated) flows and stream flows as distinctly different processes. However, there is commonly reported only a qualitative description of the deposits, from which the distinction is made. Exceptions to this are Costa and Jarrett (1981) who use the Trask sorting coefficient ( $\sqrt{d_{75}/d_{25}}$ ) to distinguish between debris flows and water-flood deposits, and Pierson and Scott (1985) and Wells and Harvey (1987) who use among other criteria, mean grain size and sorting to distinguish types of sediment-water flows. Although these studies do provide useful criteria, it remains uncertain if other sedimentological parameters of the deposits are significant discriminators of the type of flow. If other criteria do exist, and are utilized, identification of ancient deposits will be more precise. This in turn will increase the ability to: 1) develop better models of transportation and deposition; and 2) enable accurate hazard identification, and mitigation.

The purpose of this investigation is to determine which parameters are the most significant in distinguishing between debris flows and hyperconcentrated flows. Sedimentological parameters considered are Graphic Mean, Inclusive Graphic Standard Deviation, Inclusive Graphic Skewness and Graphic Kurtosis (Folk and Ward, 1957). Other parameters evaluated are mean grain size, Trask sorting coefficient, percent silt and clay, and percent clay.

#### Data Collection

The samples included in this study were collected from deposits of eight debris and hyperconcentrated flows that occurred in Utah during the spring of 1983 (Figure 1). These flows resulted from the mobilization of landslides on steep hillsides triggered by the rapid influx of water to the soils. The landslides quickly mobilized and mixed with water to form sediment-water flows. These flows travelled distances up to 6 kilometers on relatively flat gradient alluvial fans. The hyperconcentrated flows were observed at the distal ends of the deposits and represent either the transition to the more fluid trailing end of the debris flows, or floods occurring after the debris flows. All samples were collected in the summer and fall of 1983 when the deposits were relatively unmodified by subsequent erosion. A total of 65 samples were collected, of which 55 were identified as debris flows and 10 as hyperconcentrated flows.

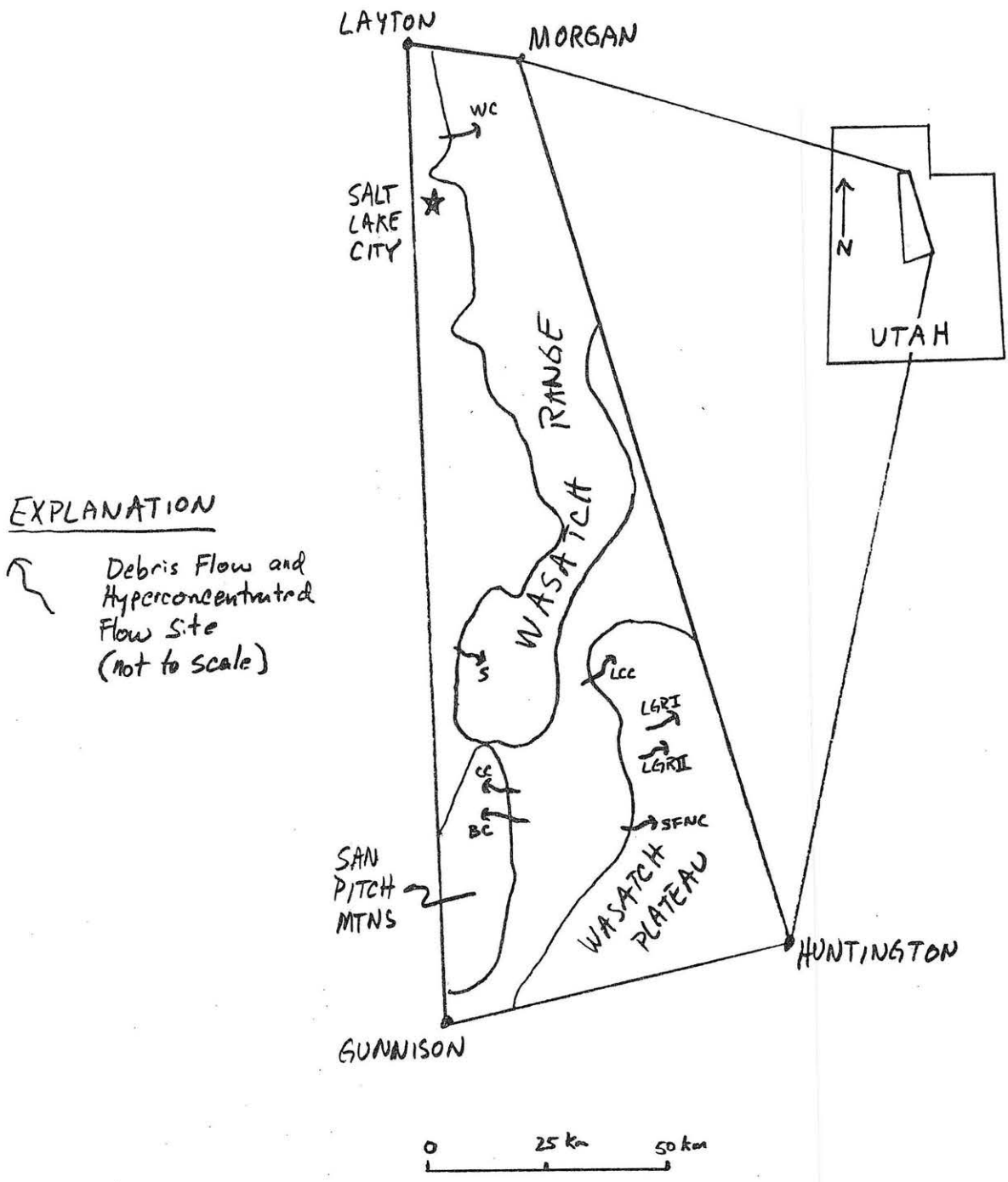


Figure 1. Location Map of Debris and Hyperconcentrated Flow Sites

WC, Ward Canyon; S, Santaquin; BC, Birch Creek; CC, Crooked Creek  
 SFNC, South Fork North Creek; LGR I, Lower Gooseberry Reservoir-I  
 LGR II, Lower Gooseberry Reservoir-II; LCC, Little Clear Creek.

The deposits were identified in the field at the time of sampling based on morphology and observable sedimentological features. Debris flows were identified as poorly sorted deposits lacking stratification and having angular clasts supported in a fine-grained matrix. Further criteria included lateral levees, terminal lobate fronts and large clasts carried in suspension. These features form as a result of having sufficient yield strength to exhibit plastic flow behavior. Debris flows had woody debris oriented parallel to the flow direction as a result of the internal shearing involved in laminar flow. The hyperconcentrated flows were identified on the basis of weakly developed stratification and a lack of a matrix of clay, levees and large clasts. Where woody debris was present in these deposits there was no preferred orientation.

Samples were collected by excavating approximately 300 cubic centimeters of the deposit. Samples were taken to include the material at the surface and to a depth of at least 10 cm. All samples were labeled and transported to the laboratory in sealed plastic sample bags. Sample location, with respect to distance from the source area and identification of the deposits were made at the time of sampling. The largest clasts included in the samples was approximately 5 cm. This was done because the intent of the sampling was to determine the rheologic properties of the flows, which is controlled primarily by the fine fraction. It is recognized that this is not always true; in particular where inertial forces dominate in flows having grain-to-grain contact of the clasts. However, field evidence at these sites suggest that fluid motion was controlled primarily by viscous forces. The error introduced in the analysis from the exclusion of the largest clasts will be discussed in a later section.

Samples were analyzed for grain size distribution in the laboratory by sieve and hydrometer techniques. Fourteen sieves were used, ranging in size from 8 mm to 0.063 mm. Hydrometer tests were performed according to Lambe (1951) with readings taken up to 24 hours. This procedure enabled determination of grain size down to 0.00013 mm. For the purpose of this investigation, clay is defined as less than 0.0004 mm; silt is between 0.0004 and 0.062 mm; sand is between 0.062 and 2 mm; and gravel is greater than 2 mm in size.

#### Data Analysis

Grain size curves of the samples were generated by plotting percent coarser by weight versus grain size in mm. Two distinct types curves were observed on these graphs. The first are the poorly sorted (well graded) curves of the debris-flow samples. The second type of curves are those from the hyperconcentrated flows which are better sorted (moderately graded). Figure 2 shows the distribution curves plotted from the average values of  $d_{95}$ ,  $d_{84}$ ,  $d_{75}$ ,  $d_{50}$ ,  $d_{25}$ ,  $d_{16}$ , and  $d_5$  of the debris-flow and hyperconcentrated-flow deposits at the Birch Creek site. These curves are representative of the curves for all eight sites.

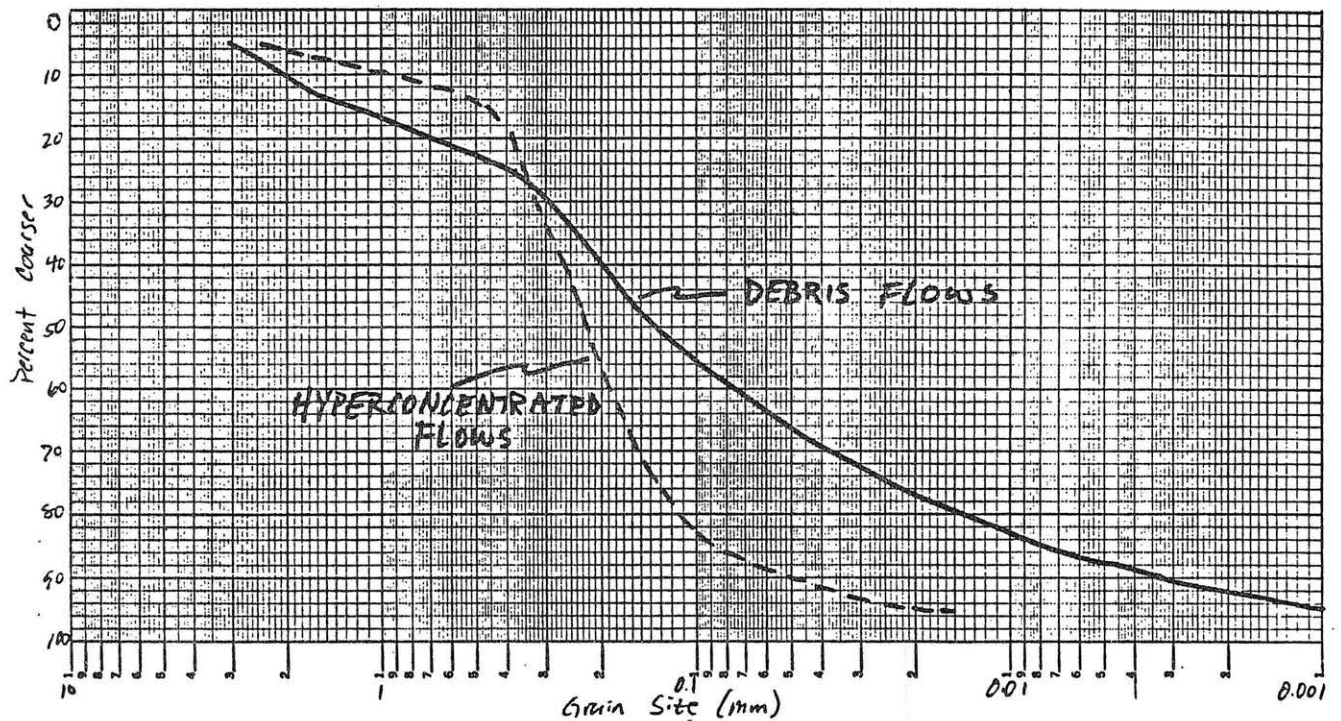


Figure 2. Grain size distribution curve for Birch Creek

Grain diameters were converted to Phi units with the following equation (Krumbein, 1938):

$$d = 2^{-\phi} \tag{1}$$

where d is the diameter in millimeters. From this:

$$\phi = - \frac{\log d}{0.30103} \tag{2}$$

In order to compare the deposits quantitatively, average size, sorting and other frequency distribution properties of each sample were determined graphically according to Folk and Ward (1957). The Graphic Mean of the samples was determined as:

$$M_z = \frac{\phi_{16} + \phi_{50} + \phi_{84}}{3} \tag{3}$$

where  $\phi_{16}$  is considered as roughly the average size of the coarsest third of the sample,  $\phi_{84}$  as the average size of the finest third, and  $\phi_{50}$  as the average size of the middle third.

The sorting was determined by measuring the Inclusive Graphic Standard Deviation (Folk and Ward, 1957).

$$\sigma_I = \frac{\phi_{84} - \phi_{16}}{4} \quad \frac{\phi_{95} - \phi_5}{6.6} \tag{4}$$

This parameter generally provides a better measure of the sorting because it includes the "tails" of the curve.

Skewness, the measure of the asymmetry of the curve, was determined by averaging the skewness of the central and extreme parts of the distribution curves. This is referred to as the Inclusive Graphic Skewness (Folk and Ward, 1957) and is defined as:

$$Ski = \frac{\phi_{16} + \phi_{84} - 2\phi_{50}}{2(\phi_{84} - \phi_{16})} \quad \frac{\phi_5 + \phi_{95} - 2\phi_{50}}{2(\phi_{95} - \phi_5)} \quad (5)$$

Perfectly symmetrical curves have  $Ski = 0.0$ , and the absolute mathematical limits are  $+1.0$  and  $-1.0$ .

Kurtosis measures the ratio of the sorting in the extremes of the distribution compared with the sorting in the central part. It is therefore a measure of the normality of the distribution; normal curves have a Graphic Kurtosis ( $Kg$ ) = 1.00 (Folk and Ward, 1957). The Graphic Kurtosis is defined as:

$$Kg = \frac{\phi_{95} - \phi_5}{2.44(\phi_{75} - \phi_{25})} \quad (6)$$

Additional parameters of the sediments used in this investigation are the mean grain size ( $\phi_{50}$ ), Trask sorting coefficient, percent silt and clay and percent clay. The Trask sorting coefficient is defined as:

$$Tr = \sqrt{\frac{d_{75}}{d_{25}}} \quad (7)$$

This sorting coefficient only considers the middle half of the distribution and therefore is probably not as good of a measure of the total sorting as is the Inclusive Graphic Standard Deviation. It is evaluated in this investigation because it has been previously used to distinguish between debris flows and waterflood deposits by Costa and Jarrett (1981).

## Results

To evaluate the difference in the deposits the mean values of the parameters mentioned above were compared to each other. If the deposits from the two flows are different they should have different mean values of size, sorting, skewness, etc. In this type of evaluation the null hypothesis is that there is no difference in the means, which can be stated as:

$$H_0: \mu_{df} = \mu_{hf} \quad (8)$$

where  $\mu_{df}$  is the mean value of a given parameter for the debris-flow deposits, and  $\mu_{hf}$  is the mean value of a given parameter for the hyperconcentrated-flow deposits. In order to show that there is a difference in the population means the null



hypothesis must be rejected in favor of the alternate hypothesis, which can be stated as:

$$H_a: \mu_{df} \neq \mu_{hf} \quad (9)$$

This type of hypothesis test is called a two-tailed-test because it is possible for  $\mu_{hf}$  to be either greater or less than  $\mu_{df}$ . For some parameters it may be appropriate to use a one-tailed test. For example it is expected that hyperconcentrated flows will have a lower sorting coefficient and lower percent clay than debris flows. However, for most parameters no knowledge of the expected difference existed before the analysis and therefore the two-tailed test was used throughout.

Because there are only ten samples of hyperconcentrated flows, and because no knowledge of normality of the samples exists the Wilcoxon Rank-Sum Test (Devore, 1982) was used to test the null hypothesis. The hypothesis tests were performed on a computer using statistics software (NH Analytical Software). This software performed the Wilcoxon Rank-Sum Test and also provided a two-tailed P-value for a normal approximation. The P-value is the probability of accepting the null hypothesis when it should be rejected. A P-value of 0.05 means that the null hypothesis is rejected at a 5 percent level of significance or confidence. Thus a lower P-value corresponds to a greater statistically significant difference in the mean values being tested. The P-value is identical to the alpha value in a Student T-Test. For this investigation, the P-value is reported and the significance is discussed rather than stating a priori at what level the null hypothesis will be rejected. Table 2 lists the mean values of the parameters tested for the two types of flows and the corresponding P-value for the hypothesis test.

Table 2. Summary of Statistics

Parameter	DF Mean	HF Mean	P-value
$\phi 50$	3.22	2.98	0.7298
Graphic Mean	3.79	3.13	0.1844
Inclusive Graphic Standard Deviation	3.10	1.84	<0.0001
Inclusive Graphic Skewness	0.27	0.23	0.4081
Graphic Kurtosis	1.03	1.68	0.0001
Trask sorting coefficient	4.68	1.90	<0.0001
Percent silt and clay	40.6	30.0	0.1056
Percent clay	14.8	5.8	0.0018

The P-values for  $\phi 50$  and the Graphic Mean indicate that the Graphic mean is a better discriminator, however for both parameters there is not a statistically significant difference between the means of the debris flows and the hyperconcentrated flows. Observations of the deposits in the field indicate that large clasts, up to boulder in size were present in the debris

flows, and not in the hyperconcentrated flows. Thus there should be a difference in the mean size of the samples, however the sampling did not include the large clasts in the debris flows. Therefore the results of these hypothesis tests are non-conclusive because of the bias of the sampling.

The two sorting parameters, Inclusive Graphic Standard Deviation and Trask sorting coefficient have the lowest P-values of all parameters. Thus there is the greatest statistically significant difference in the mean values of the sorting between debris flows and hyperconcentrated flows. The mean Trask sorting coefficient for the debris flows and hyperconcentrated flows are 4.68 and 1.91 respectively. Costa and Jarrett (1981) report a range of Trask sorting coefficients between 3.9 and 11.5 for debris and mudflows, and between 1.8 and 2.7 for waterflows. Both of these ranges agree well with the values in this study. Pierson and Scott (1985) report Graphic Standard Deviations for debris flows, transitional and hyperconcentrated streamflows as 3.0-5.0, 1.8-2.4 and 1.1-1.6 respectively. The values of the debris flows in this study agree very well with their range of debris flows. The values for the hyperconcentrated flows of this study agree very well with their transitional flows.

The P-value for the Inclusive Graphic Skewness indicate there is not a statistically significant difference between the two types of flows. Both sample means would be termed positively skewed according to Folk and Ward (1957).

The P-values for the Graphic Kurtosis indicate there is a statistically significant difference between the sample means of the two types of flows. The debris flows are mesokurtic and the hyperconcentrated flows are very leptokurtic (Folk and Ward, 1957). The physical meaning of the difference is that the debris flows are nearly normal ( $K_g = 1.0$ ) with respect to the sorting in the middle of the distribution curve and the sorting in the extremes. The hyperconcentrated flows are better sorted in the middle of the distribution than at the extremes as indicated by the  $K_g$  value significantly greater than 1.0. This well sorted central part of the distribution curve is shown in Figure 2.

The P-value for the percent silt and clay indicate there is only a weak statistically significant difference between the mean values of the two types of flows. However, there is a statistically significant difference between the percent clay in the two types of flows. The debris flows have a mean value of 14.8 percent which agrees well with reported values of the necessary clay percent to exhibit yield strength (10 percent Pierson and Scott, 1985; 11-15 percent, Wells and Harvey, 1987). The hyperconcentrated flows have a mean clay content of 5.8 percent, which is below the reported values to exhibit yield strength.

## Conclusions

Field evidence indicates there is a distinction between debris flows and hyperconcentrated flows. Debris flows are characterized by poorly sorted deposits supporting coarse angular clasts in a fine-grained matrix. Lateral levees, terminal lobate features and woody debris oriented parallel to the flow direction are additional criteria to distinguish debris-flow deposits. Hyperconcentrated-flow deposits are generally better sorted and may show stratification. Furthermore, they lack a fine grained matrix, levees, terminal lobate features, large clasts and have no preferred orientation of woody debris. These features suggest distinctly different rheologic properties which are quantifiable by analyzing sedimentological parameters of the deposits.

The best parameters for distinguishing between debris and hyperconcentrated flows are sorting, kurtosis and percent clay. Debris flows are very poorly sorted, hyperconcentrated flows are moderately sorted. Debris flows have kurtosis values near 1.0 indicating even sorting between the middle and extreme parts of the distribution curve. Hyperconcentrated flows are better sorted in the middle part of the distribution than at the extremes. The amount of clay in the debris-flow deposits is greater than the amount necessary to exhibit yield strength. Hyperconcentrated flows do not have the necessary clay percentage to have a yield strength.

Mean grain size may be a useful parameter to distinguish between the two types of flows if samples include the largest fraction of the deposits, which may be up to boulder in size. There is not a statistically significant difference between the two types of flows in skewness or in percent silt and clay.

## References

- Beverage, J. P., and Culbertson, J. K., 1964, "Hyperconcentrations of Suspended Sediment," *Journal of the Hydraulics Division, ASCE*, Vol. 90, No. HY6, pp. 117-126.
- Bradley, J. B., and McCutcheon, S. C., 1985, "The Effects of High Sediment Concentration on Transport Processes and Flow Phenomena," *in* Takei, A., ed., *Proceedings of the International Symposium on Erosion, Debris Flows and Disaster Protection, September 3-5, 1985, Tsukuba, Japan*, Toshindo Printers, Tokyo, pp. 219-225.
- Costa, J. E., 1984, "Physical Geomorphology of Debris Flows," *in* Costa, J. E., and Fleisher, P. J., eds., *Development and Applications of Geomorphology*, Springer-Verlag, Berlin, pp. .
- Costa, J. E., and Jarrett, R. D., 1981, "Debris Flows in Small Mountain Stream Channels of Colorado and Their Hydrologic Implications," *Bulletin of the Association of Engineering Geologists*, Vol. XVIII, No. 3, pp. 309-322.
- Devore, J. L., 1982, "Probability and Statistics for Engineering and the Sciences." Brooks/Cole, California, 640 p.
- Fan, J., and Dou, G., 1980, "Sediment Transport Mechanics," *Proceedings of the International Symposium on River Sediment.*, Guanghai Press, Beijing, China, pp. 1167-1177.
- Folk, R. L., and Ward, W. C., 1957, "Brazos River Bar: A Study in the Significance of Grain Size Parameters," *Journal of Sedimentary Petrology*, Vol. 27, No. 1, pp. 3-26.
- Krumbein, W. C., 1938, "Size Frequency Distribution of Sediments and the Normal Phi Curve," *Journal of Sedimentary Petrology*, Vol. 8, pp. 84-90.
- Lambe, T. W., 1951, "Soil Testing for Engineers"
- National Research Council. 1982, "Selecting a Methodology for Delineating Mudslide Hazard Areas for the National Flood Insurance Program," *Committee on Methodologies for Predicting Mudflow Areas*, National Academy Press, Washington, D. C., 35 p.
- NH Analytical Software, 1986, "Statistix: An Interactive Statistical Analysis Program for Microcomputers," NH Analytical Software, St. Paul, Minnesota.

- O'Brien, J. S., and Julien, P. Y., 1984, "Physical Properties and Mechanics of Hyperconcentrated Sediment Flows," in Bowles, D. S., ed., Proceedings of a Specialty Conference on Delineation of Landslides, Flash Floods, and Debris Flow Hazards in Utah, Logan, Utah State University, pp. 260-279.
- Pierson, T. C., and Costa, J. E., 1987, "A Rheological Classification of Subaerial Sediment-Water Flows," in Costa, J. E., and Wieczorek, G. F., eds. Debris Flows/Avalanches: Process, Recognition, and Mitigation, Geological Society of America, Reviews in Engineering Geology, Vol. 7, pp 1-12.
- Pierson, T. C., and Scott, K. M., 1985, "Downstream Dilution of a Lahar: Transition From Debris Flow to Hyperconcentrated Streamflow," Water Resources Research, Vol. 21 No. 10, pp. 1511-1524.
- Sharp, C. F. S., 1938, "Landslides and Related Phenomena," New York, Columbia University Press, 137 p.
- Smith, G. A., 1986, "Coarse-Grained Nonmarine Volcaniclastic Sediment: Terminology and Depositional Process," Geological Society of America, Bulletin, Vol. 97, No. 1, pp. 1-10.
- Takahashi, T., 1981, "Debris Flow," Annual Reviews of Fluid Mechanics, Vol. 13, pp. 57-77.
- Varnes, D. J., 1958, "Landslide Type and Process," in Eckel, E. B., ed., Landslides and Engineering, Washington D. C., Highway Research Board Special Report No. 29, pp. 20-47.
- , 1978, "Slope Movement Type and Process," in Schuster, R. L., and Krizek, R. J., eds., Landslides Analysis and Control, Washington, D. C., National Academy of Sciences, Transportation Research Board Special Report 176, pp. 11-33.
- Wells, S. G., and Harvey, A. M., 1987, "Sedimentological and Geomorphic Variations in Storm-Generated Alluvial Fans, Howgill Fells, Northwest England," Geological Society of America, Bulletin, Vol. 98, No. 2, pp. 182-198.

# THE EFFECT OF CHANNEL WIDTH ON BEDLOAD TRANSPORT

By Deborah J. Anthony

## INTRODUCTION

Many different relationships have been developed that relate parameters of channel development: channel width and depth, slope, average velocity, discharge, sediment discharge, and grain sizes for sediment and bank material. Some of these are simply rule-of-thumb relationships which show qualitative changes only (Schumm, 1977; Lane, 1955). Others fall under the general heading of regime equations or hydraulic geometry (Lacey, 1929; Leopold and Maddock, 1953), and are generally presented as power laws. These are one step beyond qualitative relationships, since they can be used to predict the magnitude of change, not just the direction.

Other equations which relate these variables are not so easily categorized. They include the basic equations of river mechanics, such as the continuity equation, and resistance formulae which relate velocity to the slope and depth (or hydraulic radius) of the channel. Also included should be the sediment transport equations which predict either bedload, suspended load, or total load as a function the above variables.

From this morass of equations, some sense of how a river behaves can be obtained. In particular, for this study, we would like to look at the relationship between the width of a channel (usually defined as the top width,  $B$ ) and the amount of bedload ( $Q_b$ ) that channel can move, given that other parameters remain constant. Three possible relationships exist, obviously. Bedload transport rate can increase with increasing width, decrease with increasing width, or an optimum width can exist where the transport rate is at a maximum.

Intuitively, the final option, an optimum width, seems the most appropriate. If an imaginary fixed discharge is allowed to spread out in a channel that becomes wider and wider, eventually the flow will become so shallow it will be below the critical unit discharge or critical shear stress necessary to initiate motion. Therefore as the width goes to infinity, transport goes to zero. Conversely, that same discharge confined to a narrow slot cannot effect the bedload to a sufficient depth to make the transport rate higher than if the flow were in a more rectangular channel.

In order to visualize what is going on, we need to identify which variables are to be held constant and which can be allowed to change. For this study, let us assume that discharge ( $Q$ ), slope ( $S$ ), and grain size ( $d_{50}$ ) are constant. Since discharge is a constant, while width changes, depth ( $H$ ) must also change. However, the cross sectional area does not remain the same, since changing depth causes a change in the velocity ( $V$ ) described by an appropriate resistance equation. The product of these three ( $B$ ,  $H$  and  $V$ ) is the only thing that remains constant.

If we assume that unit sediment transport rate ( $q_b$ ) is directly proportional to unit discharge ( $q$ ), it would seem that greater depths correspond to larger overall transport rates. However, it is the rate of change of the transport compared to the rate of change of the width which is important. If:

$$Q_b = B * q_b \dots \dots \dots (1) \text{ and}$$

$$Q_b' = (B + \Delta B) * (q_b - \Delta q_b) \dots \dots \dots (2)$$

as the width increases and the unit sediment discharge decreases each by a small amount, then  $Q_s'$  could be larger or smaller than  $Q_s$ , depending on whether the increase in the width or the decrease in the sediment transport rate has more effect on the product.

A number of different studies have touched on this problem, and of the three conclusions possible, each has proponents. Some early workers have created simple empirical models which describe broad trends (Schumm, 1977). Other studies have focused on simple proportionalities, and have tried to extrapolate beyond them (Henderson, 1966). However, more recent research has focused on the relationship between width and bedload transport rate as part of the overall adjustment available to a river, as it reacts to external and internal stimuli.

Ferguson (1986) has pointed out that in order to obtain a complete set of downstream hydraulic geometry equations for width, depth, slope and velocity (assuming discharge, sediment discharge, and sediment characteristics are given), four different equations/relationships must be developed. The two most obvious relationships to start with are the continuity equation and a resistance formula. The third popular type of equation used in hydraulic geometry analysis is some type of sediment transport equation. The final one is the most difficult to obtain. Ferguson lists several different approaches used to determine this last relationship: an empirical approach that gives a fixed relationship for one or more of the variables in question; a minimum variance approach that he described as "metaphysical"; an assumption of threshold channel conditions; an assumption of a maximum transport efficiency for the channel; or finally, a relationship based on bank stability.

#### BEDLOAD TRANSPORT INVERSELY PROPORTIONAL TO CHANNEL WIDTH

The common assumption that unit sediment transport rate is directly proportional to unit discharge raised to a certain power is the basis for Henderson's (1966) analysis. Combining the Einstein-Brown transport formula with the Chezy resistance equation, and eliminating "constants", he showed:

$$q_s \sim q^2 S^2 / d_{s0}^{1.5} \dots \dots \dots (3a) \text{ or}$$

$$q_s \sim q^k \dots \dots \dots (3b)$$

If that is true, then multiplication by the channel width (B) yields:

$$B q^k = B^{1-k} (Bq)^k = B^{1-k} Q^k \dots \dots \dots (4) \text{ and}$$

$$Q_s \sim B^{1-k} Q^k \dots \dots \dots (5)$$

Thus if k is greater than one, which Henderson believed to be the case for most transport formulae, then bedload transport is inversely proportional to width. Henderson stated explicitly that if a river increased in width, then deposition would occur due to decreased transport capacity. This would increase local slope until the transport rate increased to accommodate the upstream supply. This manipulation assumes that k is constant and not a function of q or  $Q_s$ . Equation 3b can be rearranged to look at the sediment concentration  $q_s/q$ :

$$q_s/q \sim q^{k-1} \dots \dots \dots (6)$$

Again, as long as k is greater than one, sediment concentration increases with unit discharge, a common observation.

Carson and Griffiths (1987) pointed out that this analysis

can be done with other derived or empirical equations which show unit sediment discharge as an increasing function of unit discharge, unit stream power ( $w$ ), or shear stress. Bagnold's (1977) stream power approach (Eq. 9 below) indicated that  $q_s$  was proportional to  $w$ . Since  $w = \rho QS/B = \rho qS$ , with density ( $\rho$ ) and  $S$  held constant,  $w$  is subject to the same analysis as  $q$ .

A more complex analysis of the kind described by Ferguson (1986) was undertaken for the design of stable alluvial channels, by Abou-Seida and Saleh (1987). They assumed a live bed with the ability to adjust both its width and depth in accordance with imposed fluid and sediment discharge. The equations used included continuity (not explicitly stated), the Einstein-Brown transport concept (only the straight line portion), and the Liu-Hwang resistance formula. Discharge, sediment discharge, and sediment properties are fixed, and unknowns are width, depth, and slope.

One of the apparent strengths of this method is the use of bedforms in the calculations for resistance. The final form of this model is an iterative loop that solves for the unknowns, and then checks to determine whether they predict the bedforms that were assumed at the start, and also checks for reasonable values of stream power. This loop calculates velocity (not mentioned as an unknown), and repeats until an internally consistent set of values is determined. The bedform predictor and stream power constraints can thus be seen as Ferguson's (1986) fourth equation.

The final equations were produced by algebraic manipulation of the above relationships. They appear complex, simply due to the many exponents used to determine resistance with bedforms. However, a final equation relating the sediment transport and the wetted perimeter can be given as:

$$Q_s \sim Q^a / (d_{s_0}^b S^c P)^d \dots \dots \dots (7)$$

where  $a$ ,  $b$ ,  $c$  and  $d$  are a function of resistance only. In this model, the wetted perimeter ( $P$ ) replaces the width in the primary equations, and the hydraulic radius ( $R$ ) is used instead of the depth. Using an assumed shape factor, they are converted back at the end of the program to width and depth. Assuming that  $P$  is approximately equal to  $B$ , sediment transport rate is inversely proportional to some power of width, as long as  $d$  is greater than 0, and slope, discharge, and  $d_{s_0}$  are fixed. The exponent  $d$  is a function of grain size only, and calculations showed that this number is positive for all values of  $d_{s_0}$  between 0.01 and 10 mm.

#### BEDLOAD TRANSPORT DIRECTLY PROPORTIONAL TO CHANNEL WIDTH

Of the many authors who have looked at simple relationships between the stated variables, the number that propose a direct relationship between width and bedload transport is greater than those who advocate an inverse one. For instance, one of Schumm's (1977) correlations indicated:

$$Q_s \sim (B, \text{wavelength}, S) / (H, \text{sinuosity}) \dots \dots \dots (8)$$

Since total sediment discharge is directly proportional to width and inversely proportional to depth, this would tend to imply that bedload transport is directly proportional to width, with discharge held constant. This is reinforced by Schumm's (1977) suggestion that shallow wide streams are more commonly bedload streams, while narrow streams have a larger suspended load.

Bagnold (1977) approached the problem by means of stream



power. He assumed that unit stream power and unit bedload transport rate were the same physical quantity, the time rate of energy supply and dissipation. Using data from flumes and natural rivers, he found that a strong relationship existed between unit bedload transport rate and excess stream power ( $w - w_o$ , unit stream power minus threshold unit stream power) for a fixed ratio of depth to  $d_{s0}$ . His final equation was empirical:

$$q_b = 1.6 (w - w_o)^{1.5} / w_o^{0.5} (H/d_{s0})^{-0.67} \dots \dots \dots (9)$$

At the end of this paper Bagnold states that since total bedload transport and total stream power are obtained from their unit values through multiplication by the channel width, that any relationship between  $q_b$  and  $w$  should apply to the whole river. Since  $Q_b$  is inversely proportional to depth, then it should be directly proportional to width! Bagnold apparently didn't consider the changes in unit stream power with changing depth, or note that where  $w < w_o$ , transport drops to zero.

Parker (1979) came to conclusions similar to Bagnold's using a somewhat different approach. His analysis originally dealt only with gravel bed rivers having straight channels, but he claimed a "degree of universality in coefficients as well as exponents" for his final equations. He first used dimensional analysis on all the variables, and then put these dimensionless variables into a set of hydraulic geometry relationships. In their final form, dimensionless channel width ( $B^*$ ) and depth ( $H^*$ ) (which were both scaled by  $d_{s0}$ ), and channel slope ( $S$ ) were all functions of dimensionless discharge ( $Q^*$ ) and dimensionless bedload transport ( $Q_b^*$ ). Dimensionless velocity ( $V^*$ ) was obtained from the other variables via the continuity equation.

To obtain coefficients for these relationships, Parker used velocity profile equations and field and flume data to construct his semi-empirical formulas. To solve for the 4 unknowns, Parker assumed a self formed channel which was stable, created in material identical to the bedload. This led to his stable channel paradox, in which he showed through analysis of threshold channel theory that stable banks and mobile material at the channel center were mutually exclusive. He resolved this dilemma by assuming lateral turbulent diffusion of downstream momentum, which would allow an increase in critical shear in the channel center, and a decrease near the banks, thus allowing a configuration for a stable channel.

After fixing channel geometry, Parker made four additional assumptions necessary to solve for his dimensionless variables:

$$\begin{aligned} \tau_c &= \rho g H_c S \dots \dots \dots (10) \\ \tau_c - \tau_{th} &= 0.20 \tau_{th} \dots \dots \dots (11) \\ q^* &= 11.2 (\tau^* - 0.03)^{4.5} / \tau^{*3} \dots \dots \dots (12) \\ V/u^* &= 2.5 \ln 11 (H/d_{s0}) \dots \dots \dots (13) \end{aligned}$$

The first states that in the channel center, shear stress ( $\tau$ ) can be defined by the conventional equation, ignoring lateral turbulent diffusion of downstream momentum, while the second states that this central shear stress is only 20% above the threshold value ( $\tau_{th}$ ). The last two equations (where  $q^*$  is dimensionless unit discharge,  $\tau^*$  is Shields stress, and  $u^*$  is the shear velocity) are semi-empirical, and were fitted by eye to flume and field data from Peterson and Howells (1973).

After some algebraic manipulation, Parker presents different

groups of equations in which dependent and independent variables are mixed. Some of these are hydraulic equations only, showing, for instance, the relationship:

$$H^* = 0.866 (Q^* / B^*)^{0.83} \dots \dots \dots (14)$$

between width, depth and discharge. Several of these were tested against field data with good results. However, a more complete set of equations included  $Q_b^*$ , but these were not tested against outside data. The final equation for width was:

$$B^* = 3.09 \times 10^4 Q_b^{* 1.296} Q^*^{-0.296} \dots \dots \dots (15)$$

This shows a direct relationship between width and bedload transport rate. However, in deriving this relationship, Parker neglected any effects of bedforms or channel planform, and he assumed a channel where the gravel bedload is near the threshold of motion, hardly indicative of most natural rivers. However, his inclusion of bank stability shows thought for the processes which might cause channel width adjustments.

Julien and Simons (1984) constructed a different set of hydraulic relationships. Their analysis is more straight forward than Parker's (1979), since it identifies four unknowns (width, depth, velocity, and slope) found from four equations. Given in this analysis are discharge, sediment discharge, and grain size. The four relationships include the ever popular continuity and resistance formulae. In place of a bedload transport law, the Shields parameter ( $\tau^*$ ) is used, and this equation scales the depth. The final equation shows some similarities to Parker's work, in that it involves the bank erosion, and thus can be used to scale the width/depth ratio. This final equation is an evaluation of the lateral shear at the bank, and is derived from the equation of motion, emphasizing the effects of centrifugal force, cross stream pressure gradient, and bed shear:

$$\tau_{x,r} \sim (\rho V^2 H) / ((\gamma_s - \gamma) B d_s) \dots \dots \dots (16)$$

Algebraic manipulation yields the following:

$$B \sim Q^{.53} d_s^{-.33} \tau^{* 0.2} \dots \dots \dots (17)$$

$$H \sim Q^{.4} d_s^0 \tau^{* -0.6} \dots \dots \dots (18)$$

Since Shields stress is a surrogate for bedload transport rate in this analysis, the above equations show a direct relationship between transport rate and width, and an inverse relationship between depth and transport rate. While these downstream hydraulic geometry relations show only trends, they agree in general with the equations mentioned above. However, using Shields parameter as a surrogate for bedload transport poses some problems, especially for the relationship between the transport or erosion rate (for the banks), and the threshold value of the Shield's parameter.

#### BEDLOAD TRANSPORT WITH AN OPTIMUM WIDTH

One of the first individuals to assume that an optimum channel width existed for bedload transport was Gilbert (1914). On the basis of his flume experiments, he determined that a channel whose width/depth ratio was between 2 and 25 had a maximum transport capacity. He noted that the value of this ratio increased as the discharge and slope increased, and decreased as sediment size increased, but he developed no equations to quantify this relationship.

The work of White et al (1982) was noted by Ferguson (1966)

under the category of maximum transport efficiency. This group assumed constant, fixed discharge and slope, and then solved for channel width, depth, velocity, and sediment transport. To do this, they used the White, Paris and Bettess friction relationship for their resistance equation, and the Ackers and White sediment transport formula. Both these sets of equations are semi-empirical, based on generally accepted principles of sediment transport and channel resistance, but calibrated using flume data. The continuity equation is not mentioned, but must be assumed to be a third equation in the analysis.

One more equation or relationship is needed to solve for the four variables listed above. White et al. (1982) assumed a condition of maximum sediment transport exists. Their approach to this final relationship is not to devise an equation, but with 3 equations and 4 unknowns, to create a program which will give a family of solutions. When this family of solutions is graphed (Fig 1.), a width which corresponds to a maximum sediment transport is apparent.

When this maximum transport rate is made a constant, and the slope is allowed to vary with fixed discharge, then the results are the second curve in Fig. 1. At the position of the optimum width calculated before, the slope now reaches a minimum. Thus maximizing sediment transport at a given discharge and slope is equivalent to finding the shallowest slope for a given discharge and sediment transport capacity, and both will occur at the same width, given the same values. The idea of a minimum slope necessary to move a given bedload has been elaborated on by other authors (Change, 1980; Yang and Song, 1979).

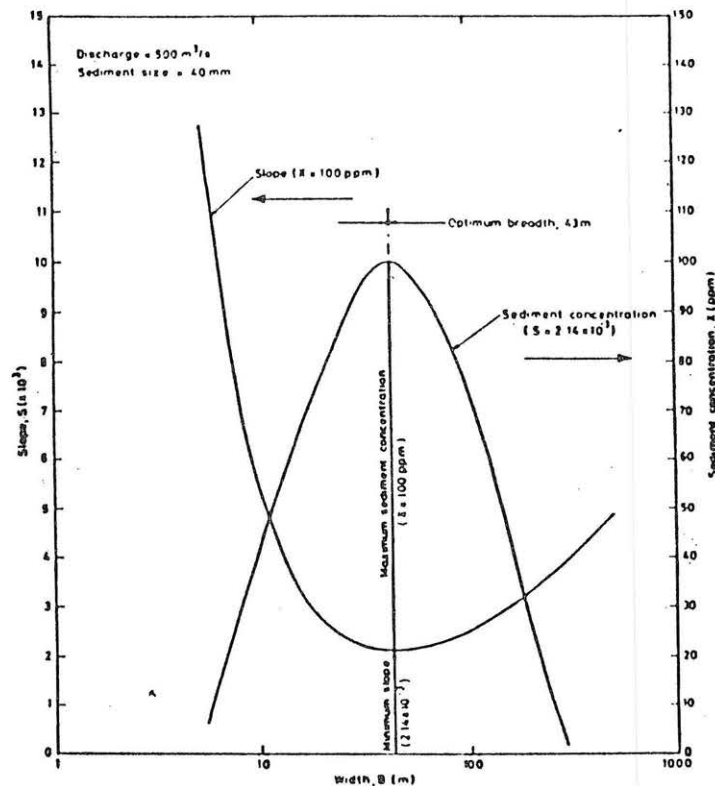


Fig. 1. Plot of model generated values of slope and sediment concentration versus width (White et al., 1982).

In this study, no equation was created to "force" a maximization of bedload transport capacity. From equations which describe sediment transport, resistance, and continuity only, a family of values was calculated, and only one set corresponded to a maximum transport rate. The value of this analysis depends heavily on the sediment transport and friction equations. The authors state that these equations have been tested and agree well with values obtained from sand and gravel bed channels. However, they were developed and calibrated using rectangular flume data, with no width adjustments occurring. No final equation relating width and sediment transport was given. Presumably an iterative computer analysis would need to be run for each set of variables.

Carson and Griffiths (1987) approached the problem of an optimum channel width in a slightly different way. After reviewing several of the above studies, they concluded that a maximum transport capacity (MTC) channel does exist. Given a fixed discharge, slope,  $d_{50}$ , and Manning's "n" roughness coefficient, they solved for bedload transport, width, and depth.

The equations used by Carson and Griffiths are much simpler than those proposed by White et al (1982). Their bedload transport formula is an equation based on excess Shields stress:

$$Q_s = B q_s = k B (M_s - E_c)^m = k B (H - H_c)^m j^m \dots \dots \dots (19)$$

where  $k$  is a constant of proportionality,  $M_s$  is the channel Shields stress,  $E_c$  is the critical Shields stress necessary to initiate motion, and  $m$  is an exponent. This equation was rewritten in terms of critical depth ( $H_c$ ), since all other terms in the Shield's parameter are considered constant ( $= j$ ).

To eliminate the depth term, so that  $Q_s$  can be determined as a function of width only, an equation which is a combination of continuity and resistance was developed:

$$V = (1/n) H^{4/3} S^{1/2} = Q / H B \dots \dots \dots (20)$$

$$B H^c = n Q / S^{1/2} = z \dots \dots \dots (21)$$

For Manning's equation,  $c$  is equal to 1.67. For this problem, since  $Q$ ,  $n$  and  $S$  are given,  $z$  is a constant, and thus critical depth can be replaced by width in the first equation.

In order to find the MTC channel, White et al (1982) found a family of solutions, one of which represented maximum bedload transport for that channel. However, Carson and Griffiths took the first derivative of  $Q_s$  with respect to  $B$  and set it equal to zero to find this maximum. This condition exists when:

$$H = c H_c / (c - m) \dots \dots \dots (22)$$

With three equations and three unknowns, solving for the MTC channel width gave:

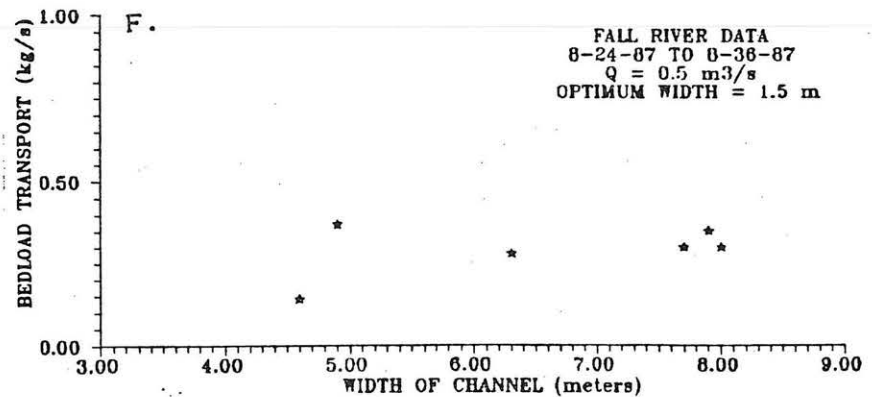
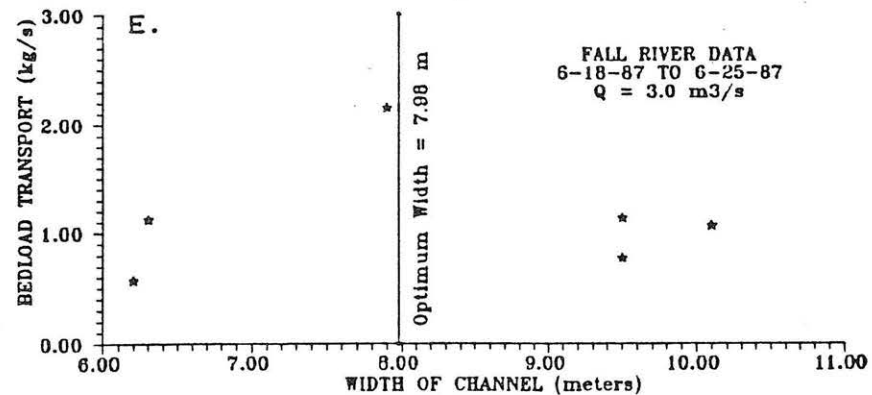
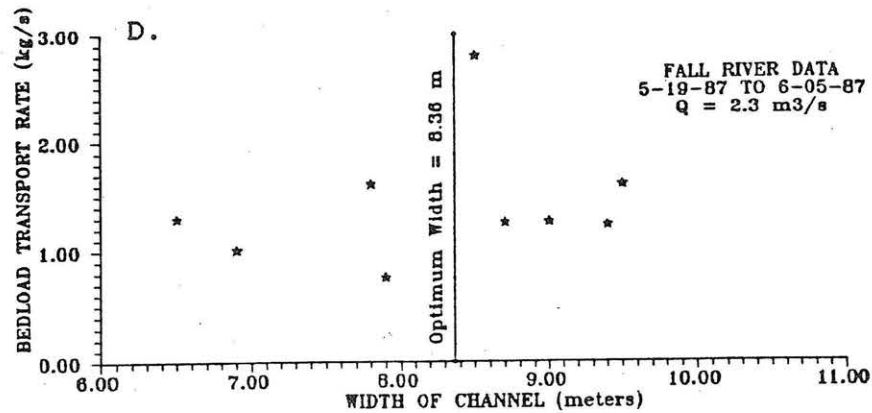
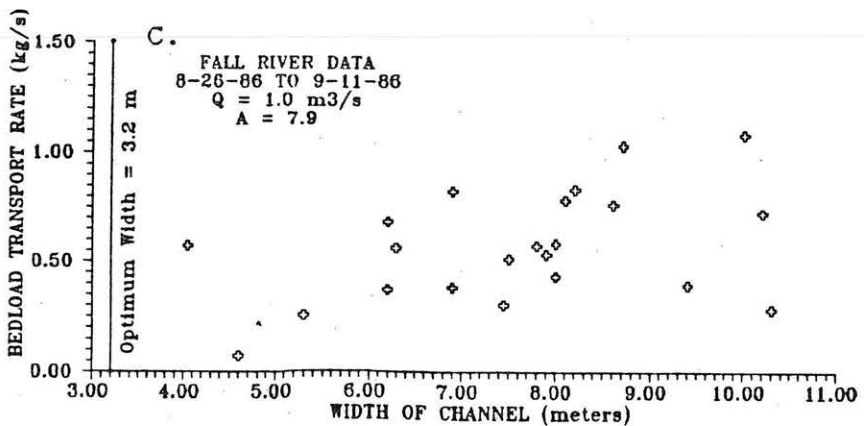
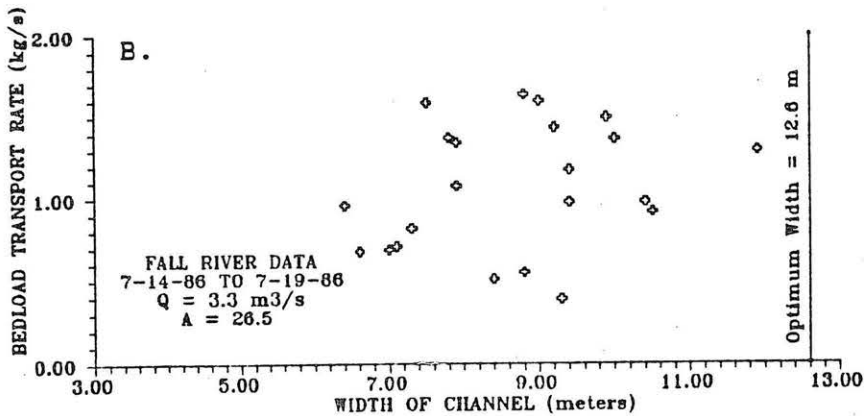
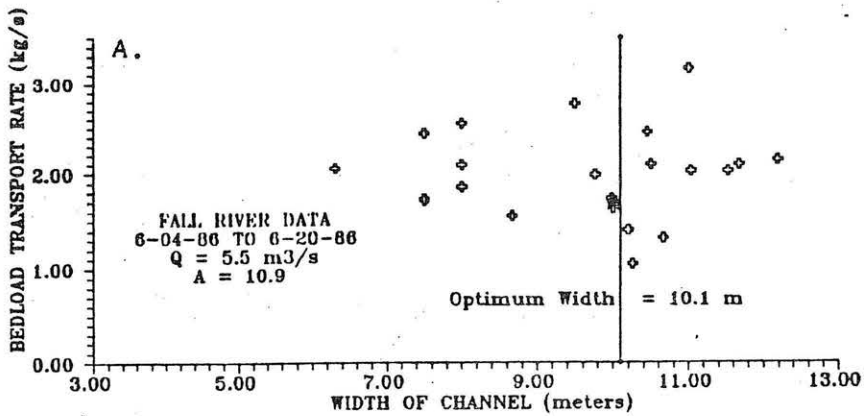
$$B = z (j (c-m) / c E_c)^{1/m} \dots \dots \dots (23)$$

The values of  $z$  and  $j$ , defined above, are fixed for constant  $S$ ,  $Q$ ,  $n$ , and  $d_{50}$ . Assuming  $c$  is 1.67 (Manning's equation) and  $m$  is 1.5, the following expression for an optimum width/depth ratio ( $A$ ) was developed. Note that the coefficient  $k$  has dropped out.

$$A = (2.24 \times 10^{-3} Q n S^{2.17}) / (E_c (G_s - 1) d_{50})^{2.67} \dots (24)$$

$G_s$  is the specific gravity of the sediment, and all other terms are defined above. Note that this equation shows the same relationship between optimum width/depth ratio, discharge, slope and grain size as Gilbert (1914) described. This analysis to obtain the optimum width depth ratio was done without considering the effects of channel sidewalls. A somewhat more complex

Fig 2. Bedload transport rate versus width for 1986 and 1987 field data.



spread and makes the 1987 values more accurate. Of these 1987 graphs, the first two appear to show maxima at about 8 to 8.5 m.

The addition of a value for the optimum width, calculated using the method of Carson and Griffiths (1987) helps to clarify these graphs. Figs. 2 a. and b. have optimums which are near the limits of the widths shown in the data set. Figs. 2 d. and e. show optimums which are near those indicated by the data. However, Figs. 2 c. and f. show optimum widths which are ridiculously narrow for the channel, and will be discussed later.

Table I shows values for width and depth calculated using Parker's equations. Only straight channel sections were used. Values for depth calculated using only discharge and width show good agreement with the data. However, when sediment transport is used to predict width, the values become ridiculous, differing from the real values by five orders of magnitude.

TABLE I. DATA COMPARISON WITH PARKER'S EQUATIONS

CROSS SECTION	GRAIN SIZE	DISCHARGE	ACTUAL DEPTH	PREDICTED DEPTH	ACTUAL WIDTH	PREDICTED WIDTH
	mm	m <sup>3</sup> /s	m	m	m	m
1B	1.5	5.35	0.85	0.79	10.1	3.8x10 <sup>5</sup>
13B	1.5	4.80	0.99	1.06	6.4	6.2x10 <sup>5</sup>
22B	1.5	6.05	1.03	1.06	8.0	8.1x10 <sup>5</sup>
1D	1.0	2.56	0.44	0.48	10.1	7.7x10 <sup>5</sup>
13D	1.0	3.18	0.66	0.83	6.4	4.7x10 <sup>5</sup>
22D	1.0	3.99	0.74	0.83	8.0	2.5x10 <sup>5</sup>

Finally, Carson and Griffiths (1987) optimum width/depth ratio "A" is calculated at various discharges (Table II). At high flows, good agreement exists between the data and A with no bank effects. However, at low discharges, this value is too small, and the value with bank effects is much closer to the real ratio. This same effect can be seen in Figs. 2 c. and f., at low flows. The value calculated for B on these graphs has no bank effects, and should be larger. This is a curious result, since at low flows, width depth ratios are large, (where bank effects should be negligible), and at bankfull discharges, ratios are smaller, and bank effects should be more pronounced. However, Carson and Griffiths note that the equations converge when the bottom shear stress in the channel is ten times the critical Shield's stress. At bankfull discharges in Fall River, the shear stress is about 12 N/m<sup>2</sup>, while the critical value is 1.2 N/m<sup>2</sup>. At low discharge, the average is 2 to 3 N/m<sup>2</sup>, while the critical value is 0.8 N/m<sup>2</sup>.

TABLE II. MTC CHANNEL WIDTH-DEPTH RATIO

CROSS SECTION	DISCHARGE m <sup>3</sup> /s	MANNING'S "n"	D50 mm	"A"	"A"	"A"
				ACTUAL	NO BANK	BANK
1B	5.35	0.053	1.5	12.2	11.9	40
13B	4.80	0.047	1.5	6.4	8.8	35
22B	6.19	0.048	1.5	7.9	11.6	41
1D	2.56	0.037	1.0	22.8	10.9	39
13D	3.18	0.038	1.0	9.7	14.0	44
22D	3.99	0.044	1.0	10.8	20.3	55
13A	2.47	0.037	1.2	11.1	11.4	41
22A	2.82	0.046	1.2	12.9	16.3	48
1E	1.01	0.031	1.0	45.2	6.9	32
13E	1.05	0.033	1.0	19.4	7.5	33
22E	0.64	0.029	0.7	41.6	9.4	37

## SUMMARY AND CONCLUSIONS

An examination of the investigations into the connection between channel width and bedload transport capacity shows a distinct break between the "old" and "new" methodologies. Older studies looked at broad trends, and their findings were often not quantified. Empirical equations were the only ones produced.

In contrast, the newer approach tends to see the width and transport capacity adjustments in the broader context of overall channel adjustment to changing upstream controls (discharge, sediment supply, and sediment caliber). This second group builds models, which are partly based on well known and accepted hydraulic "laws". However, as Ferguson (1986) has pointed out, these laws are not sufficient to predict all the unknowns, and so other principles are necessary. All models require some form of sediment transport equation, and no sediment transport equation is "right", with most based on some empirical calibration. The final relationship is one where most studies diverge, and the categories have already been enumerated. In the final analysis it can be seen that these models are also based to a greater or lesser extent on empirically derived or calibrated equations.

In comparing old and new approaches it is surprisingly evident that they can not be differentiated by ultimate conclusions. Each of the three possible relationships between bedload transport and width has both old and new proponents, and what the new models have is predictive capability only. The direction of change has not been agreed upon, but the amount of change can be predicted to several significant digits.

Carson and Griffith (1987) claim that what is missing in many models is the threshold value for the initiation of motion, and that this threshold value, if included, would show that an MTC channel exists. Their straightforward derivation, based as it is on the well entrenched idea of threshold Shields stress, has indeed shown this. Abou-Seida and Saleh (1987) have disregarded the threshold value by only using the straight line portion of the Einstein-Brown graph. Parker (1979), in contrast, requires that straight gravel channels are just above the shear stress threshold value. These explicit or implicit assumptions may be what put these studies on either side of the optimum channel width graph, seeing only increasing or decreasing trends.

However, it would seem that the trend they see should be reversed. Parker (1979) supports a direct relationship, while his channels are just above threshold, where small decreases in width would cause major increases in unit transport rate. Abou-Seida and Saleh (1987) are using the portion of the Einstein graph where unit transport rates are high, and small increases in width should increase overall bedload transport. However, their model is calibrated with data from relatively fine grained systems, most with  $d_{50}$  smaller than medium sand, and they constrain their P/R ratio to between 12 and 30. In contrast Parker's model is based on gravel transport, and calibrated with data from large rivers.

In conclusion:

- (1) There is no consensus in the literature concerning the relationship between width and bedload transport capacity, given that other factors such as discharge remain constant.
- (2) The fact that an optimum width exists for maximum sediment

transport appears correct, from a number of different approaches, including iterative computer analysis, and the assumption of threshold conditions.

(3) Models which show a consistent trend relating the two variables may have ignored threshold values, or they may be calibrated for usage on narrow ranges of stream variables.

(4) Field data for a small meandering stream shows good correlation with the idea of an optimum channel width as presented by Carson and Griffiths.

#### APPENDIX-REFERENCES

- Abou-Seida, M.M., and M. Saleh, 1987. Design of stable alluvial channels. Jour. of Hydral. Res., v. 25, n.4. pp. 433-446.
- Bagnold, R.A., 1977. Bedload transport by natural rivers, Water Resources Res., v. 13, n. 2, pp. 303-312.
- Carson, M.A. and G.A. Griffiths, 1987. Influence of channel width on bedload transport capacity, J. Hydr. Div., ASCE v. 113, n. 12, pp. 1489-1509.
- Chang, H.H., 1980. Stable alluvial channel design. J. Hydr. Div., ASCE, v. 106, HY5, pp. 873-891.
- Ferguson, R.I., 1986. Hydraulics and hydraulic geometry. Progress in Physical Geography, v. 10, n.1, pp 1-31.
- Gilbert, G.K., 1914. The transport of debris by running water. USGS Professional Paper 86.
- Griffiths, G.A., 1984. Extremal hypotheses for river regime: an illusion of progress. Water Resources Res., v.20, n. 1, pp 113-118.
- Henderson, F.M., 1966. Open Channel Flow, Macmillan Publishing Co., New York, N.Y.
- Julien, P.Y. and D.B. Simons, 1984. Analysis of Hydraulic geometry relationships in Alluvial Channels, Rept. CER83-84 PYJ-DBS45. Colorado State University, Ft. Collins, Co. 47 p.
- Lacey, G., 1929. Stable channels in alluvium. Proc. Inst. Civ. Engrs., v. 229, pp 259-292.
- Lane, E.W., 1955. The importance of fluvial morphology in hydraulic engineering. ASCE Proc., v. 81, n. 745, 17p.
- Leopold, L.B., and T. Maddock, Jr., 1953. The hydraulic geometry of stream channel and some physiographic implications. USGS Prof. Paper 242, 57 p.
- Parker, G., 1979. Hydraulic geometry of active gravel rivers. J. Hydr. Div., ASCE, v. 105, n.9, pp 1185-1201.
- Peterson, A.W. and R.F. Howells, 1973. A compendium of solids transport data for mobile boundary channels. Rept. HY1973-ST3, Dept. of Civil Engineering, Univ. of Alberta, Edmonton, Canada.
- Schumm, S.A., 1977. The Fluvial System. John Wiley and Sons, New York, N.Y., 338 p.
- White, W.R., R. Betess and E. Paris, 1982. Analytical approach to river regime. J. Hydr. Div, ASCE, v. 108, HY10, pp 1179-1193.



## DESIGN OF STABLE ALLUVIAL CHANNELS

By Jayamurni WARGADALAM

**Abstract :** Chronological development methods of designing stable alluvial channel are presented. Three old formulas (Lacey, Lane, and Simons and Albertson) and three recent formulas (Chang, Hey and Thorne, and Abou Seida and Saleh) are discussed. Favorable comparisons of Lacey, Lane, Hey and Thorne, and Simons and Albertson formulas are made with data from Colorado River ( $d_{50} = 0.33$  mm) and flume data ( $d_{50} = 0.93$  mm and  $d_{50} = 0.19$  mm).

### INTRODUCTION :

The problem of determining a stable, cross section geometry and slope of an alluvial channel has been the subject of considerable research over hundred years, since Chezy proposed his single equation in about 1775 and continues to be of great practical interest. For a channel in an alluvial material the stable conditions are achieved through the adjustment of three factors, channel width, channel depth and channel slope. The three factors, to each of which nature gives definite equilibrium values to suite definite imposed conditions, require three equations. The imposed conditions are the rate of flow and the rate of sediment transport to be carried through the channel.

An excellent definition of stable or regime channel was presented by Lane in 1952 (Simon, 1957) as follows :

"A stable channel is an unlined earth canal for carrying water, the banks and bed of which are not scoured by the moving water and in which objectionable deposits of sediment do not occur."

There are two main theories of stable channel design: the regime theory and the analytical theory. The regime theory is an empirical theory which relies on available data and attempts to determine appropriate relationships from the data. The usefulness of this theory depends on the quality of the data

and the validity of the assumed form of the relationships. The analytical theory relies on specifying equations which describe the dominant individual processes such as sediment transport, flow resistance, and bank stability. This approach can only be successful if the dominant processes are correctly identified and appropriate equations exist to describe them adequately. Recently, there are some new analytical approaches introduced by involving the modern concepts of fluid mechanics and sediment transport.

This paper is concerned with the chronological development of stable channel design. Some selected design procedures are discussed. By using the data from Colorado River;  $d_{50} = 0.33\text{mm}$  and flume data;  $d_{50} = 0.93\text{ mm}$  and  $d_{50} = 0.19\text{ mm}$  (Haynie 1964), Wetted perimeter, hydraulic radius and bed slope are computed with Lacéy, Lane and Hey and Thorne formulas. The results are plotted on the curves developed by Simons and Albertson as comparisons.

#### REVIEW OF LITERATURE :

The design of stable channels in alluvial materials has been a subject to study and research by many investigators in the past. Several factors are interrelated and serve to make the subject much more complicated than a superficial examination would indicate.

Base on approaches used by investigators, the method for designing stable channel can be distinguished into four methods as follows :

1. Permissible Velocities Method
  2. Tractive Force Method
- Both methods used analytical approach.
3. Regime Theory
  4. Sediment Transport - Computer modelling.

### Tractive Force :

In 1937 Lane presented the paper which might be considered the first attempt at a deductive, rational solution of the stable channel in easily scoured materials should have high bed-width to depth ratios.

Lane, 1955 presented a method of designing stable channel which was based on securing a distribution of the tractive force along the sides and bottom of the channel. It was found that maximum shear on the bed was approximately equal to  $\gamma DS$  and on the sides it was about 0.76 of  $\gamma DS$ , see figure 1. The effect of side slopes was treated as a factor,  $K$ , which is the ratio of the tractive force required to start motion on the sloping side to that force required.

$$K = \cos \phi \sqrt{1 - \frac{\tan^2 \phi}{\tan^2 \theta}}$$

where

$\phi$  = the angle of the side slope of the canal

$\theta$  = the angle of repose of the material. (fig. 4)

The permissible shear stress on the side slope is,

$$\tau_{ss} = K \times \tau_c$$

$\tau_c$  is critical shear stress given on fig. 2 or computed from Shields parameter :

$$\frac{\tau_c}{(\gamma_s - \gamma_w) ds} = 0.047 \text{ (Meyer - Peter and Muller, 1948)}$$

### Regime Theory :

This theory was introduced by Kennedy in 1895 based on his observations of stable canal in the Pubyab and then it was continued by Lindley in 1919.

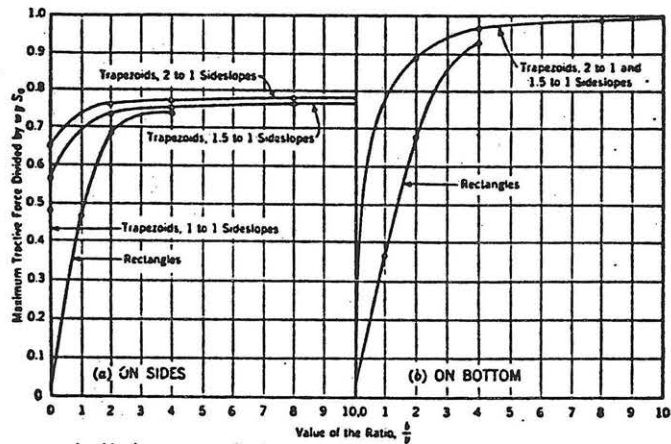
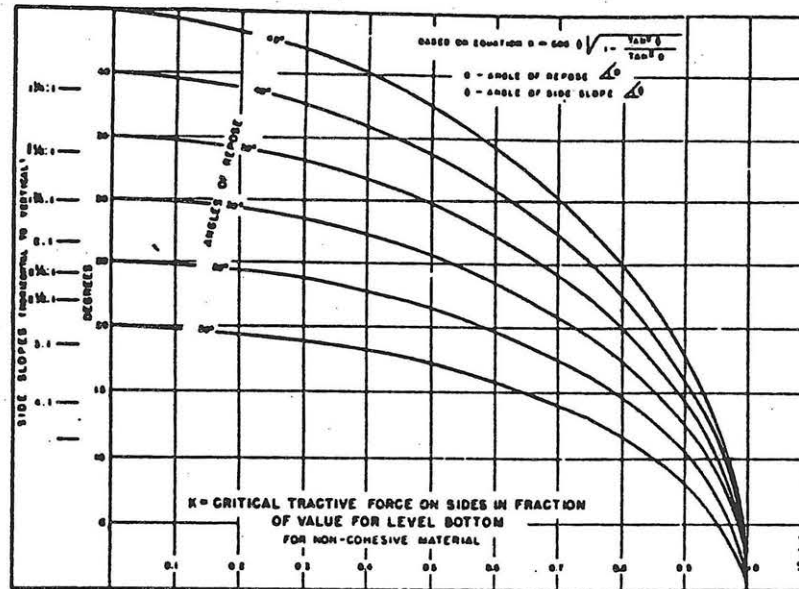


FIG. 1.—MAXIMUM TRACTIVE FORCES IN A CHANNEL



- K = Critical tractive force on sides in fraction of value for level bottom for non-cohesive material. Acc. to Lane (1953)

FIG. 3

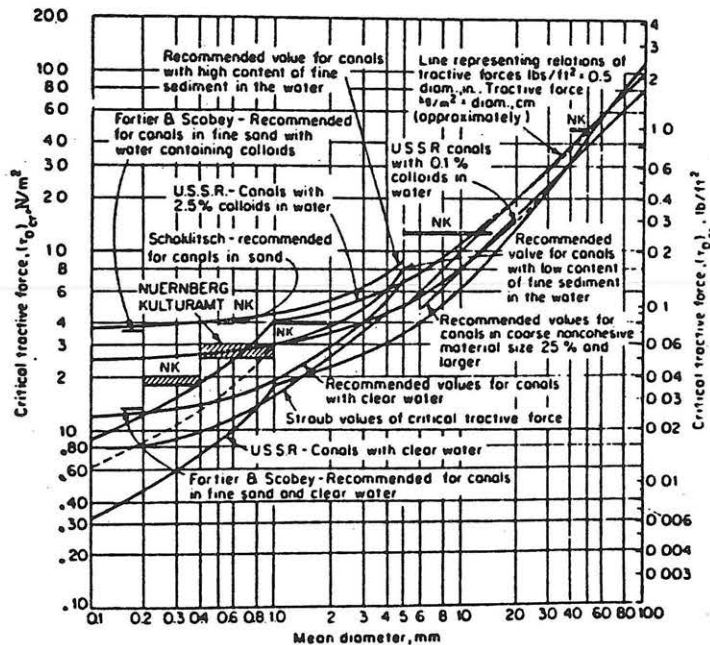
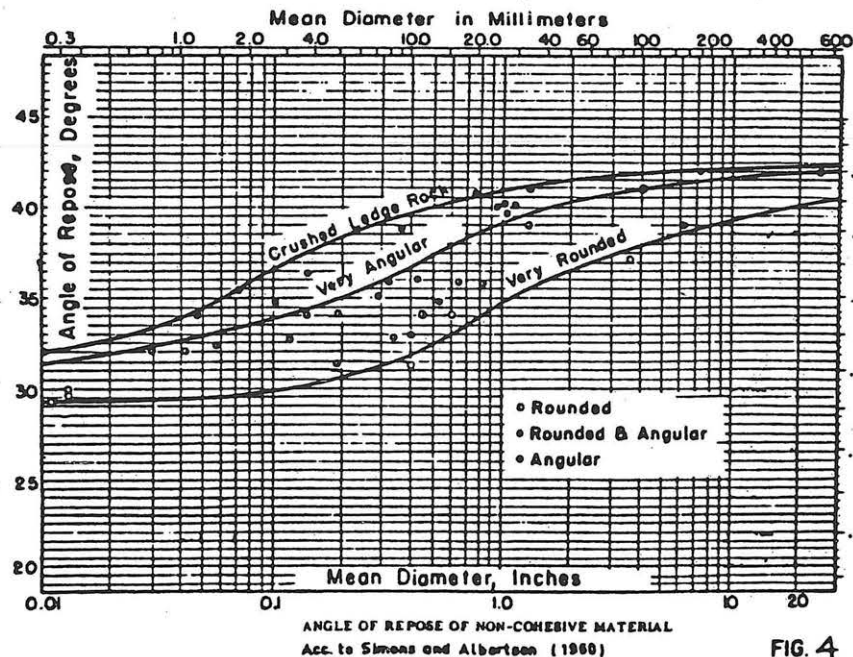


Fig. 2 Critical shear stress as function of grain diameter. [After LANE (1953).]



ANGLE OF REPOSE OF NON-COHESSIVE MATERIAL Acc. to Simons and Albertson (1960)

FIG. 4

In 1930, G. Lacey introduced one of the more important contributions to the design of regime canals. Lacey substituted the hydraulic radius (R) for the depth (D), and the wetted perimeter (P) for the width (W). He also introduced the silt factor (f).

Lacey initial equations were,

$$V = 1.17 (Rf)^{1/2}$$

$$Af^2 = 3.8 V^5$$

$$P = 2.668 Q^{1/2}$$

Later, he modified the first equation become

$$V = 1.155 (Rf)^{1/2}$$

Lacey also arrived at the equation

$$V = \frac{1.3458}{Na} R^{3/4} S^{1/2}$$

where  $Na = 0.0225 f^{1/4}$  = a coefficient of absolute rugosity

$$f = 1.59 d_{50}^{1/2}$$
 = silt factor

Above equations can be restated in term of discharge as follows:

$$P = 2.668 Q^{1/2}$$

$$R = 0.4725 (Q/f)^{1/3}$$

$$A = 1.26 Q^{5/6} / f^{1/3}$$

$$S = 0.00055 f^{5/3} / Q^{1/6}$$

Simons and Albertson, 1963, have analysed a large number of Indian and American Canal. The results presented are valid for sediment concentrations 500 p.p.m and Froude number 0.3. The result of their studies are presented in some curves that can be used for designing of stable channels.

In 1986, Hey and Thorne introduced a regime type equations for mobile gravel-bed rivers based on the data obtained from 62 stable gravel bed river in the United Kingdom. They provided some equations that not only can be used for designing a straight channel, but also can be used for designing of meandering mobile gravel bed channels or for the design of channel with a pool riffle bed topography. The effect of vegetation on the bank is also considered in their equations.

Their practical design equations are as follows :

Mean depth,  $D = 0.22 Q_b^{0.37} D_{50}^{-11}$  , m, Vegetation types I - IV.

Maximum depth,  $D_m = 0.20 Q_b^{0.36} D_{50}^{-0.56} D_{84}^{0.35}$  ; m, vegetation types I-IV

Slope,  $S = 0.087 Q_b^{-0.43} D_{50}^{-0.09} D_{84}^{0.84} Q_s^{0.10}$  ; vegetation types I - IV

Wetted perimeter, P :

$P = 4.53 Q_b^{0.49} Q_s^{-0.1}$  ; m, vegetation type I

$P = 3.65 Q_b^{0.49} Q_s^{-0.1}$  vegetation type II

$P = 3.02 Q_b^{0.49} Q_s^{-0.1}$  vegetation type III

$P = 2.65 Q_b^{0.49} Q_s^{-0.1}$  vegetation type IV

Hydraulic Radius, R :

$R = 0.15 Q_b^{0.41} Q_s^{-0.02} d_{50}^{-0.14}$  ; m vegetation type I

$R = 0.16 Q_b^{0.41} Q_s^{-0.02} d^{-0.14}$  vegetation type II & III

$R = 0.17 Q_b^{0.41} Q_s^{-0.02} d^{-0.14}$  vegetation type IV

Width, B :

$B = 3.67 Q_b^{0.45}$  ; m general equation

$B = 4.33 Q_b^{0.50}$  vegetation type I

$B = 3.33 Q_b^{0.50}$  vegetation type II

$B = 2.73 Q_b^{0.50}$  vegetation type III

$B = 2.34 Q_b^{0.50}$  vegetation type IV

Velocity, V :

$V = 1.70 Q_b^{0.10} Q_s^{0.03} d_{50}^{0.18}$  ; m, vegetation type I

$V = 2.02 Q_b^{0.10} Q_s^{0.03} d_{50}^{0.18}$  vegetation type II

$V = 2.14 Q_b^{0.10} Q_s^{0.03} d_{50}^{0.18}$  vegetation type III

$V = 2.54 Q_b^{0.10} Q_s^{0.03} d_{50}^{0.18}$  vegetation type IV

Notes :

Vegetation type I : grassy bank with no trees or shrubs

II : 1-5% tree/shrub cover

III : 5-50% tree/shrub cover

IV : greater than 50% shrub cover or  
incised into flood plain.

Meander arc length or riffle spacing, Z :

$Z = 6.31 W, m$  vegetation type I - IV

Sinuosity,  $p = \frac{S_v}{S}$  vegetation type I - IV  
 $S_v =$  valley axis slope.

Riffle width,  $R_w = 1.034$

Riffle mean depth,  $R_d = 0.951 D$

Riffle maximum depth,  $R_{dm} = 0.912 D_m$ .

## Sediment Transport Formula - Computer Modelling :

In 1980, Chang proposed his formula for designing stable alluvial canal. He says that the equilibrium condition for the regime channel, as well as graded streams treated by geologist, may be conceptually considered as the condition of minimum stream power ( $\gamma QS$ ) for an alluvial channel. His definition for the hypothesis of minimum stream power,

"For an alluvial channel, the necessary and sufficient condition for equilibrium is when the stream power is a minimum subject to given constraints. Hence, an alluvial channel with given water discharge and sediment inflow tends to establish its width, depth and slope such that the stream power or slope is a minimum."

In his formula, he uses Manning equation for flow resistance and three sediment transport formula, Du Boys, Einstein - Brown and Engelund- Hansen. He found that except in the flow region of low shear stress, the Engelund-Hansen sediment formula gives better result than Einstein-Brown formula. Both the Engelund-Hansen formula and Einstein-Brown formula are inadequate for flow in the low shear stress region. However, the Du Boys are found adequate for canals with low shear stress corresponding to incipient sediment movement. Fig. 13 shows the flow diagram of computational procedure of designing stable channel.

Abou-Seida and Saleh, 1987 developed computer programs for designing stable alluvial channels. They used Liu-Hwang resistance equation and Einstein-Brown sediment transport concept. They make limitation conditions for the design of canals in equilibrium that,

$$\text{Stream power} < \text{Critical power}$$

The model was verified using field data from Pakistan, India, UNited States, New Mexico and Egypt.

Fig. 14 and 15 show the flow chart of program of computational procedure.



The values of Ca, X and Y are from fig. 16 a, b and c or from equations:

$$C_{\text{ripple}} = 22.30 + 26.44L - 84.9L^2 - 165L^3 \quad \text{for } d_{50} \geq 0.45 \text{ mm}$$

$$C_{\text{ripple}} = 11.05 + 3.75L - 0.15L^2 \quad \text{for } d_{50} < 0.45 \text{ mm}$$

$$C_{\text{dune}} = 13.88 + 15.62L + 8.84L^2$$

$$x = 0.64 + 0.1305L - 0.49L^2 + 0.7716L^3 \quad \text{for } d_{50} \geq 0.35 \text{ mm}$$

$$x = 0.6113 + 0.387L + 0.2027L^2 + 0.0371L^3 \quad \text{for } d_{50} < 0.35 \text{ mm}$$

$$y = 0.362 + 0.1219L + 0.0577L^2$$

in which

$$L = \log(d_{50})$$

The value of F (settling velocity) can be computed with equation:

$$F = \sqrt{\frac{2}{3} + \frac{36\nu^2}{gds^3(\gamma_s/\gamma - 1)}} - \sqrt{\frac{36\nu^2}{gds^3(\gamma_s/\gamma - 1)}}$$

ds = bed material size

$\gamma_s$  and  $\gamma$  = specific weight of the bed particles and water

$\nu$  = Kinematic viscosity.

The equations are used for finding the velocity and the slope as follows :

$$V = 0.046[C_d]^{3.30} \left[ \frac{d_s^{1.8} q_s}{F q} \right]^{3.30-y} [R]^{3.3(\alpha-y)+y}$$

where

V = velocity in m/s

$d_{50}$  = median grain size in mm

$q_s/q$  = sediment concentration in p.p.m.

R = hydraulic radius in meters

$$Q = 10^{-10.22} [C_d]^{3.30} \left[ \frac{d_s^{1.8} q_s}{F q} \right]^{2.3-x} [S]^{3.3(y-x)-3.3} P$$

where

Q = water discharge in m<sup>3</sup>/s

S = channel slope

P = wetter perimeter in meter

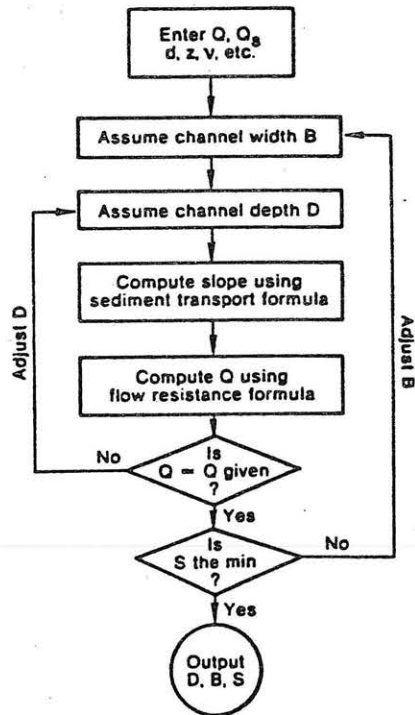


FIG. 13—Flow Diagram Showing Major Steps of Computation

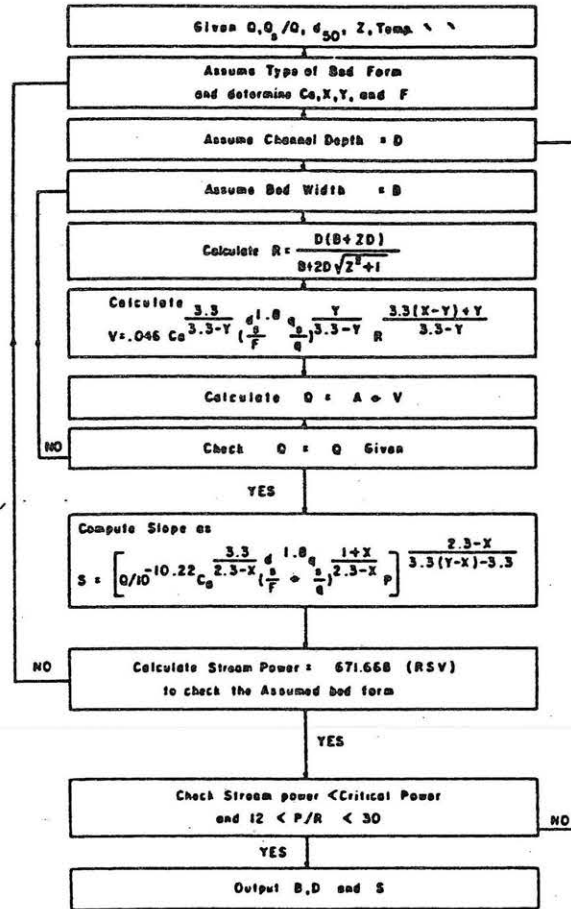


Fig. 14, Flow chart of program A.  
Organigramme du programme A.

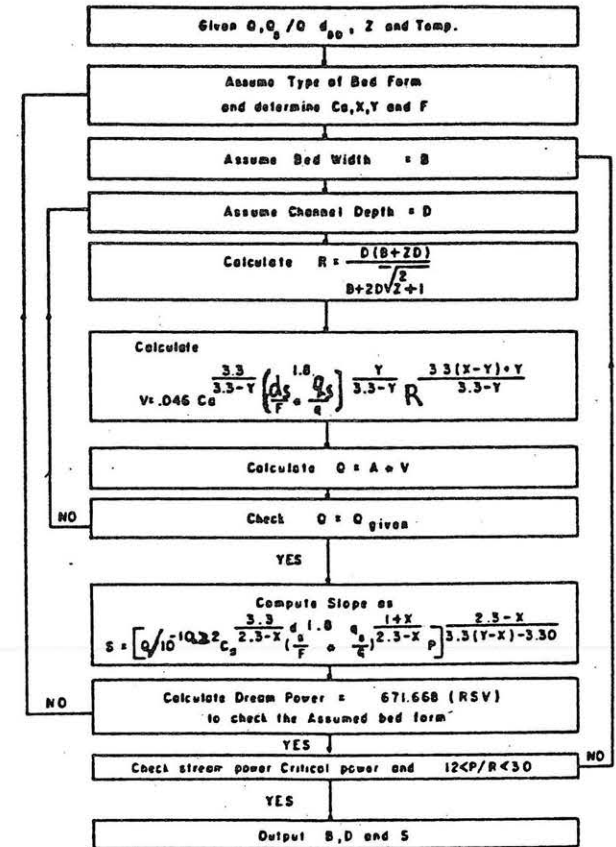


Fig. 15 Flow chart of program B.  
Organigramme du programme B.

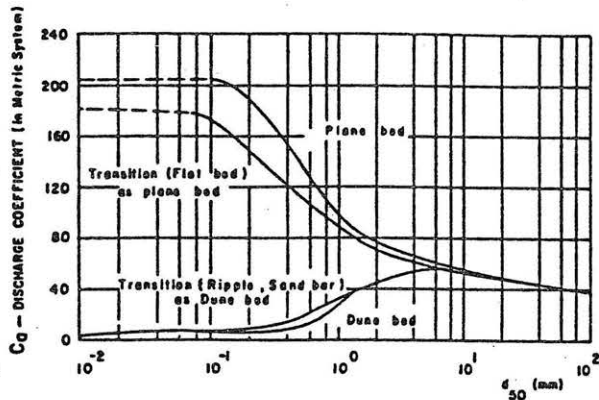


Fig. 16<sup>a</sup>  $C_q$  as a function of  $d_{50}$  and bed forms (after Liu and Hwang, 1958).

Tracé de  $C_q$  en fonction du  $d_{50}$  pour diverses formes de lit (d'après Liu et Hwang, 1958).

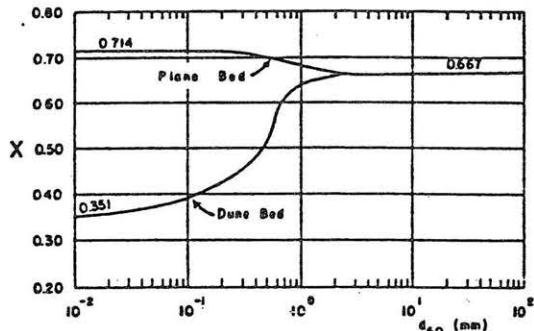


Fig. 16<sup>b</sup> Variation of  $X$  with  $d_{50}$  (after Liu and Hwang, 1958).

Variation de  $X$  en fonction du  $d_{50}$  (d'après Liu et Hwang, 1958).

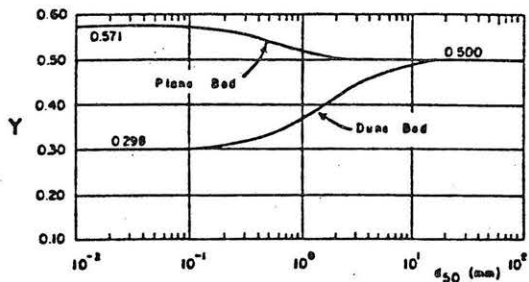


Fig. 16<sup>c</sup> Variation of  $Y$  with  $d_{50}$  (after Liu and Hwang, 1958).

Variation de  $Y$  en fonction du  $d_{50}$  (d'après Liu et Hwang, 1958).

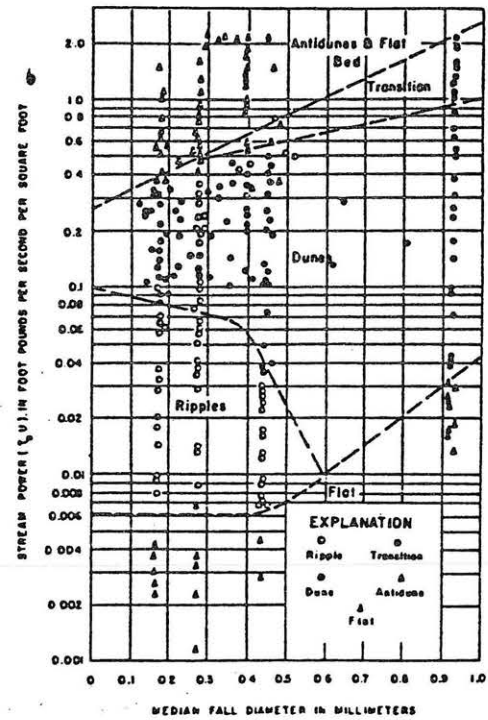


Fig. 17

Relation of bed form to stream power and medium fall diameter (after Simons and Richardson, 1966).

Diagramme donnant les formes de lit en fonction de la puissance érosive et du diamètre de chute moyen (d'après Simons et Richardson, 1966).

Fig. 17 is used for checking the bed form  
 The stream power is checked with equations,

where  $\text{stream power} < 10^N$   $\leftarrow$  critical power  
 $\text{stream power (in ft lb/ft}^3) = 671.668(RSV)$

in which

$R$  = hydraulic radius in m  
 $S$  = non-dimensional slope  
 $V$  = velocity in m/s

$$N = 0.87d_{50} - 0.56 \quad \text{for } d_{50} \leq 0.3 \text{ mm}$$

$$N = 0.424d_{50} - 0.427 \quad \text{for } d_{50} > 0.3 \text{ mm}$$

#### COMPUTATION :

By using the data from Colorado River ( $d_{50} = 0.33$  mm) and flume data ( $d_{50} = 0.93$  mm and  $d_{50} = 0.19$  mm), have computed the values of wetted perimeter ( $P$ ), hydraulic radius ( $R$ ), wetted area ( $A$ ) and slope ( $S$ ). Three formulas were used in this computation, Lacey, Lane and Hey and Thorne. The results are plotted on the curves derived by Simons and Albertson as a comparison, fig. 18, 19, 20 and 21.

Sediment transport formulas (Chang and Abou-Seida and Saleh) were not included in computation because they are more complicated and need computer programs.

#### RESULTS :

1. Fig. 18 shows the relation between wetted perimeter  $P$  and discharge  $Q$ . Lacey and Hey and Thorne formulas give the same results as Simons and Albertson formula type B (sandbed and cohesive banks). This result indicates that Hey and Thorne formula not only can be used for gravel material, but also can be used for fine sand. For small discharge ( $< 100$  cfs), Lane formula give the same result as Simons and Albertson type B. For big discharge, it has the same slope as Simons & Albertson but smaller coefficient.

2. Fig. 19 shows the relation between hydraulic radius  $R$  and discharge  $Q$ . For big discharge, Hey and Thorne formula does not fit Simons and Albertson formula but for small discharge it fits Simons and Albertson formula. Lacey formula is similar with Simons and Albertson formula. For big discharge, Lane formula fits Simons and Albertson formula type B but for small discharge it is far from Simons and Albertson formula.
3. Fig. 20 shows the relation between wetted area  $A$  and discharge  $Q$ . Almost all formulas have the same results except Lane formula for small discharge that has smaller coefficient.
4. Fig. 21 shows relation between average velocity  $V$  and  $R^2S$ .  
 For  $R^2S > 0.001$  ; Lacey, Lane and Hey and Thorne results are around the data collected by Simons.  
 For  $R^2S < 0.001$  ; Lane results computed by using flume data are far from Simons data.

#### CONCLUSIONS :

1. Regime theory is more appropriate to use in designing stable alluvial channel than tractive force theory. It was developed by using many data such as India, Pakistan, U.S.A. and United Kingdom. Using flume data also gives a good result in computation.
2. Lacey, Hey and Thorne and Simons and Albertson formulas have almost the same result in designing stable channel.
3. Hey and Thorne formula can be used in more general condition from fine bed material up to gravel. This formula involves more parameters in its equations such as material size, sediment discharge rate and vegetation.
4. Lane formula gives different result from other formulas especially if flume data are used in computation.

▲ Lacey;  $d_{50} = .33$  mm    × Lane;  $d_{50} = .33$  mm    □ Hey&Thorne;  $d_{50} = .33$  mm  
 ▲ Lacey;  $d_{50} = .93$  mm    × Lane;  $d_{50} = .93$  mm    ■ Hey&Thorne;  $d_{50} = .93$  mm  
 ▲ Lacey;  $d_{50} = .19$  mm    × Lane;  $d_{50} = .19$  mm    ■ Hey&Thorne;  $d_{50} = .19$  mm

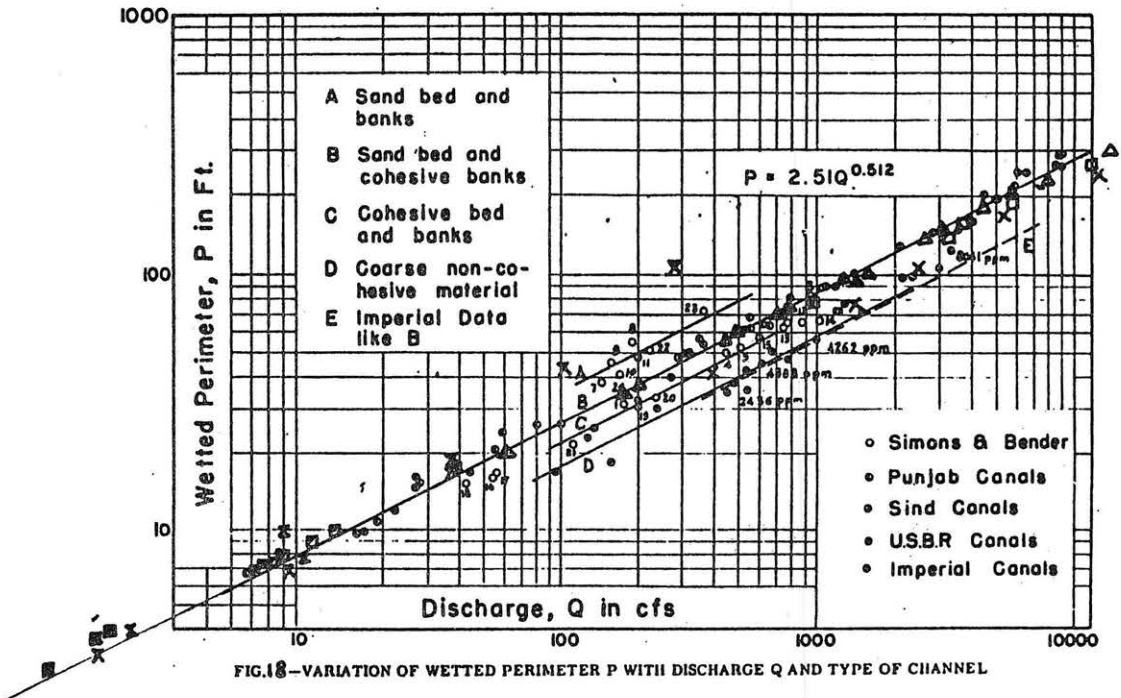


FIG.18—VARIATION OF WETTED PERIMETER P WITH DISCHARGE Q AND TYPE OF CHANNEL

▲ Lacey;  $d_{50} = .33$  mm    × Lane;  $d_{50} = .33$  mm    □ Hey&Thorne;  $d_{50} = .33$  mm  
 ▲ Lacey;  $d_{50} = .93$  mm    × Lane;  $d_{50} = .93$  mm    ■ Hey&Thorne;  $d_{50} = .93$  mm  
 ▲ Lacey;  $d_{50} = .19$  mm    × Lane;  $d_{50} = .19$  mm    ■ Hey&Thorne;  $d_{50} = .19$  mm

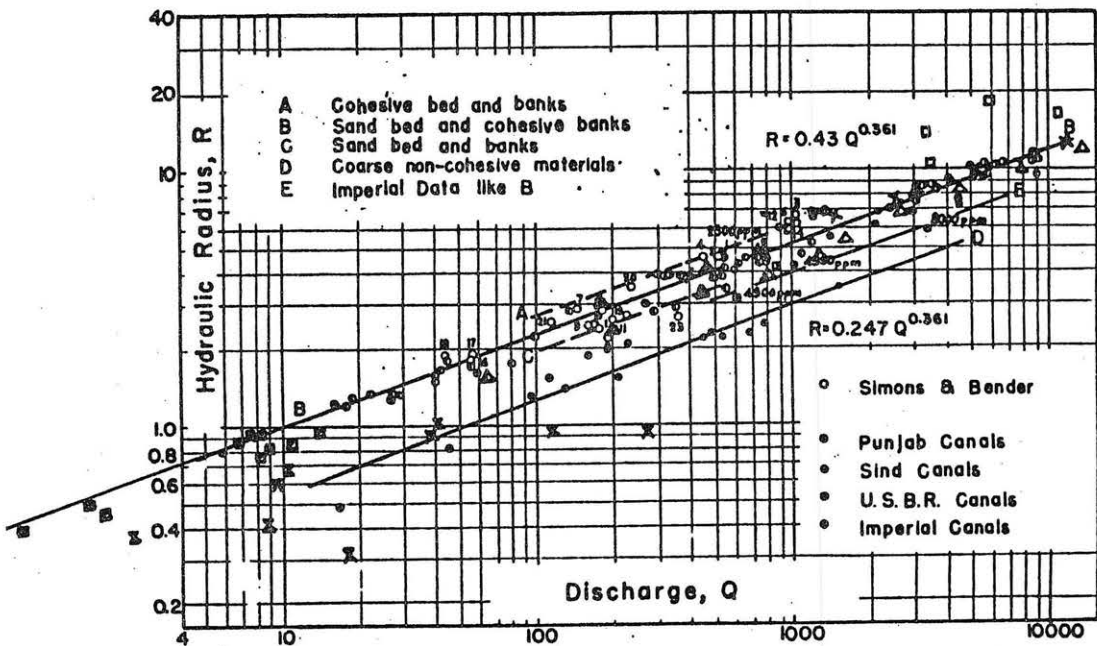


FIG.19—VARIATION OF HYDRAULIC RADIUS R WITH DISCHARGE Q AND TYPE OF CHANNEL, ALL DATA

▲ Lacey;  $d_{50} = .33$  mm    × Lane;  $d_{50} = .33$  mm    □ Hey&Thorne;  $d_{50} = .33$  mm  
 ▲ Lacey;  $d_{50} = .93$  mm    × Lane;  $d_{50} = .93$  mm    □ Hey&Thorne;  $d_{50} = .93$  mm  
 ▲ Lacey;  $d_{50} = .19$  mm    × Lane;  $d_{50} = .19$  mm    □ Hey&Thorne;  $d_{50} = .19$  mm

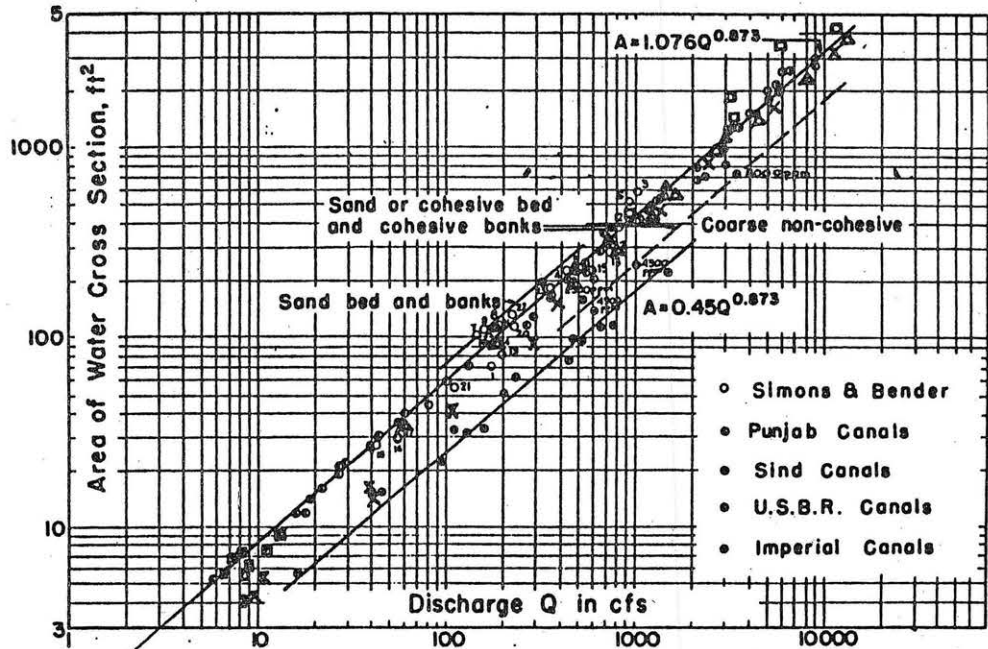


Fig. 26 VARIATION OF AREA OF WATER CROSS SECTION A WITH DISCHARGE Q AND TYPE OF CHANNEL

▲ Lacey;  $d_{50} = .33$  mm    × Lane;  $d_{50} = .33$  mm    □ Hey&Thorne;  $d_{50} = .33$  mm  
 ▲ Lacey;  $d_{50} = .93$  mm    × Lane;  $d_{50} = .93$  mm    □ Hey&Thorne;  $d_{50} = .93$  mm  
 ▲ Lacey;  $d_{50} = .19$  mm    × Lane;  $d_{50} = .19$  mm    □ Hey&Thorne;  $d_{50} = .19$  mm

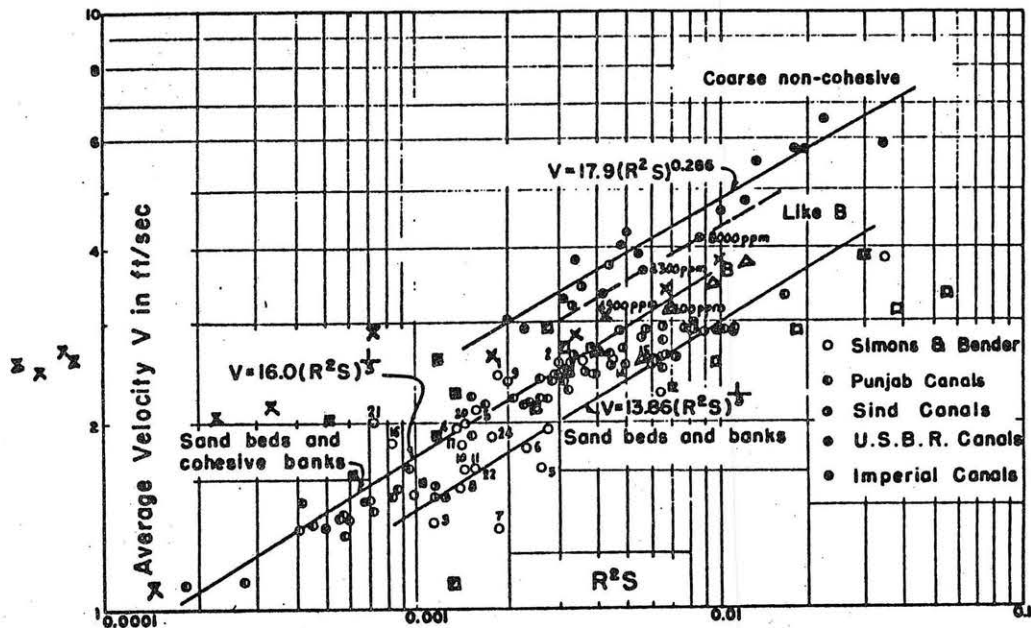


FIG. 26-VARIATION OF AVERAGE VELOCITY V WITH  $R^2S$  AND TYPE OF CHANNEL, ALL DATA

REFERENCES :

1. Abou- Seida, M.M. and Saleh, M., 1987, Design of Stable Alluvial Channels, Journals of Hydraulic Research, Vol. 25, No. 4. pp. 433-446.
2. Breusers, H.N.C., 1981, Lecture Notes on Sediment Transport, International Course in Hydraulic Engineering, Delft.
3. Carson, M.A. and Griffiths G.A., 1987, Influence of Channel Width on Bed Load Transport Capacity, Journal of Hydraulic Engineering, ASCE, Vol.113, No. 12, pp. 1489-1509.
4. Chang, H.H., 1980, Stable Alluvial Canal Design, Journal of the Hydraulics Division, ASCE, Vol. 106, No. 5, pp. 873-891.
5. Chang, H.H., 1986, River Channel Changes: Adjustments of Equilibrium, Journal of Hydraulic Engineering, Vol. 112, No.1, pp. 43-55.
6. Griffiths, G.A., 1981<sup>a</sup>, Stable Channel Design in Gravel-Bed Rivers, Journal of Hydrology, Vol. 52, pp.291-305.
7. Griffiths, G.A., 1981<sup>b</sup>, Flow Resistance in Coarse Gravel Bed Rivers, Journal of Hydraulic Engineering, ASCE, Vol. 107, NO.7, pp.899-918.
8. Griffiths, G.A., 1983, Stable Channel Design in Alluvial Rivers, Journal of Hydrology, Vol. 65, pp. 259-270.
9. Griffiths, G.A., 1984, Extremal Hypotheses for River Regime: An Illusion of Progress, Water Resources Research, Vol. 20, No. 1, pp.113-118.
10. Guo C.Y. and Hughes W.C., 1984, Optimal Channel Cross Section with Freeboard, Journal of Irrigation and Drainage Engineering, Vo. 110, No. 3, pp. 304-314.
11. Haynie, R.M., 1964, Design of Stable Channels in Alluvial Materials, Colorado State University, Ph.D. Dissertation, 100 p.
12. Henderson, F.M., 1963, Stability of Alluvial Channels. Transaction, ASCE, Vol. 128, Part I, No. 3440, pp. 657-720.
13. Hey, R.D. and Thorne, C.R., 1986, Stable Channel with Mobile Gravel Beds, Journal of Hydraulic Engineering, ASCE, Vo. 112, No.8, pp. 671-689.
14. Hey, R.D. and Thorne, C.R., 1988, Stable Channel with Mobile Gravel Beds : Discussions, Journal of Hydraulic Engineering, ASCE, Vol. 114 No. 3, pp. 342-344.
15. Kellerhals, R., 1967, Stable Channels with Gravel-Paved Beds, Journal of the Waterways and Harbors Division, ASCE, Vo.93 pp.63-84.
16. Lane, E.W., 1955, Design of Stable Channels, Transactions, ASCE, Vol. 120, No.2776, pp. 1234-1279.
17. Osman, A.M. and Thorne, C.R., 1988, Riverbank Stability Analysis. I: Theory, Journal of Hydraulic Engineering, ASCE, Vol. 114, No.2, pp. 134-150.
18. Osman, A.M. and Thorne, C.R., 1988, Riverbank Stability Analysis. II: Applications, Journal of Hydraulic Engineering, ASCE, Vol. 114, No.2, pp. 151-172.
19. Simons, D.B., 1957, Theory and Design of Stable Channels in Alluvial Materials, Colorado State University, Ph.D. Dissertation, 394 p.
20. Simons, D.B. and Senturk, F., Sediment Transport Technology, Water Resources Publications, Fort Collins, Colorado, 1977.
21. Simons D.B. and Albertson, M.L., 1963, Uniform Water Conveyance Channels in Alluvial Material, Transactions, ASCE, Vol.128, Part I, No. 3399, pp. 65-167.
22. Simons, D.B., Richardson, E.V. and Julien, P.Y., 1987, Highway in the River environment, U.S. Department of Transportation, Federal Highway Administration.
23. Stevens, M.A. and Nordin, C.F., 1987, Critique of the Regime Theory for Alluvial Channels, Journal of Hydraulic Engineering, ASCE, Vol. 113, No. 11, pp. 1359-1380.
24. Trent, R.E. and Brown, S.A., 1984, An Overview of Factors Affecting River Stability, Transportation Research Record 950, Vol. 2, pp. 156-163.
25. White, W.R., Bettess, R. and Paris, E., 1982, Analytical Approach to River Regime, Journal of Hydraulics Division, ASCE, Vol. 108, No. 10, pp. 1179 - 1193.



## SEDIMENT EXTRACTORS

by Tabassum Zahoor

**Abstract:** Many investigators have performed experiments with the vortex tube ejectors but the early reported results were applicable quantitatively only for field flow conditions similar to the experimental flow conditions. However lately researchers [11, 14] have made an analytical study of the flow inside a vortex tube and developed a design procedure to predict the performance and the design parameters. The method is in the form of design graphs, with worked example. The performance prediction is more complicated, although an approximate method is included.

### INTRODUCTION

One of the major problems faced by Hydraulic engineers concerned with the design of irrigation works and hydroelectric schemes is the control of sediment entering the irrigation and power canals. When an irrigation canal takes off from the headworks, its slope is usually smaller than that of the parent stream, so that water can reach the points above the stream where irrigation is required. If heavy sediment load enters the canal, the canal will be unable to transport the whole load under such small slope and part of the load will be deposited in the canal itself. In order to prevent clogging and costly maintenance operations, it must be removed from the water at the canal intake or transported through the canal system with a minimum of accumulation within the canal prism and structures.

The purpose of this study is to present the various sediment exclusion and ejection techniques available to the design engineer. Special emphasis will be given to vortex tube type sand ejector.

### METHODS OF SEDIMENT CONTROL

The methods of sediment control can be broadly classified into two categories depending on whether the control is effected at the canal headworks or in the canal downstream. Whenever possible, an attempt should be made to exclude the sediment from the canal at the headworks. The device used for this purpose is known as excluder. If it is not practicable to remove all coarse material entering the canal at the headworks, structures can be built in the main canal to extract the excess sediment from it. The structure used for this purpose is known as ejector. In some cases both the excluder and the ejector are required to control the sediment load in the canal.

In literature [3, 7, 8, 12] following sediment control devices are discussed based on excluders or ejectors principle. i) slot; ii) step; iii) settling basin; iv) deflecting vanes; v) skimming weir; vi) drawing-off of slow moving currents; vii) separation of top and bottom water - tunnel types; viii) curved currents; ix) sluices; x) still pond; xi) grillage.

Whenever the cross-sectional area of a channel carrying water-sediment mixture is increased, the velocity and turbulence in the channel are naturally decreased. Depending on the size of the suspended material, the velocity of flow and the length of the channel with increased cross-section, some particles will settle down on the bottom. This method of sediment control is very efficient but very small velocities and long channels are required to remove very small sizes; hence it becomes expensive. The sloop, the step and the settling basin work on the above principle. A slot is a depressed channel across the bottom of the canal or in front of the headworks. As the sediment-laden water passes over it, part of the sediment is dropped into it and can be removed (Fig. 1). In case of streams carrying high loads of fine sediment, settling basins are provided for sediment removal. Settling basins are effective in removing material as fine as 0.072 mm. In case of a step, the bottom of the channel is gradually depressed forming a small basin at the downstream end of which the bottom rises abruptly to the normal canal invert (Fig. 2). The material deposited in a slot, step or settling basin is scoured out by high velocity flow through the sluices provided for the purpose. Alternately, the sediment deposited in the settling basin can be dredged out.

Recognizing the fact that sediment in flowing water is distributed nonuniformly in the vertical, the sediment entering the canal can be considerably reduced by keeping off slow-moving bottom layers having high sediment concentration. This is achieved either by using deflecting vanes (Fig. 3) or by using skimming weir or raised sills.

Sluices are used to flush out the deposit in slots and settling basins. Sluices are also used in excluders and ejectors. When they are used in excluders, they are usually of sufficient capacity to pass the entire low flow of the canal.

A still pond is situated just upstream of the sluice and is separated from the main flow by providing a divide wall (Fig. 4). Provision of a divide wall creates an area of low velocity at the canal intake when the sluice is closed and increases the area of influence of the sluice when it is open.

Sometimes a grill can be placed on the bed to permit the rolling down of the coarse sediment and relatively clear water drawn from below the grill.

The devices described above can be used either individually or in combination as excluders or ejectors.

#### VORTEX TUBE EJECTORS

Tests of the vortex tubes sand trap were first reported by Parshall [3, 7, 6]. The vortex tube sand trap was described as a tube with an opening along the top and placed in the bed of a canal at an angle of about  $45^{\circ}$  to direction of flow. Figure 5 shows various types of the vortex tube sand traps tested by Parshall. As the water passes over the opening, a spiral motion was set up within the tube. Material traveling along the canal bed was drawn or dropped into the tube and

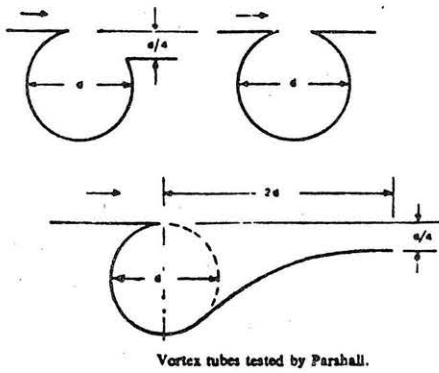
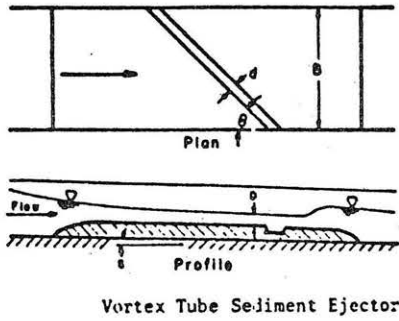


Fig. 5. Vortex tube.

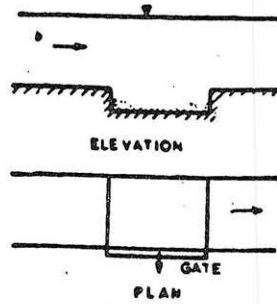


Fig. 1. Slot.

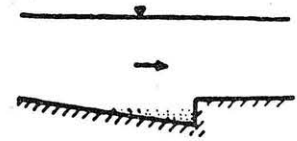


Fig. 2. Step.

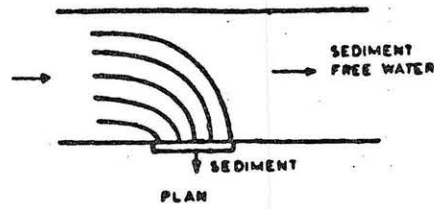


Fig. 3. Deflecting vanes.

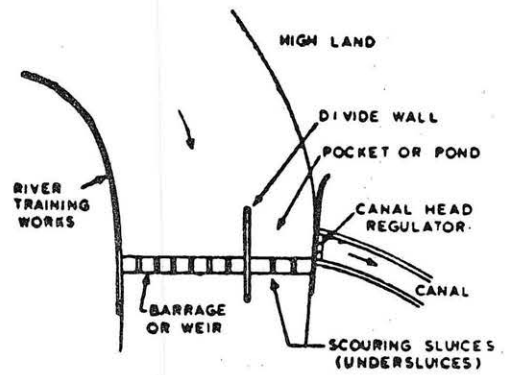


Fig. 4. Typical headworks for a canal

carried to an outlet where it was discharged into a return channel. The device was observed to be very effective in removing large material even the size of cobblestones.

Rohwer et al. [9] reported the results of tests conducted on vortex tubes installed in channels 8 ft and 14 ft wide. The tubes used were 4 in. and 6 in. in diameter set at various angles of the flow. Conclusions from these tests were given as (1) The tubes were most active when the depth of water in the channel was slightly less than critical; (2) Straight or tapered tubes were equally efficient in removing sand; (3) Angle of tube for angles less than  $90^\circ$  to the direction of flow had little effect on efficiency; (4) Efficiencies of trapping were conspicuously better when elevations of the upper and lower lips were the same; (5) The tube would remove from 70% to 90% of bed load carried by the flume; (6) Tubes in a channel that was 8 ft wide seemed to be more efficient in sand removal than ones installed in a channel 14 ft wide; and (7) When the Froude number of the flow immediately upstream from the tube exceeded 1.3, a considerable amount of sand and gravel was thrown out of the tube and re-entered the channel.

A tube 0.2 ft in diameter with one-quarter of the circumference cut away and installed in a flume 2-ft wide was studied by Koonsman [5,6]. The sand used for the test had a size range of 0.4 to 1.1 mm with a median diameter of 0.7 mm. Concentrations of sand ranged from 0.09 to 0.68 in percent by weight. Velocity of flow varied from 1.3 to 5.5 fps while depth ranged from 0.2 ft to 0.6 ft with corresponding Froude number,  $F$ , varied from 0.5 to 1.5. The elevation of the downstream lip was varied relative to the upstream one. Results from these tests showed that: (1) highest trapping efficiencies (92%) were noted near a Froude number of 1.0; (2) Efficiencies decreased as the depth of flow increased; (3) Efficiencies decreased as concentration was increased beyond a certain point depending also on the depth of flow; (4) Optimum operation was noted when the lips were at the same elevation; and (5) Percentage of flow removed from the tube varied from 2.7% to 15.5% depending on velocity and depth of flow over the tube. The reason given for the apparent decrease in efficiency with increasing depth was that greater quantities of sediment were being moved and more of this material was in suspension at greater depths.

In a design study by Ahmad [1, 2, 9] the vortex type ejector was found to be superior to the frontal type and was, therefore, preferable to the common ones used in Pakistan. The vortex type gave greater efficiencies at less discharge extractor ratios (percent of total flow removed) under similar operating conditions. The following recommendations were made regarding the design of the vortex tube: (1) The structure should be designed so that the Froude number of flow at the tube is equal to 0.8. (2) Diameter of the tube should be equal to water depth in the channel at a Froude number equal to 0.8. (3) The two lips of the opening slit should be at the same elevation. (4) Opening of the slit should be one-sixth of tube circumference. (5) Under conditions of heavy silt concentration, a long tube may not work efficiently. In this case, shorter tubes should be used, each equipped with an independent discharge pipe.

Robinson [9] suggested the following design criteria for the successful operator of vortex tube sand trap: (1) The velocity and depth of flow across the station containing the tube should be such that the Froude number approximate 0.8. (2) The percentage of flow removed by the tube is a function of the depth and velocity of flow in the channel as well as width of opening area, angle, and length of tube. The flow removed usually ranges from 5% to 15% of the total. (3) The width of opening should usually be in the range of 0.5 ft to 1.0 ft. (4) The ratio of length of tube to width of opening ( $l/d$ ) should not exceed 20 with the maximum length of tube being approximately 15 ft. (5) The tube angle should be  $45^\circ$ . (6) Straight tubes operate as well as tapered ones. (7) The elevation of the upstream and downstream lips of the tube can be the same rather than having the downstream one lower. (8) The shape of the tube does not seem to be particularly important as long as this shape is such that material entering the tube is not allowed to escape back into the channel. A pipe with a portion of the circumference removed seems to operate as well as other prefabricated shapes. (9) The required area of the tube can be approximated by the relationship  $AT = 0.06 DL \sin \theta$ . (10) With the foregoing design specification, the tube can be expected to remove approximately 80% of the sediment with size greater than 0.50 mm. The trapping efficiency of smaller sizes will be considerably lower.

The above mentioned investigators had performed experiments with the vortex tube sediment ejector but the reported results are applicable quantitatively only for field flow conditions similar to the experimental flow conditions. To describe the hydraulics of the flow of the water-sediment mixture through the vortex tube Sanmuganathan and White [11, 14] have developed an analytical method which would allow a design engineer, knowing the field condition, to design a vortex tube ejector and confidently predict its performance.

Sanmuganathan [11] developed an analytical method to study the flow inside a vortex tube based on the assumptions: (1) The friction in the vortex tube is negligible. (2) The swirling flow component in the vortex tube can be represented by a forced vortex. (3) The component of velocity in the channel along the vortex remains unchanged during the entry into the vortex tube, so that just below the slit the component has the same value as that in the channel. Subsequently, however, on entry into the main tube this velocity could change.

Based on these assumptions, Sanmuganathan [11] developed two basic equations describing the control of flow through vortex tube; extraction ratio and minimum velocity of sediment movement in the tube.

$$U_0 = C_v^* \sqrt{2g(H_T - H_0)} \quad (1)$$

$$V_{to} = \sqrt{2g(H_T - H_0)} \cdot \frac{k \cdot C_v}{\sqrt{1+k^2}} \cdot \frac{1}{\cosh y} \quad (2)$$

where

$$C_v^* = \sqrt{1 - \frac{k^2 C_v^2}{2}} \tan hy$$

If  $t/d$  is chosen so that  $k = 1.0$  (i.p.  $t/d = 0.3$ ) then

$$\frac{V_{to}}{\sqrt{2g(H_T - H_0)}} = \frac{0.693}{\text{Cosh } \gamma}$$

$$C_v = 0.98$$

$$\gamma = 0.2422 \ell/d$$

$U_o$  = average velocity in the pipe outlet (m/s);

$V_{to}$  = tangential velocity at entry to vortex tube (m/s);

$H_0$  = pressure head in the vortex tube at the outlet (m);

$$H_T = h + (V \sin\theta)^2/2g \text{ (m);}$$

$\ell$  = length of tube (m);

$d$  = diameter of vortex tube (m).

The purpose of the analysis was to determine the dimension of tube or number of tubes that will extract the maximum amount of sediment at the expense of an allowable quality of abstracted water. The tube should be self cleaning and the head drop across the tube should be minimal to assist easy disposal of the extracted sediment.

The two basic design equations are included as graphs (Figs. 6 and 7) of  $U_o$  versus  $(H_T - H_0)$  and  $V_{to}$  versus  $(H_T - H_0)$  for various  $\ell/d$ . For estimation of trap efficiency a graph (Fig. 8) is provided between ratio of settling velocity to shear velocity versus trap efficiency for various values of extraction. A design procedure developed by White and Sanmuganathen [14, 11] to estimate the trap efficiency and geometric parameters is discussed in the next section. A flow chart of the designed procedure is included in Fig. 10.

The sediment extractor methods discussed above have their own operational limitations depending on the water requirement, sediment extraction ratio, and location. The amount of water required for the operation of excluder and ejectors varies from 0.5% for settling basins to 100% for tunnel type excluders. Similarly the trapping efficiency of the devices varies with the area provided. Vortex tube type sediment ejectors are very efficient in removing the sand particles in the range of 0.5 mm. A study to compare the vortex tube type silt extractor with the frontal type was reported by Ahmad [2]. The withdrawals of the vortex tube and conventional type ejectors as percent of canal discharge were plotted against efficiency of silt ejectors. Figure 11 shows that a vortex tube eject can be more efficient with less discharge extraction as compared to conventional frontal type ejectors.

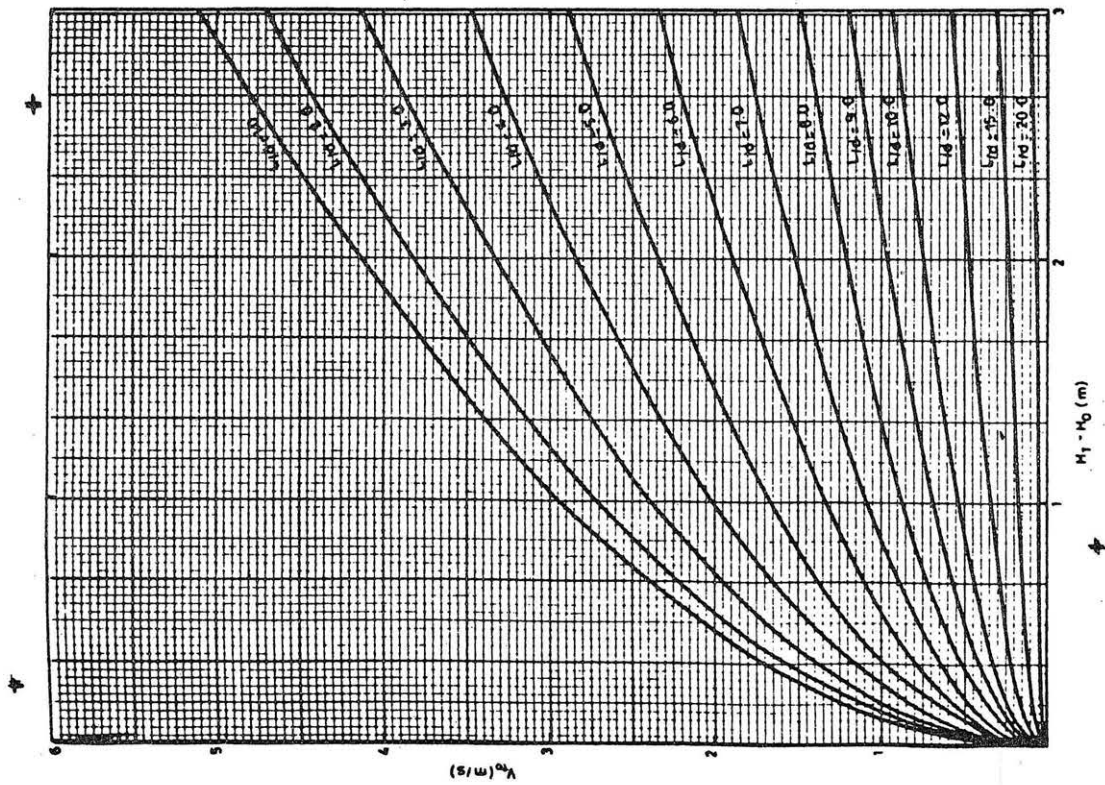


Fig. 6. Design graph  $V_0$  versus  $H_T - H_0$  for varying  $L/d$

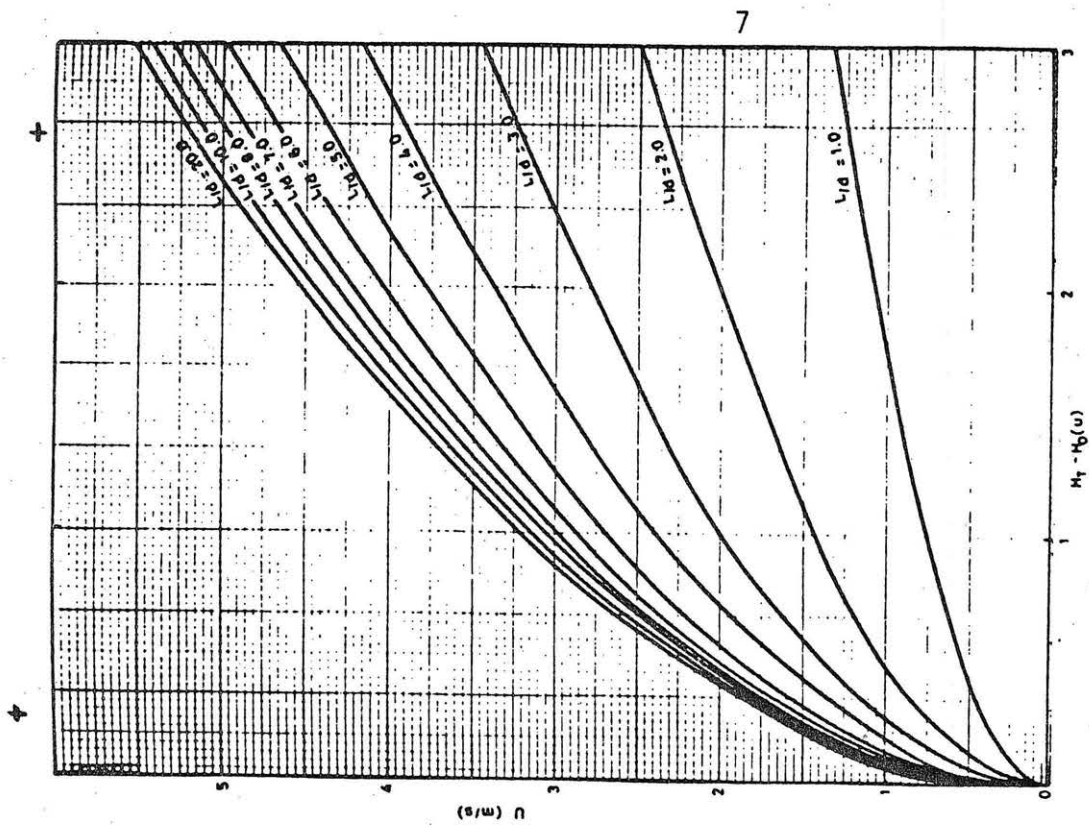


Fig. 7. Design graph  $U_0$  versus  $H_T - H_0$  for varying  $L/d$

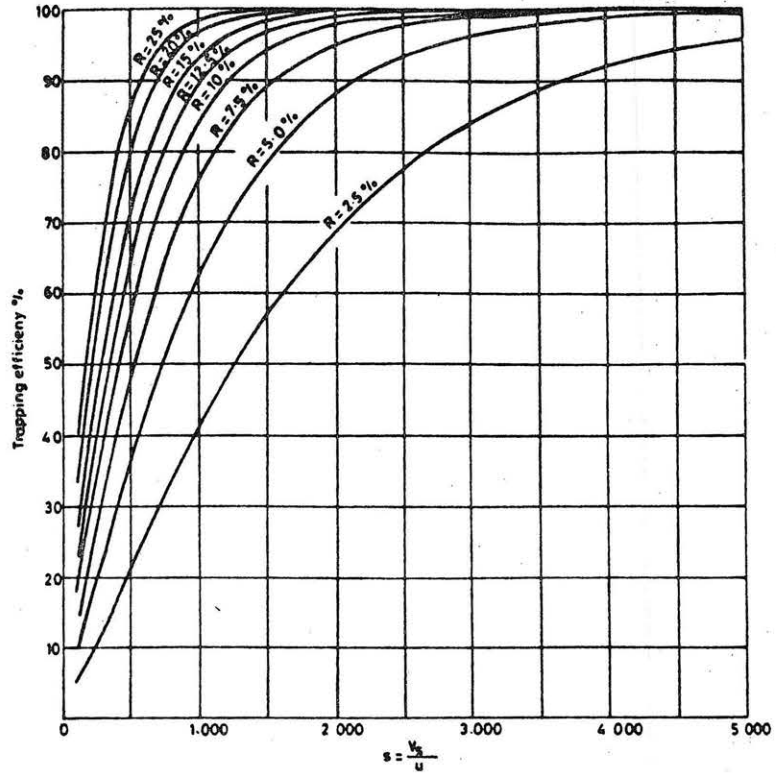


Fig. 8. Variation of trapping efficiency with  $s$

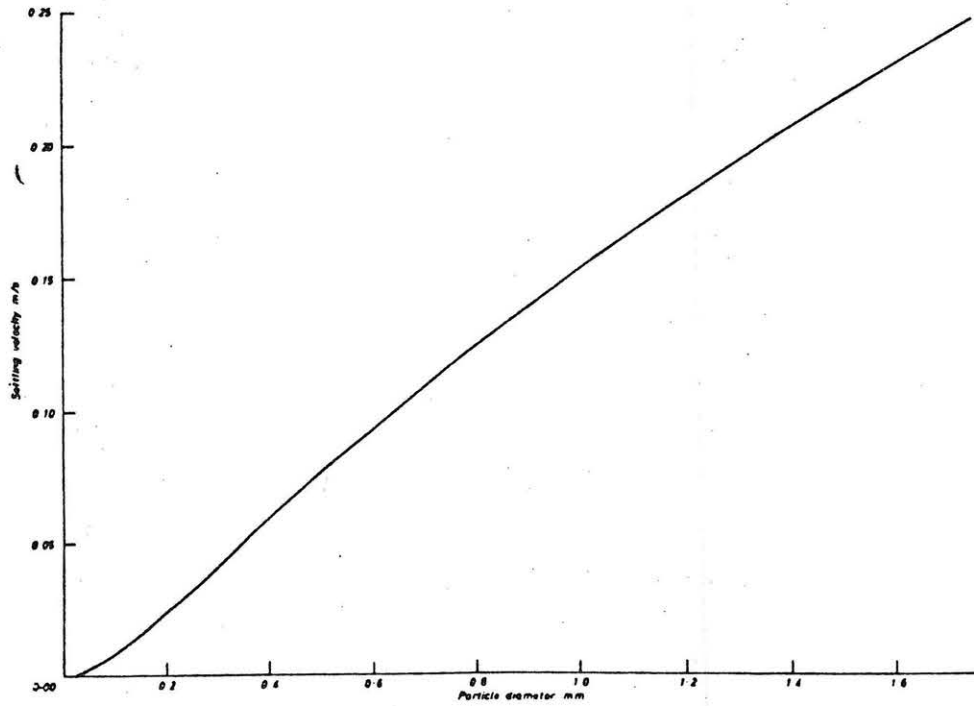


Fig. 9. SETTLING VELOCITIES OF SAND ( $S=2.65$ ) IN WATER AT 20°C



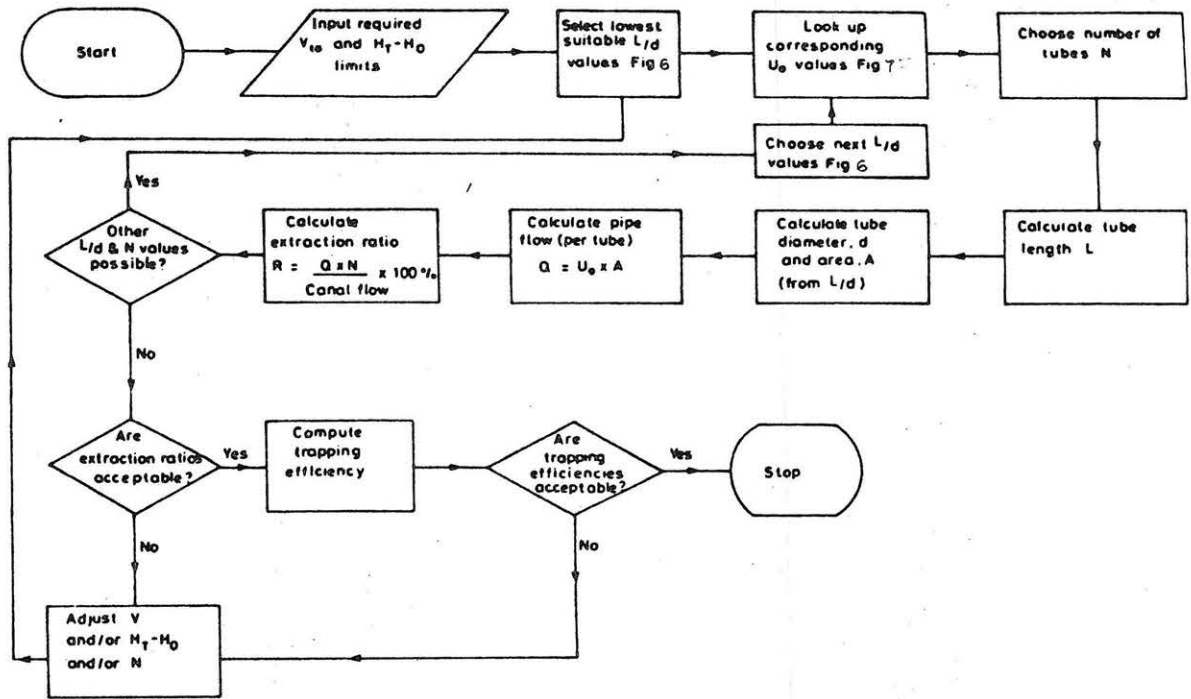


Fig. 10. Flow diagram of design procedure

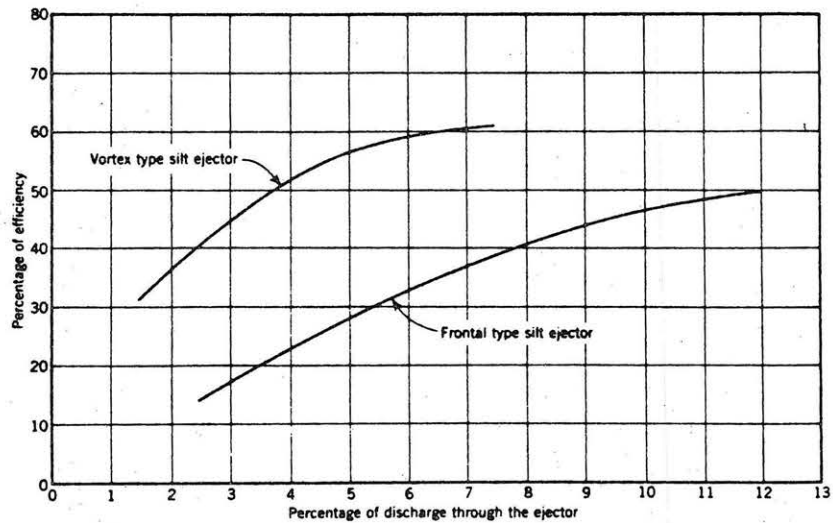


FIG. 11—COMPARISON OF VORTEX TYPE AND CONVENTIONAL TYPE EJECTOR

## DESIGN PROCEDURES

## a) For Vortex Tube Design

## 1. Assemble data:

Obviously, the more data that is available, the more reliable the design will be. However, the vortex tube can be designed with fairly limited data, which is listed below:

- i. Canal cross-section at vortex tube site.
- ii. Design flow in canal.
- iii. Design depth in canal.
- iv. Allowable extraction ratio for normal operation and occasional tube flushing.
- v. Analysis of sediment in canal -- particularly  $D_{75}$  and  $D_{90}$  and specific gravity of sediment.
- vi. Mean temperature at site -- to calculate water viscosity.

2. Calculate sediment settling velocities,  $V_s$  :

Diameters of various sediment fractions are easily measured using sieve analysis. Then some method is needed to relate diameter to settling velocities. Figure 9 gives the variation of settling velocity,  $V_s$ , with diameter,  $D$ . The values of Fig. 9 were taken from Gibbs et al. (1971).

3. Set limits on  $H_T - H_0$  suitable to site conditions:

The head across the vortex tube ( $H_T - H_0$ ) needs to be large enough for extraction to be relatively insensitive to small changes in water levels, 10 cm has been found to be a reasonable minimum. Also it needs to be small so that the extracted water can be used or disposed of without extensive excavations, i.e., the system should be designed to operate under gravity.

4. Calculate  $V_{to} \geq V_{s75}$  :

Since sediment in natural canals is graded, the question arises as to which sediment diameter to consider. The recommended guidelines are:

$$V_{to} \geq V_{s75} \quad \text{for normal operation under design conditions;}$$

$$V_{to} \geq V_{s90} \quad \text{for occasional flushing after tube shutdown, etc.}$$

These are not strict design rules. If problems are encountered with finding a suitable tube geometry to satisfy the criteria for  $V_{to}$ , then these values may be relaxed.

5. From Fig. 6 and using  $H_T - H_0$  and  $V_{to}$ , a suitable range of  $\ell/d$  values can be found.

6. Using  $\ell/d$  and  $H_T - H_0$ ,  $U_0$  the velocity along the vortex tube can be found from Fig. 7.

7. The values of  $\ell/d$  give values of tube diameter,  $d$ , for various tube lengths. Lengths being dependent on the number of tubes chosen for investigation. Once the diameter is known the tube cross-section Area,  $A$ , can be calculated.

8. From the values of  $U_0$ ,  $A$ , and  $Q$ , values of extraction ratio may be calculated.

- b) For Estimation of Trap Efficiency
1. Assembly data:
    - i. The average velocity in the channel,  $\bar{u} = Q/Ac$ .
    - ii. Calculate extraction ratio.
    - iii. The sediment grading from sieve analysis say  $D_{10}$ ,  $D_{30}$ ,  $D_{50}$ ,  $D_{70}$  and  $D_{90}$ .
  2. Calculations
    - i. Calculate shear velocity,  $u_* = \bar{u}/15$ .
    - ii. Calculate settling velocities ( $V_{s10}$ ,  $V_{s30}$ ,  $V_{s50}$ ,  $V_{s70}$ ,  $V_{s90}$ ) from Fig. 9.
    - iii. Calculate values for each sediment grading ( $S_{10}$ ,  $S_{30}$ ,  $S_{50}$ ,  $S_{70}$ ,  $S_{90}$ ) where  $S = V_s/u_*$ .
  3. From graph (Fig. 8) obtain values for  $P_{R10}$ ,  $P_{R30}$ ,  $P_{R50}$ ,  $P_{R70}$ ,  $P_{R90}$ . These are the trapping efficiencies for different sediment fractions. From these values, the overall value of  $P_R$  is obtained from

$$P_R = \frac{1}{5} [P_{R10} + P_{R30} + P_{R50} + P_{R70} + P_{R90}]$$

4. Assume that  $P_R \approx 1.3 P$ . One may obtain the final trapping efficiency from

$$P = \frac{P_R}{1.3}$$

The method described, is an approximate graphical method. For accurate computation of trapping efficiency, a more complex procedure is given in reference [14].

#### DESIGN EXAMPLE

This example is of a moderately sized canal, with fine sediment. Water is at a premium in this area and no extraction can be afforded. Therefore the extracted water and sediment are to be discharged into a settling pond with the water being reintroduced into the canal further downstream.

#### a) Design Data - Canal

Bed width	16.0 m
Design depth	0.75 m
Design discharge	16.0 m <sup>3</sup> /s
Minimum flow	10.5 m <sup>3</sup> /s
Maximum extraction	2.0 m <sup>3</sup> /s
Section	Trapezoidal
Side slopes	1.1

## b) Design Data - Sediment Characteristics

Sediment grade	Sediment diameter (mm)	Settling velocity* (m/s)
D <sub>5</sub>	0.16	0.017
D <sub>15</sub>	0.23	0.029
D <sub>25</sub>	0.29	0.039
D <sub>35</sub>	0.34	0.048
D <sub>45</sub>	0.41	0.061
D <sub>50</sub>	0.45	0.068
D <sub>65</sub>	0.55	0.084
D <sub>75</sub>	0.71	0.110
D <sub>85</sub>	0.99	0.152
D <sub>90</sub>	1.35	0.197
D <sub>95</sub>	1.35	0.197

## c) Preliminary Calculations

In this particular example it was decided to limit the maximum  $H_T - H_0$  to be 0.6 m due to local conditions. A minimum value of  $H_T - H_0 = 0.1$  m would seem to be reasonable, so that the extraction ratio is not too sensitive to small fluctuations in canal water level. Using these values and the sediment settling velocities, value of  $\ell/d$  can be found from Fig. 6 and hence value of  $U_o$  from Fig. 7. This in turn, leads to values for the extraction ratio. Several examples are given in the tables below.

No. of tubes = 1; Length of tubes = 16 m.

$V_{to}$ (m/s)	$H_T - H_0$ (m)	$\ell/d$	$d$ (m)	$A$ (m <sup>2</sup> )	$U_o$ (m/s)	$Q_t$ (m <sup>3</sup> /s)	$R$ (%)	Note
0.1	.10	12	1.3	1.327	1.0	1.327	8.3*	Min. $H_T - H_0$ , therefore limits $\ell/d$
0.2	.38	12	1.3	1.327	2.0	2.654	16.6	
0.1	.15	13	1.2	1.131	1.25	1.414	8.8	
0.2	.59	13	1.2	1.131	2.45	2.771	17.3	
0.1	.24	14	1.1	0.95	1.55	1.473	9.2	
0.2	.95	14	1.1	0.95	3.15	2.993	18.7	$H_T - H_0$ above permissible limits

\*used in worked example.

\*From Gibbs et al., using Fig. 9.

No. of tubes = 2; Length of tubes = 8 in.

$V_{to}$ (m/s)	$H_T - H_0$ (m)	$l/d$	$d$ (m)	$A$ (m <sup>2</sup> )	$U_o$ (m/s)	$Q_t$ (m <sup>3</sup> /s)	$R$ (%)	Note
0.1	.10	12	0.70	0.385	1.0	0.770	4.8	Note that here the same criteria as above are being met, with a lower extraction ratio.
0.2	.38	12	0.70	0.385	2.0	1.540	9.6	
0.1	.15	13	0.60	0.283	1.25	0.708	4.4	
0.2	.59	13	0.60	0.283	2.45	1.387	8.7	

No. of tubes = 3; Length of tubes = 5.33 m.

0.1	0.10	12	0.45	0.159	1.0	.477	3.0	Note that here the same criteria as above are being met, with a lower extraction ratio.
0.2	0.38	12	0.45	0.159	2.0	.954	6.0	
0.1	.15	13	0.40	0.126	1.25	.472	3.0	
0.2	.59	13	0.40	0.126	2.45	.926	5.8	

Normally, one would select two or three options from the tables above according to local conditions, availability of pipe, etc., and would then go on to calculate trapping efficiency.

b) Trap Efficiency

This example includes only Option 1, with  $R = 8.3\%$ .

1. Assembly data:

$$\bar{U} = Q/Ac = 1.33 \text{ m/s}$$

$$V_{to} = 0.1 \text{ m/s}$$

$$R = 8.3\%$$

$$U^* = \bar{U}/15 = 0.0887 \text{ m/s}$$

2. Calculations:\*

Sediment grading $D$ (mm)	Settling velocities $U_s$ (m/s)	$S$	$P_R^{**}$ (%)
0.20	0.024	0.2706	33
0.31	0.043	0.4848	50
0.45	0.068	0.7666	68
0.60	0.093	1.0485	81
1.35	0.199	2.2435	97

$$P_R = \frac{1}{5} [33 + 50 + 68 + 81 + 97] = 65.8\%$$

\* Computations are for  $D_{10}$ ,  $D_{30}$ ,  $D_{50}$ ,  $D_{70}$  and  $D_{90}$ , respectively.

\*\* Fig. 8.

Final trapping efficiency:

$$P = \frac{P_R}{1.3} = 51\%.$$

#### CONCLUSION

Despite the fact that different types of sediment controlling devices have been used in the past to varying extents, it is not possible, to specify any one type of device as the best solution under any given condition. The method of design and performance production for vortex tube silt ejector can be used during design stage with confidence. However, the method does not provide the engineering judgment that is required for final choice. It provides only the data that helps the final choice.

## REFERENCES

1. Ahmad, M., "Some aspects of design of head works to exclude sediment from canals," IAHR, 4th meeting, Bombay 1951.
2. Ahmad, M., "Vortex tube sand trap," discussion, Transaction, ASCE Volume 127, part III, 1962.
3. Garde, R. J., Ranga Raju, K. G., "Mechanics of sediment transportation and alluvial stream problems," Wile Eastern It. 1985.
4. Ghotankar, S. T., "A review of some aspects of the design of head works to exclude coarse bed sand from canals," IAHR, 4th meeting, Bombay 1951.
5. Koonsman, G. L., "Efficiency of a vortex tube sand trap," M.S. thesis, June 1950, Civil Engineering, CSU.
6. Koonsman, G. L., Albertson, M. L., "Design characteristics of the vortex tube sand trap," IAHR, 4th meeting, Bombay 1951.
7. Melone, M. Anthony, "Exclusion and ejection of sediment from canals," M.S. thesis, 1974, Civil Engineering, CSU.
8. Melone, A. M., Richardson, E. V., Simons, D. B., "Exclusion and ejection of sediment from canals," Civil Engineering, CSU, 1975.
9. Robinson, A. R., "Vortex tube sand trap," Transactions, ASCE Volume 127, part III, 1962.
10. Thorne, C. R., Bathurst & Hay, "Sediment transport in gravel-bed rivers."
11. Sanmuganathan, K., "Design of vortex tube silt extractors," Hydraulic Research Stations, Wallingford, U.K., 1976.
12. Uppal, H. L., "Sediment excluders and extractors," IAHR, 4th meeting, Bombay, 1951.
13. Vanoni, V. A., ed., "Sedimentation engineering," ASCE Manuals and Reports on Engineering Practice #54, 1975.
14. White, S. M., "Design manual for vortex tube silt extractors," Report # OD37, 1981, Hydraulics Research Station, Wallingford, U.K.

## CHANNEL STABILIZATION

By Rob Wassum

**ABSTRACT:** The overall objective of this report is to evaluate the stability of an existing channel system and recommend measures for its control. Short-term and long-term changes can be expected on channel systems as a result of natural and man-made influences. Numerous types of channel control and bank stabilization devices are available to accommodate these changes. The upper reaches of the Little Wekiva River, in Orange County, in Central Florida, is currently experiencing stabilization problems. A portion of this channel system will be investigated and recommendations will be made concerning its stability. This report was submitted to Dr. Pierre Y. Julien in partial fulfillment of the requirements of CE 717, River Mechanics, Colorado State University, Fort Collins, Colorado, Spring 1988.

### INTRODUCTION

In 1960, Orange County, Florida, experienced substantial flood damages caused by Hurricane "Donna". As a result of that experience, Orange County developed a water management plan to alleviate flooding problems. The plan primarily relied upon the construction of a series of canal systems and lake level controls for removing flood waters from the urbanized areas to less populated agricultural areas.

As a result of recent increase in urbanization, the existing drainage systems are no longer adequate. The upper reaches of the Little Wekiva River is an example of a channel system which is experiencing stabilization problems as a result of increased runoff due to the increase in impervious areas.

A portion of the Little Wekiva River will be investigated in this report and recommendations will be made concerning its stability.

### SCOPE OF STUDY

The primary goal of this study is to evaluate the stability of an existing channel system and to recommend measures for its control. The stability analysis used in this study breaks down into the following tasks:

1. Generate water surface profiles under existing conditions.
2. Evaluate the channel stability under existing conditions using the following methods: critical shear stress, permissible tractive force, and permissible velocity.
3. If the channel is determined to be unstable, then modify the channel and regenerate the water surface profiles.
4. Evaluate the channel stability under modified conditions.



5. If the channel is determined to be unstable, then remodel the channel and/or provide necessary reinforcement, i.e. riprap, etc.

#### DESCRIPTION OF STUDY AREA

The study site is located in the Little Wekiva Watershed, in Orange County, in Central Florida. The area of the basin is 236 acres.

The existing stormwater conveyance system consists of a storm sewer system, retention pond, and canal system. The storm sewer system conveys runoff into the retention pond which outfalls into the canal system. This canal system flows northeasterly for a distance of approximately 4300 feet outfalling into Lawne Lake. A portion of this canal system is the subject of this report.

The topography of the area is relatively flat with land usage as follows: 33.8% woods and grasses, 33.6% residential, 20.3% commercial, 6.8% open space, and 5.5% open water.

For the purpose of this study, the basin was divided into 10 subbasins based on hydrologic and hydraulic features.

#### DESCRIPTION OF INPUT DATA

Input data can be classified into two major groups: hydrologic and hydraulic. Hydrologic data are required in the simulation of flood hydrographs and hydraulic data are used in computation of water surface profiles. Some of the selected hydrologic and hydraulic data are discussed below:

##### Rainfall

The rainfall data used in this study was obtained from Orange County Water Management Department. The Orange County rainfall distribution was used to calculate rainfall depth at each time interval.

##### Soil

Soil data were taken from the U.S. Department of Agriculture, Soil Conservation Service Soil Survey Interim Report of May, 1985. The basin consisted entirely of type 'D' soils. The portion of the canal under consideration, consists of noncohesive fine sands with a mean diameter of 0.140 mm. The specific gravity is assumed to 2.65.

##### SCS Runoff Curve Number

The SCS Runoff Curve Number was used to compute surface runoff based upon land use and soil type.

##### Channel Cross-Sections

Cross-sections are necessary for determining the shape and geometry of channels for flood profile computations. Field-surveyed channel cross-sections and engineering data on

control structures were obtained from the Orange County Survey Department.

### Channel Roughness Coefficients

Analysis of flow in open channels requires information on the roughness characteristics of the channel. Channel roughness coefficients are dependent upon a number of factors such as stage and discharge, vegetation, size and shape of channel, degree of irregularity, and obstructions. Estimation of channel roughness coefficients requires considerable experience and judgement. This parameter can have significant effect on the simulated flood elevations. The coefficients used in this study were assessed based on field inspections and aerial photography and are 0.03 and 0.08 for the main channel and overbank areas, respectively.

### Runoff Hydrographs

The Santa Barbara Urban Hydrograph (SBUH) computer model was used to generate the storm hydrograph for the 25 year, 24 hour storm event.

### Design Storm

The 25 year, 24 hour storm event is the required design storm for designing canals, ditches, or culverts for drainage external to the developed area per Orange County Drainage Regulations (1986).

## METHODS OF COMPUTATION

### Water Surface Profiles

The HEC2 computer model, developed by the U.S. Army Corps of Engineers (1982), was used to generate the water surface profiles. The computational procedure is based on the solution of the one-dimensional energy equation with energy loss due to friction evaluated with Manning's equation. This computational procedure is generally known as the Standard Step Method. The following assumptions are implicit in the analytical expressions used in the program:

1. Flow is assumed to be steady because time-dependent terms are not included in the energy equation.
2. Flow is assumed to be gradually varied because the energy equation is based on the premise that a hydrostatic pressure distribution exists at each cross section.
3. Flow is assumed to be one dimensional because the energy equation is based on the premise that the total energy head is the same at all points in the cross-section.
4. Small channel slopes, say less than 1:10, are assumed because the pressure head which is a component of the water surface elevation in the energy equation is represented by the water depth measured vertically.

### Average Boundary Shear Stress

The shear force is the shear developed on the wetted area of the channel and it acts in the direction of flow. This force per unit wetted area is called the average boundary shear stress  $\tau_0$  and can be expressed as:

$$\tau_0 = \gamma R S_f \dots\dots\dots (1)$$

Generally speaking, for trapezoidal channels of the shapes ordinarily used in canals, the average boundary shear stress on the bottom is close to the value  $\tau_0$ , and on the side slopes close to  $0.76 \tau_0$  (Chow, 1959).

### Critical Boundary Shear Stress

The critical boundary shear stress is the minimum amount of shear stress exerted by the passing stream currents required to initiate soil particle motion. The two methods used in this study for estimating the critical boundary shear stress are the Shield's Diagram and Method of Permissible Tractive Force.

#### Shield's Diagram

Many experiments have been conducted to develop an explicit relationship for the beginning of motion. A relationship has been determined experimentally by Shields and others (Federal Highway Administration (FHWA), 1987). The relationship is given in Fig. 1. At conditions of incipient motion, the average boundary shear stress  $\tau_0$  is designated the critical boundary shear stress,  $\tau_c$ . This method is widely accepted and used for analysis of noncohesive particles. The procedure for the Shield's Diagram is as follows:

1. Estimate the mean particle diameter,  $D_s$ .
2. Compute the shear velocity,  $V_*$ .

$$V_* = \sqrt{\frac{\tau_0}{\rho}} \dots\dots\dots (2)$$

3. Compute the boundary reynolds number,  $R_*$ .

$$R_* = \frac{V_* D_s}{\nu} \dots\dots\dots (3)$$

4. Determine the dimensionless shear stress  $F_*$ , from the Shields Diagram, Fig. 1.
5. Compute the critical shear stress on the bed,  $\tau_c$ .

$$\tau_c = F_* (\gamma_s - \gamma) D_s \dots\dots\dots (4)$$

6. Estimate the angle of repose  $\phi$ , from Fig. 2.
7. Compute the coefficient K, using Lane's relationship between the critical shear stress on the bed and side slope.

$$K = \sqrt{1 - \frac{\sin^2 \theta}{\sin^2 \phi}} \dots \dots \dots (5)$$

This relationship is valid when the streamlines are horizontal (Julien, 1987).

8. Compute the critical shear stress on the side slope,  $\tau_{cs}$ .

$$\tau_{cs} = K \tau_c \dots \dots \dots (6)$$

Method of Permissible Tractive Force

The method of permissible tractive force (critical shear stress) was developed by the United States Bureau of Reclamation (USBR). It is a graphical procedure based upon field and laboratory experiments (Chow, 1959). The following procedure is valid for fine noncohesive particles and straight channels and is as follows:

1. Estimate the mean particle diameter,  $D_s$ .
2. Estimate the sediment content in the water (clear, low, or high).
3. Determine the permissible tractive force,  $\tau_p$ , on the channel bed from Fig. 3.
4. Estimate the angle of repose  $\phi$ , from Fig. 2.
5. Compute the coefficient K, using Eq. 5.
6. Compute the permissible tractive force on the side slope  $\tau_{ps}$ , using Eq. 6.

Method of Permissible Velocity

A third method for evaluating the stability of an open channel is the method of permissible velocity (Fortier and Scobey, 1926, Simons and Senturk, 1977). The maximum permissible velocity is the greatest mean velocity that will not cause erosion of the channel body. This method has been used extensively for the design of earth canals in the United States and is valid for channels composed of noncohesive materials with small slopes. Table 1 summarizes the permissible velocities and the procedure is as follows:

1. Compute the mean channel velocity,  $V_m$ .
2. Estimate the mean particle diameter,  $D_s$ , and classify the channel material (fine sand, etc.)
3. Estimate the sediment content in the water (clear, colloidal particles, or noncolloidal particles).
4. Determine the permissible velocity from Table 1.

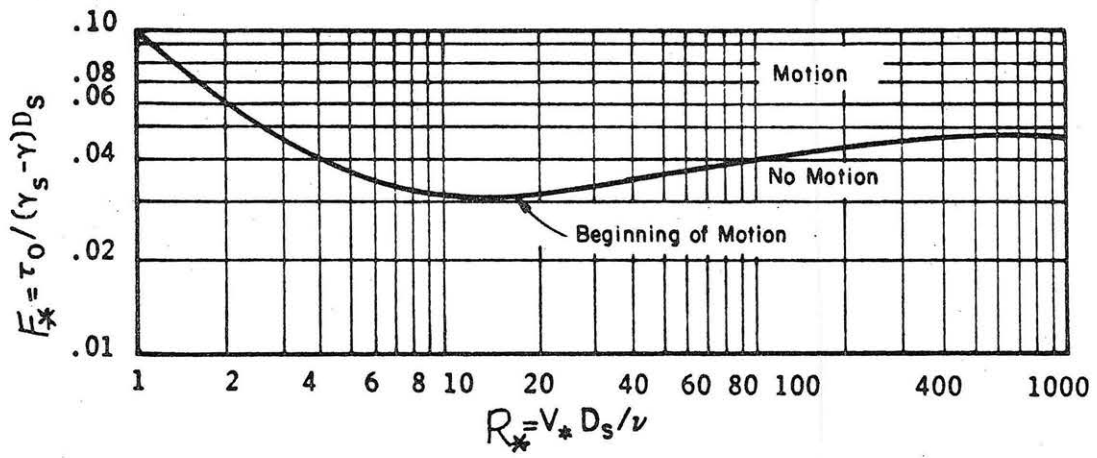


Fig. 1. Shield's Diagram for beginning of motion (after FHWA, 1987).

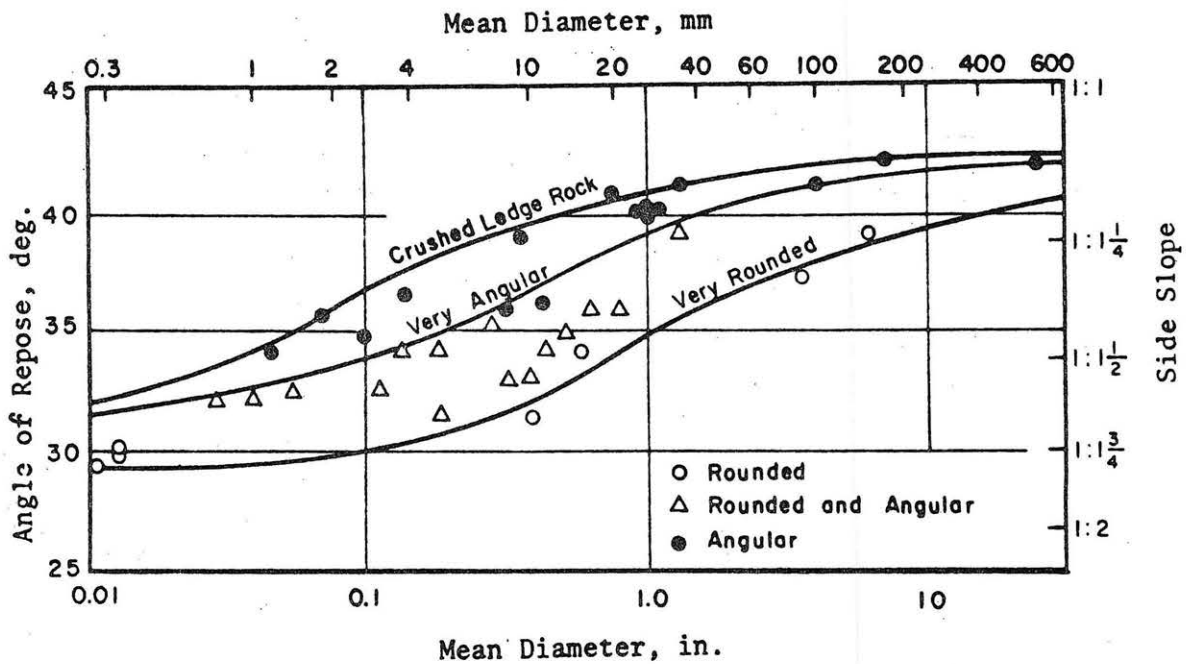


Fig. 2. Angle of Repose (after FHWA, 1987)

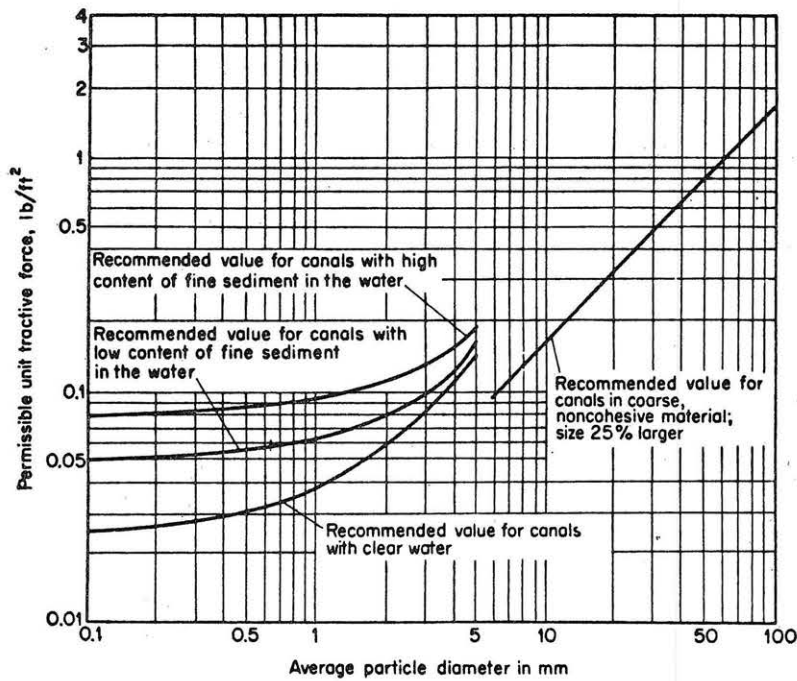


Fig. 3. Recommended Permissible Tractive Forces for Canals in Noncohesive Material (after Chow, 1959).

Original material excavated for canals	n	Mean velocity, After Aging, of Canals (d ≤ 3 ft)					
		Clear water, no detritus		Water transporting colloidal silt		Water transporting noncolloidal silts, sands, gravels or rock fragments	
		ft/sec	m/sec	ft/sec	m/sec	ft/sec	m/sec
1. Fine sand (colloidal)	.02	1.5	0.46	2.50	0.76	1.50	0.46
2. Sandy loam (noncolloidal)	.02	1.45	0.53	2.50	0.76	2.00	0.61
3. Silt loam (noncolloidal)	.02	2.00	0.61	3.00	0.91	2.00	0.61
4. Alluvial silt when noncolloidal	.02	2.00	0.61	3.50	1.07	2.00	0.61
5. Ordinary firm loam	.02	2.50	0.76	3.50	1.07	2.25	0.69
6. Volcanic ash	.02	2.50	0.76	3.50	1.07	2.00	0.61
7. Fine gravel	.02	2.50	0.76	5.00	1.52	3.75	1.14
8. Stiff clay (very colloidal)	.025	3.75	1.14	5.00	1.52	3.00	0.91
9. Graded, loam to cobbles, when noncolloidal	.03	3.75	1.14	5.00	1.52	5.00	1.52
10. Alluvial silt when colloidal	.025	3.75	1.14	5.00	1.52	3.00	0.91
11. Graded, silt to cobbles, when colloidal	.03	4.00	1.22	5.50	1.68	5.00	1.52
12. Coarse gravel (noncolloidal)	.025	4.00	1.22	6.00	1.83	6.50	1.98
13. Cobbles and shingles	.035	5.00	1.52	5.50	1.68	6.50	1.98
14. Shales and hard pans	.025	6.00	1.83	6.00	1.83	5.00	1.52

Table 1. Maximum Permissible Velocities (after Simons and Senturk, 1977).

SECNO	QCH cfs	$Y_0$ ft	$V_M$ fps	$\tau_0$ lb/ft <sup>2</sup>	$\tau_{os}$ lb/ft <sup>2</sup>	Shield's Diagram $\tau_c$ lb/ft <sup>2</sup>	Shield's Diagram Stability
2090	200	5.37	2.63	0.122	0.093	0.0016	Unstable
2698	200	4.54	2.87	0.156	0.119	0.0015	Unstable
2830	200	5.48	1.92	0.065	0.049	0.0017	Unstable
3300	200	5.84	1.90	0.063	0.048	0.0017	Unstable
3620	200	3.78	3.16	0.196	0.149	0.0015	Unstable

Shield's Diagram $\tau_{cs}$ lb/ft <sup>2</sup>		Permissible Tractive Force				Permissible Velocity	
Stability		$\tau_p$ lb/ft <sup>2</sup>	Stability	$\tau_{ps}$ lb/ft <sup>2</sup>	Stability	$V_p$ fps	Stability
0.0009	Unstable	0.050	Unstable	0.029	Unstable	2.00	Unstable
0.0009	Unstable	0.050	Unstable	0.029	Unstable	2.00	Unstable
0.0010	Unstable	0.050	Unstable	0.029	Unstable	2.00	Stable
0.0010	Unstable	0.050	Unstable	0.029	Unstable	2.00	Stable
0.0009	Unstable	0.050	Unstable	0.029	Unstable	2.00	Unstable

Table 2. Stability Analysis Results - Existing Conditions

SECNO	QCH cfs	$Y_0$ ft	$V_M$ fps	$\tau_0$ lb/ft <sup>2</sup>	$\tau_{os}$ lb/ft <sup>2</sup>	Shield's Diagram $\tau_c$ lb/ft <sup>2</sup>	Shield's Diagram Stability
2090	200	5.37	1.87	0.060	0.046	0.0017	Unstable
2698	200	4.26	2.00	0.071	0.054	0.0016	Unstable
2830	200	5.50	1.40	0.032	0.025	0.0018	Unstable
3300	200	4.24	2.01	0.072	0.055	0.0016	Unstable
3620	200	3.46	2.64	0.131	0.099	0.0015	Unstable

Shield's Diagram $\tau_{cs}$ lb/ft <sup>2</sup>		Permissible Tractive Force				Permissible Velocity	
Stability		$\tau_p$ lb/ft <sup>2</sup>	Stability	$\tau_{ps}$ lb/ft <sup>2</sup>	Stability	$V_p$ fps	Stability
0.0007	Unstable	0.050	Unstable	0.029	Unstable	2.00	Stable
0.0007	Unstable	0.050	Unstable	0.029	Unstable	2.00	Stable
0.0008	Unstable	0.050	Stable	0.029	Stable	2.00	Stable
0.0007	Unstable	0.050	Unstable	0.029	Unstable	2.00	Unstable
0.0007	Unstable	0.050	Unstable	0.029	Unstable	2.00	Unstable

Table 3. Stability Analysis - Modified Conditions

## Riprap Design

When available in sufficient size, rock riprap is usually the most economical material for bank protection. Rock riprap has many other advantages over other types of protection (FHWA, 1987).

In the absence of waves and seepage, the stability of rock riprap particles on a side slope is a function of:

1. The magnitude and direction of the stream velocity in the vicinity of the particles.
2. The angle of the side slope.
3. The characteristics of the rock including the geometry, angularity, and density.

The following particle stability analysis to be used for riprap design has first been derived by Stevens (1968), (FHWA, 1987). As a result, the stability factor for rock riprap on side slopes where the flow has a non-horizontal velocity vector is related to properties of the rock, side slope and flow by the following equations:

$$SF = \frac{\cos\theta + \tan\phi}{\eta'\tan\phi + \sin\theta \cos\beta} \dots\dots\dots (7)$$

$$\beta = \tan^{-1} \left[ \frac{\cos\lambda}{\frac{2\sin\theta}{\eta\tan\phi} + \sin\lambda} \right] \dots\dots\dots (8)$$

$$\eta = \frac{2\tau_0}{(\gamma_s - \gamma) D_s} \dots\dots\dots (9)$$

$$\eta' = \eta \left[ \frac{1 + \sin(\lambda + \beta)}{2} \right] \dots\dots\dots (10)$$

If SF is greater than unity, the riprap is stable; if SF is unity, the rock is in the condition of incipient motion; if SF is less than unity, the riprap is unstable.

The procedures for designing riprap for channel bed and bank stabilization is described below.

### Riprap Design - Channel Bed

The following procedure is applicable to the stability of riprap on the channel bed under downslope flow (FHWA, 1987). For downslope flow over a plane bed inclined at an angle  $\hat{\theta}$  is equivalent to an oblique flow on a side slope with  $\theta = \hat{\theta}$  and  $\lambda = 90^\circ$ . Refer to Fig. 4.

1. Estimate the average boundary shear stress on the channel bed,  $\tau_0$ , using Eq. 1.
2. Compute the channel bed slope angle,  $\hat{\theta}$ .



3. Estimate the angle of repose for the riprap,  $\phi$ .
4. Assume an appropriate value of the stability factor, SF.
5. Compute the stability number,  $\eta$ , using Eqs. 7 and 10.
6. Compute the mean riprap size,  $D_S$ , using Eq. 9.

#### Riprap Design - Channel Bank

The following procedure is applicable to the stability of riprap on the channel bank when the velocity along the bank has no downslope component (i.e., the velocity vector is along the horizontal), (FHWA, 1987). For horizontal flow along a side slope, the equations relating the stability factor, the stability number, the side slope angle, and the angle of repose for the rock are obtained with  $\lambda = 0^\circ$ . Refer to Fig. 4.

1. Estimate the average boundary shear stress on the channel bank,  $\tau_{os}$ , using Eq. 1.
2. Compute the channel bank slope angle,  $\theta$ .
3. Estimate the angle of repose for the riprap,  $\phi$ .
4. Assume an appropriate value of the stability factor, SF.
5. Compute the ratio,  $S_m$ .

$$S_m = \frac{\tan \phi}{\tan \theta} \dots \dots \dots (11)$$

6. Compute the stability number,  $\eta$ .

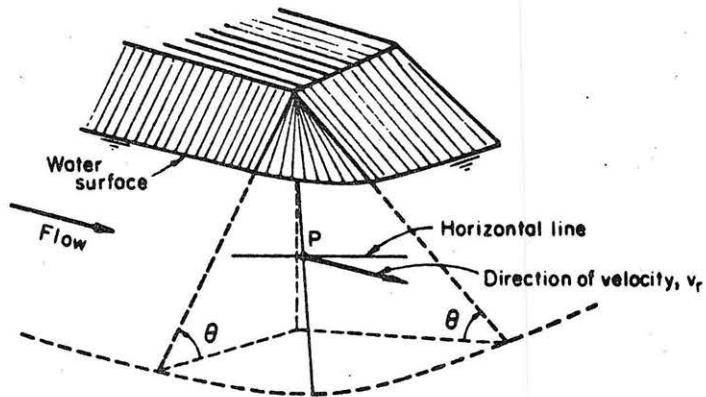
$$\eta = \frac{S_m^2 - SF^2}{S_m^2 SF} \cos \theta \dots \dots \dots (12)$$

7. Compute the mean riprap size,  $D_S$ , using Eq. 9.

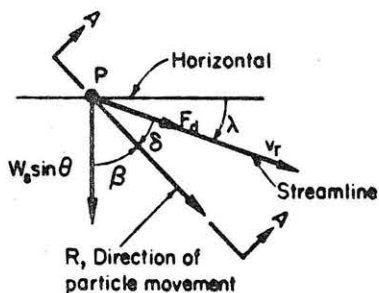
#### Riprap Design - Channel Bends

The velocity method for riprap design will be used to determine the riprap requirements for the channel bends (FHWA, 1987). The procedure is as follows:

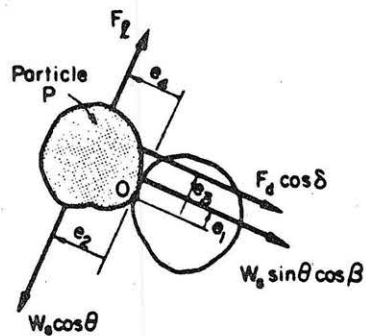
1. Compute the channel bank slope angle,  $\theta$ .
2. Compute the mean channel velocity,  $V_m$ .
3. Compute the average flow depth in the bend,  $Y_0$ .
4. Estimate the angle  $\lambda$ , as shown in Fig. 4. The angle  $\lambda$  ranges from 0 to 20 degrees depending upon the sharpness of the bend. The streamlines in a bend are deflected downward on the outer bank,  $\lambda$  is positive, and upward on the inner bank,  $\lambda$  is negative.
5. Estimate the mean stone size,  $D_S$ .
6. Estimate the angle of repose,  $\phi$ .
7. Compute the ratio,  $D_S/Y_0$ .
8. Convert the mean channel velocity  $V_m$ , to the velocity against the stone  $V_S$ , using Fig. 5.



(a) General view



(b) View normal to the side slope



(c) Section A-A

Fig. 4. Diagram for the Riprap Stability Conditions (after FHWA, 1987).

9. Apply correction factor to  $V_s$ . The size of stone required to resist displacement from direct impingement of the current as might occur with a sharp change in stream alignment is greater than that which would occur in a straight channel. Therefore, a factor which would vary from 1 to 2 depending upon the severity of the attack by the current, should be applied to the velocity  $V_s$ .
10. Compute the stability number,  $\eta$ , (FHWA, 1987).

$$\eta = \frac{0.60V_s^2}{(S_s - 1)gD_s} \dots\dots\dots (13)$$

11. Compute the angle,  $\beta$ , using Eq. 8.
12. Compute the stability number for the particles on the embankment slope,  $\eta'$ , using Eq. 10.
13. Compute the stability factor, SF, using Eq. 7.
14. Steps 5 to 13 are repeated until the desired stability factor is obtained.

Slope	Slope Angle degrees	Required Riprap Diameter	
		Straight Channel inches	Channel Bend inches
1.75:1	29.74	2.7	48.0
2:1	26.57	2.2	9.0
2.5:1	33.69	1.0	3.5
3:1	18.43	0.8	1.5
3.5:1	15.95	0.7	1.1
4:1	14.04	0.6	0.8

Table 4. Required Riprap Diameter for Various Channel Bank Slope Angles

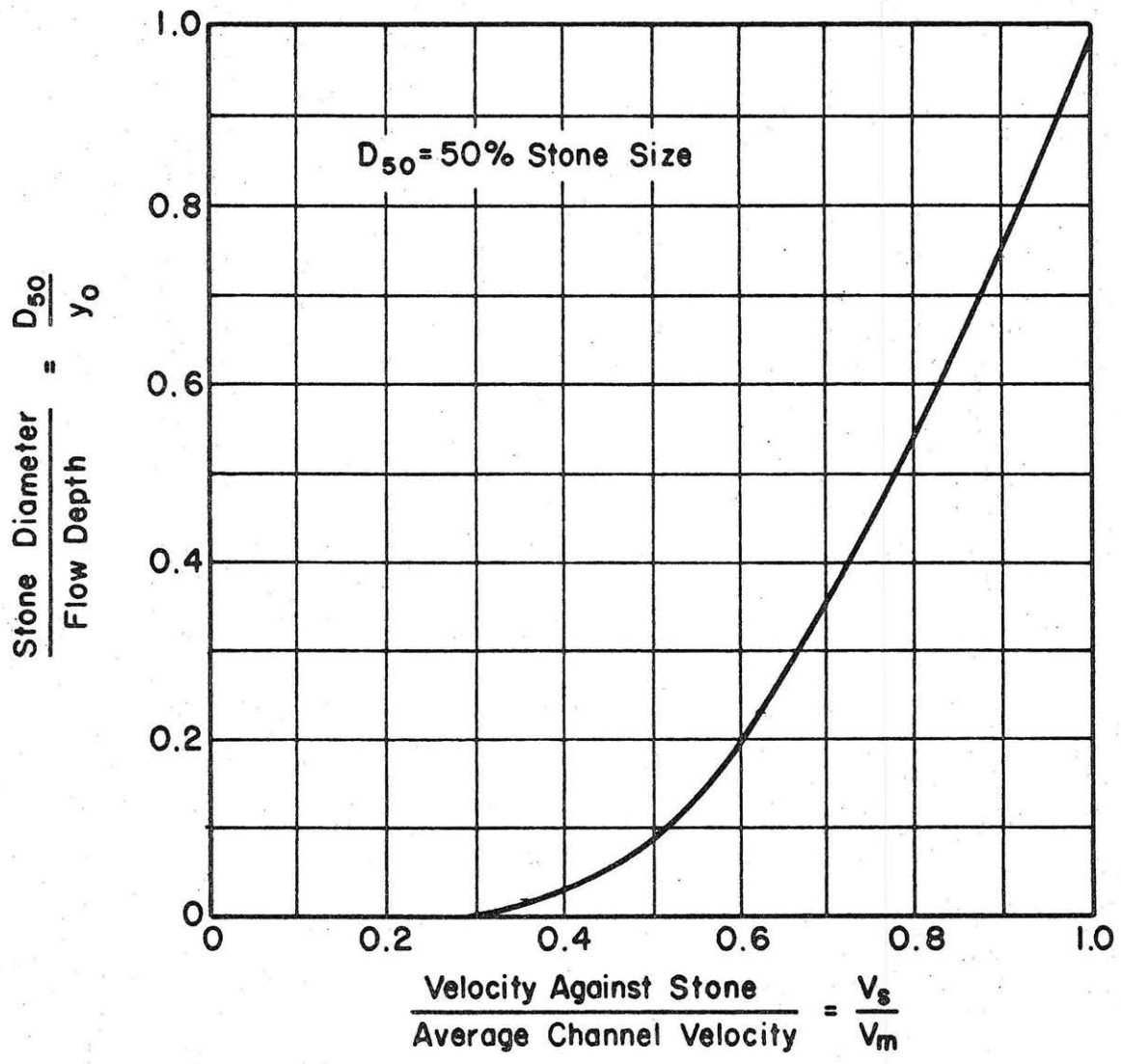


Fig. 5. Velocity Against Stone on Channel Bottom (after FHWA, 1987).

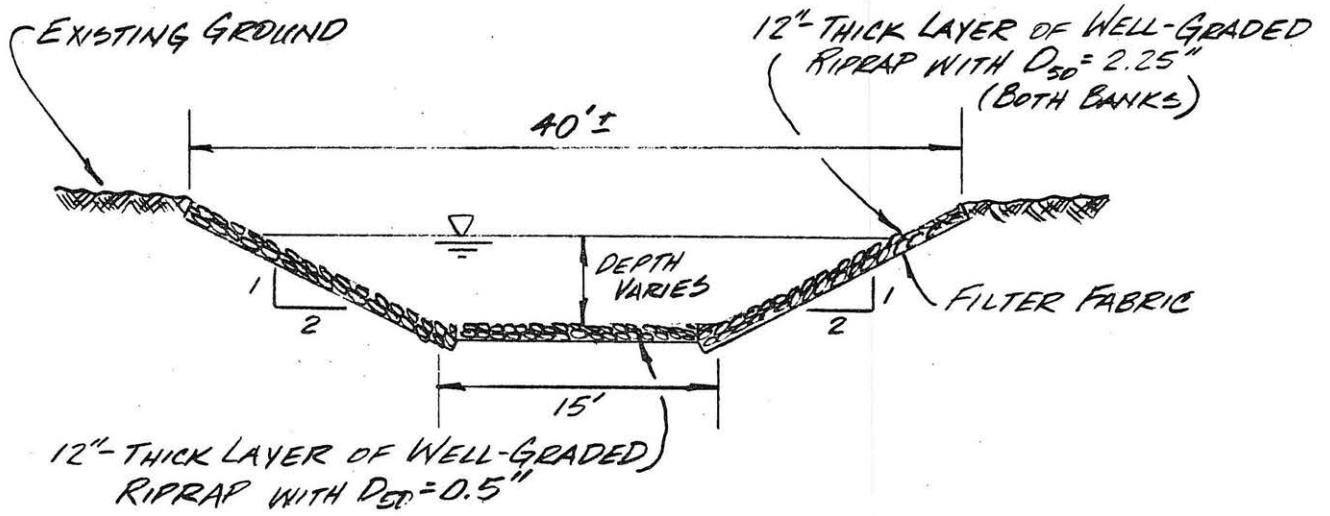


Fig. 6. Proposed Channel Cross-Section

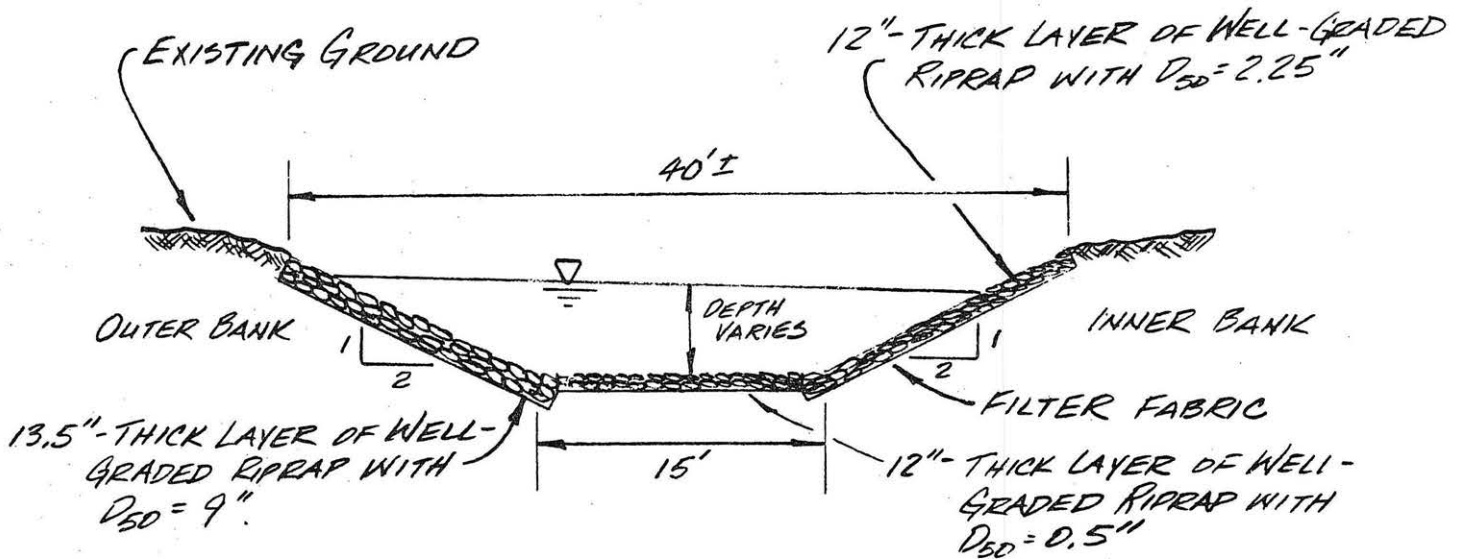


Fig. 7. Proposed Channel Bend Cross-Section

## SUMMARY

Channel stabilization is becoming increasingly important in areas of high urbanization. As a result of increased runoff due to the increase in impervious areas, existing channel systems are unable to accommodate the peak flood flows.

The methods of the Shields Diagram, permissible tractive force, and permissible velocity for stability analysis and Stevens method and velocity against the stone for riprap design are just a few of the many methods available. As more test sites are setup and stabilization devices installed and monitored, the validity of the above methods, as well as others, will be proven with time and as a result our knowledge of channel stabilization will continue to grow.

## CONCLUSIONS

Based upon my review of channel stabilization, I conclude that:

1. The Little Wekiva River is experiencing stabilization problems.
2. The threshold condition for the beginning of particle motion depends on the channel geometry, material characteristics, and flow conditions.
3. Many experiments have been conducted to develop an explicit solution for the beginning of motion.
4. Riprap is a possible stabilization alternative.
5. The use of vegetation as a stabilization alternative requires additional consideration.
4. The stability of riprap is very sensitive to the channel bank slope angle.
5. The velocity and shear stress are significantly higher on the outer bank of a channel bend.
6. Side slope stability methods for straight channels are not applicable to channel bends.
7. The effects of vegetation are not accounted for in the methods presented in this report.
8. The effects of riprap gradation, thickness, and shape on stability methods requires additional consideration.
9. The methods for determining velocity in straight and curved channels requires additional consideration.
10. The effects of variation in roughness on the Shield's parameter requires additional consideration.

## APPENDIX I. REFERENCES

- Chow, Ven Te, 1959, Open-Channel Hydraulics, McGraw-Hill Book Company, New York, New York.
- Federal Highway Administration, 1987, Highways in the River Environment, U.S. Department of Transportation, Washington, D.C.
- Julien, Pierre Y., 1987, Teaching Guide to Erosion and Sedimentation, Colorado State University, Fort Collins, Colorado.

- Orange County, Florida, 1986, Orange County Subdivision Regulations, Orlando, Florida.
- Simons, Daryl B. & Senturk, Fuat, 1977, Sediment Transport Technology, Water Resources Publications, Fort Collins, Colorado.
- U.S. Army Corps of Engineers, 1982, HEC2, Water Surface Profiles, Users Manual, The Hydrologic Engineering Center, Davis, California.
- Vanoni, Vito A., editor, 1977, Sedimentation Engineering, American Society of Civil Engineers, ASCE Manuals and Reports on Engineering Practice No. 54, Headquarters of the Society, New York, New York.

#### APPENDIX II. NOTATION

- $\beta$  = Angle defined in Fig. 4, degrees.
- $D_s$  = Mean diameter of particle, feet.
- $M$  = Stability number, dimensionless.
- $M'$  = Stability number for the particles on the embankment
- $F_*$  = Dimensionless shear stress.
- $\gamma$  = Unit weight of water, lbs./cu.ft.
- $\gamma_s$  = Unit weight of soil particle, lbs./cu.ft.
- $K$  = Ratio of critical shear stress on embankment to the bed critical shear stress.
- $\lambda$  = Angle defined in Fig. 4, degrees.
- $\nu$  = Kinematic viscosity of water, sq.ft./sec.
- $\phi$  = Angle of repose, degrees.
- $\rho$  = Density of water, lbm./cu.ft.
- $R$  = Hydraulic radius, feet.
- $R_*$  = Boundary Reynolds number.
- $S_f$  = Slope of the energy grade line, ft./ft.
- $SF$  = Stability factor for riprap design.
- $S_m$  = Ratio used in riprap design.
- $S_s$  = Specific gravity of soil particle.
- $\tau_o$  = Average boundary shear stress on bed, lbf./sq.ft.
- $\tau_{os}$  = Average boundary shear stress on bank, lbf./sq.ft.
- $\tau_c$  = Critical boundary shear stress on bed, lbf./sq.ft.
- $\tau_{cs}$  = Critical boundary shear stress on bank, lbf./sq.ft.
- $\tau_p$  = Permissible tractive force on bed, lbf./sq.ft.
- $\tau_{ps}$  = Permissible tractive force on bank, lbf./sq.ft.
- $\theta$  = Channel bank slope angle, degrees.
- $\Theta$  = Channel bed slope angle, degrees.
- $V_*$  = Shear velocity, ft./sec.
- $V_m$  = Mean channel velocity, ft./sec.
- $V_p$  = Permissible velocity, ft./sec.
- $V_s$  = Velocity against stone, ft./sec.
- $Y_o$  = Average flow depth, ft.